

# Green Water Credits for the Upper Tana Basin, Kenya. Phase II – Pilot Operations

## Biophysical assessment using SWAT

November 2009

**Author**

J.E. Hunink  
W.W. Immerzeel  
P. Droogers

**Client**

ISRIC

**Report FutureWater: 84**



**FutureWater**

Costerweg 1G  
6702 AA Wageningen  
The Netherlands

+31 (0)317 460050

[info@futurewater.nl](mailto:info@futurewater.nl)

[www.futurewater.nl](http://www.futurewater.nl)

# Preface

Green Water Credits create a market mechanism between upstream farmers and downstream water users. A proof-of-concept in the Tana basin, Kenya, confirmed the feasibility of the financial mechanism and showed that the implementation of Green Water Credits can significantly reduce the problems related to water scarcity in the basin, improve basin storage capacity, at the same time giving opportunities to the rural poor.

This study is part of the second phase of Green Water Credits (co-ordinated by ISRIC and supported by the International Fund for Agricultural Development (IFAD) and the Swiss Agency for Development and Cooperation (SDC)) focusing on operational design and aiming at a more detailed assessment of the Green Water Credits mechanisms. This report resumes the biophysical assessment prepared during this phase and quantifies the impact of Green Water Credits practices on the green and blue water and sediment fluxes in the basin. This leads to the identification of potential target areas that will be the baseline for the following studies on the socio-economic and institutional aspects for pilot operation.



## Summary

This biophysical assessment quantifies the impact of Green Water Credits practices on the green and blue water and sediment fluxes in the Upper Tana basin. The analysis leads to identification of potential target areas for GWC pilot operation on biophysical grounds. This required a distributed modeling approach (SWAT) accounting for the heterogeneities in the basin in terms of precipitation regime, topography, soil characteristics and land use. The developed tool quantifies the benefits of the management practices on erosion reduction and green and blue water flows in the basin.

The analysis revealed that basin-wide implementation of tied ridges leads to a reduction of sediment input into the Masinga reservoir of about a million tons. Mulching leads to a reduction of unbeneficial soil evaporation of more than 100 million cubic meters per year. The enhancement of groundwater recharge through the different practices will improve the usage of the natural storage capacity in the basin by about 20%. These benefits were quantified crop-specific as well as site-specific.

The distributed approach allowed assessing the spatial distribution of the extent to which each practice contributes to the different GWC objectives. The most effective practices were determined for each response unit (unique in topography, soil and land use) and the maximum reachable change was assessed. This gives detailed insight on the location of the optimum sites for pilot operation from a biophysical point of view.



# Table of contents

<b>1</b>	<b>Introduction</b>	<b>9</b>
<b>2</b>	<b>Baseline information</b>	<b>11</b>
2.1	Basin delineation	11
2.1.1	Data source	11
2.1.2	Methodology	12
2.1.3	Results	13
2.2	Climate	15
2.2.1	Climate conditions	15
2.2.2	Data needs	16
2.2.3	Data sources	17
2.2.4	Dataset evaluation	21
2.2.5	Conclusion	28
2.3	Land cover	29
2.3.1	Data sources	29
2.3.2	Dataset evaluation	29
2.3.3	Conclusion	32
2.4	Soils	33
2.4.1	Data sources	33
2.4.2	Conclusion	36
2.5	Streamflow	37
2.5.1	Data source	37
2.5.2	Dataset evaluation	37
2.5.3	Conclusion	38
2.6	Reservoirs	41
<b>3</b>	<b>Baseline model analysis</b>	<b>43</b>
3.1	Introduction	43
3.2	Model set up	44
3.2.1	Distributed model input	44
3.2.2	Hydrological response units	44
3.3	Calibration and model performance	45
3.4	Crop-based assessment	49
3.5	Temporal responses	51
3.6	Heterogeneity and spatial distribution	53
<b>4</b>	<b>Options for Green Water Credits</b>	<b>61</b>
4.1	Potential benefits	61
4.2	Proposed Green Water Credit management practices	61
4.2.1	Permanent vegetative contour strips	62
4.2.2	Mulching	62
4.2.3	Tied ridges	63
4.3	Technical background	63
4.3.1	Soil evaporation	63
4.3.2	Soil Erosion	64
4.3.3	Runoff Curve Number	66
4.4	Scenario definition	67
4.5	Scenario analysis	67
4.5.1	Key indicators	68
4.5.2	Crop-based evaluation	70



4.5.3	Spatial analysis	72
4.6	Results	75
4.6.1	Most effective practices	75
4.6.2	Potential target area identification	76
4.7	Conclusions	78
<b>5</b>	<b>References</b>	<b>80</b>



## Tables

Table 1: Characteristics of locally obtained meteorological stations.....	18
Table 2: Characteristics of meteorological stations.....	20
Table 3: Characteristics of different meteorological data sources.....	22
Table 4: Missing values in the estimated (FEWS) and observed datasets.....	22
Table 5: Average soil moisture characteristics of dominant soils in the Upper Tana catchment	34
Table 6. Availability of flow data from stream gauges.....	38
Table 7. Availability of reservoir related variables.....	38
Table 8. Reservoir characteristics.....	41
Table 9. Parameters used for sensitivity analysis.....	46
Table 10. Boundary values and calibrated value of multiplier used for calibration.....	46
Table 11. Performance coefficients for the calibration points.....	48
Table 12. P factor for different management practices, as was studied in the United States (Wischmeier and Smith, 1978).....	65
Table 13. P factor for different management practices, as was studied for West Africa (Roose, 1977).....	65
Table 14. Runoff curve numbers according to different types of land covers (USDA-SCS, 1972) .....	66
Table 15. Parameter changes for each of the scenarios.....	67
Table 16. Values of the key indicators for the baseline situation and the 3 scenarios.....	68
Table 17. Absolute and relative changes (green = increase, red = reduction) of the key indicators for the 3 scenarios compared to the baseline situation.....	69

## Figures

Figure 1: Green Water Credits bridging the gap in the water cycle.....	9
Figure 2: The SRTM Digital Elevation Model at 250 m resolution.....	11
Figure 3: Subbasin delineation with a threshold area of 15.000 ha.....	12
Figure 4: Contour lines (500 m) used for the subdivision of the upstream subbasins.....	13
Figure 5: The derived stream network.....	14
Figure 6: The delineated subbasins using the modified delineation methodology.....	14
Figure 7: Frequency distribution of the difference in elevation within each subbasin, without and with refinement using contour lines.....	15
Figure 8: Agro-climatic zones of the Upper and Middle Tana Basin.....	16
Figure 9: Agro-ecological zones of the Upper and Middle Tana basin.....	16
Figure 10: Isohyetal map of the Rainfall distribution in the Upper Tana River Basin (Source: MWD 1992).....	17
Figure 11: Location of the stations with locally obtained data.....	18
Figure 12: Availability of stations in the Weather Underground archive.....	19
Figure 13: Location of the active meteorological weather stations.....	20
Figure 14: Rainfall estimate obtained from the FEWS network (24/11/2000).....	21
Figure 15: Daily rainfall during March 2001 of the EMBU station according to the observations (GSOD) and the estimates (FEWS).....	23
Figure 16: Scatterplots of observations (GSOD) and the estimates (FEWS) of the Nyeri station (left) and the Embu station (right).....	24
Figure 17: Scatter plot of observed and estimated monthly accumulated rainfall.....	25



Figure 18: Comparison of monthly averages measured at the 3 weather stations with the accumulated FEWS estimates. ....	25
Figure 19: Residual (estimate - observed) mean per month of the 3 stations .....	26
Figure 20: Monthly total of April 2002 from the FEWS rainfall estimations.....	27
Figure 21: Observed (GSOD) and estimated (FEWS) yearly total rainfall amounts of the Meru station .....	27
Figure 22: Total rainfall of 2002 in mm, accumulated with the FEWS rainfall estimations .....	28
Figure 23: Evaluation of different mapped cultivated areas of the Africover dataset with recent satellite imagery (source: Google Earth).....	30
Figure 24: Detail of mapped agricultural areas according to the Africover dataset (in green) with recent satellite imagery (source: Google Earth).....	31
Figure 25: Detail of recent remote sensing imagery, classified in the Africover dataset as “open trees with closed to open shrubs” (source: Google Earth).....	31
Figure 26: Units classified as irrigated area, (Africover – yellow; Globcover – red) around the Masinga Dam .....	32
Figure 27: Landcover map as used in the SWAT model, main source: Africover dataset, corrected by comparison with recent satellite imagery .....	33
Figure 28: Dominant soil types of the Upper Tana catchment (KenSOTER-version 2).....	34
Figure 29: Available Water Capacity of dominant soils of the Upper and Middle Tana catchment (KenSOTER-version 2) .....	35
Figure 30: Rootable depth of dominant soils of the Upper and Middle Tana catchment (KenSOTER-version 2) .....	35
Figure 31. Location of gauging stations for which data have been obtained.....	37
Figure 32. Comparison between similar data from two sources at Garissa. GAR originates from Global Runoff Discharge Data and 4G01 from University of Nairobi.....	39
Figure 33. Comparison between similar data from two sources at Grand Falls. GRF originates from Global Runoff Discharge Data and 4F13 from University of Nairobi. ....	40
Figure 34. Outflow from main reservoirs in Tana .....	41
Figure 35: The 5 main reservoirs included in the basin delimitation .....	42
Figure 36: Total yearly basin rainfall (FEWS precipitation estimates) .....	43
Figure 37. Total precipitation for 2005 (left) and 2006 (right).....	44
Figure 38. The defined hydrological response units (HRUs). ....	45
Figure 39: Location of the calibration points in the basin.....	47
Figure 40: Simulated and observed inflow of the Masinga Reservoir.....	48
Figure 41: Simulated and observed inflow of the gauge 4DD01 (Thiba river, Kamburu Reservoir).....	49
Figure 42: Evapotranspiration split in crop transpiration (T) and soil evaporation (E) per crop for the dry year (2005) and the wet year (2006) (for meaning of codes, see Figure 27). ....	50
Figure 43: Percentage of total evapotranspiration used for crop transpiration for the dry year (2005) and the wet year (2006). ....	50
Figure 44: Water entering the streams by surface runoff and drainage (Blue Water) for the dry year (2005) and the wet year (2006). ....	51
Figure 45: Total actual sediment loss per crop for the dry year (2005) and the wet year (2006). ....	51
Figure 46: Total basin precipitation and Blue Water, being the sum of surface runoff and groundwater discharge.....	52
Figure 47: Main components of water balance of 2005 (dry) and 2006 (wet) .....	53
Figure 48. Actual evapotranspiration for 2005 (dry) and 2006 (wet) in mm.....	54
Figure 49. Actual transpiration for 2005 (dry) and 2006 (wet) in mm.....	55
Figure 50. Actual soil evaporation for 2005 (dry) and 2006 (wet) in mm. ....	56



Figure 51. Percentage of total actual evapotranspiration used for Green Water for 2005 (dry) and 2006 (wet).....	57
Figure 52. Blue Water (water entering the streams by surface runoff and baseflow) for 2005 (dry) and 2006 (wet) in mm. ....	58
Figure 53. Deep groundwater recharge for 2005 (dry) and 2006 (wet) in mm. ....	59
Figure 54. Erosion for a dry year (2005, top) and a wet year (2006, bottom) in ton/ha/yr .....	60
Figure 55. Example of permanent vegetative contour strips (source: NRCS) .....	62
Figure 56. Example of tree loppings used as a mulch in the Quesungual system (Honduras) to reduce the loss of rainwater through runoff and evaporation (source: FAO).....	62
Figure 57. Example of graded contour ridges with cross ties lower than the main ridges to retain water between the cross ties, but allow excess rainwater to flow between the ridges rather than spill over or break the main ridges (source: FAO).....	63
Figure 58: Impact of soil evaporation compensation factor ESCO on depth of evaporation extraction.....	64
Figure 59: Relative changes of some of the key indicators for the 3 scenarios compared to the baseline situation (2005, dry) .....	70
Figure 60: 'Business as usual' water balance of the 3 major cultivated crops for the two reference years.....	71
Figure 61: Changes of the crop water balances for the 'vegetative contour strips' scenario compared to the baseline scenario .....	71
Figure 62: Changes of the crop water balances for the 'mulching' scenario compared to the baseline scenario .....	72
Figure 63: Changes of the crop water balances for the 'tied ridges' scenario compared to the baseline scenario .....	72
Figure 64: Spatial distribution of relative erosion reduction for the contour strips (left) and tied ridges (right) scenarios for the wet year.....	73
Figure 65: Spatial distribution of relative reduction of soil evaporation for the mulching scenario for a dry year (left) and a wet year (right).....	74
Figure 66: Spatial distribution of relative increase in groundwater recharge (left) and reduction of runoff (right) for the contour strips scenario for a wet year. ....	74
Figure 67: Spatial distribution of most effective practices with a positive impact on transpiration (left) and groundwater recharge (right) for a dry year (2005).....	75
Figure 68: Spatial distribution of most effective practices reducing erosion for a dry year (left) and a wet year (right). ....	76
Figure 69: Spatial distribution of relative changes of four selected parameters for target area identification: erosion reduction (a), groundwater recharge (b), transpiration (c) and evaporation (d). ....	77
Figure 70: Spatial distribution of potential target areas.....	78





# 1 Introduction

Green Water Credits (GWC) is a mechanism for payments to land users in return for specified soil and water management activities that determine the supply of fresh water at source and reduction of soil erosion from rainfed fields. These activities are presently unrecognized and unrewarded. Direct payment will enable better management and therefore less damaging runoff, more beneficial infiltration, more groundwater recharge and more stream base flow, particularly in the dry season. At the same time, GWC will provide a reliable, predictable diversification of rural incomes, enabling communities to adapt to economic, social and environmental change through asset-building in the shape of stable soils, more reliable local water supply, improved crops and infrastructure.

GWC focus is on a market failure in water supply: farmers and pastoralists manage all fresh water and land at source but their land and water management activities are unrecognized and unrewarded. Green Water Credits rectifies the market failure by supporting upstream water producers in return for specified water management services that determine supplies to consumers downstream (Figure 1).

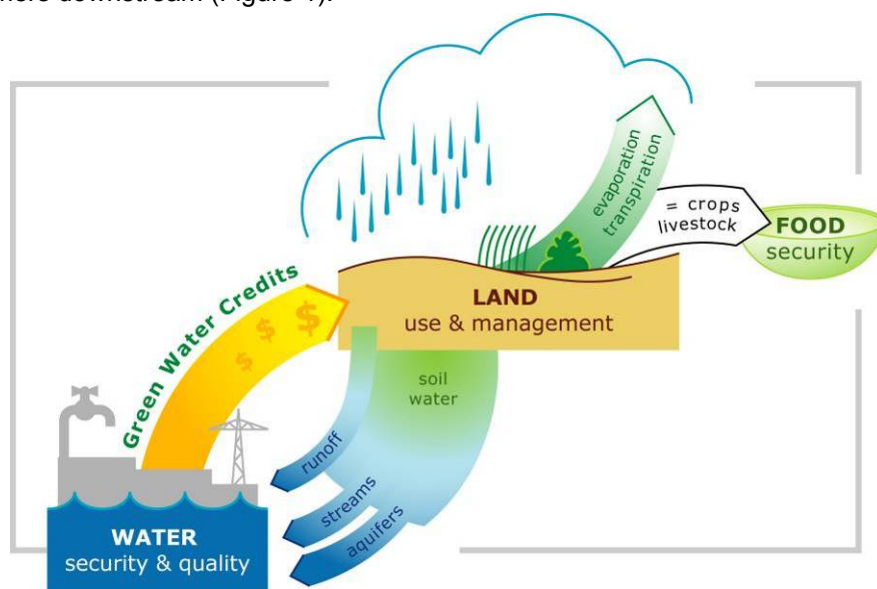


**Figure 1: Green Water Credits bridging the gap in the water cycle**

GWC is implemented in the following program components:

- Phase I, *Proof of Concept*: Completed for the Upper Tana basin in 2007
- Phase II, *Pilot Operation*: Operational design, management information system, capacity building, and communications strategy by the end of 2011. Fund-raising for Phase III is included in Phase II.
- Phase III, *Implementation*: 2011 onwards
- Phase IV, *Regional and global up-scaling*

In Kenya, proof-of-concept studies during Phase I showed that the implementation of Green Water Credits can significantly reduce the problems related to the growing demands for hydro-power generation, municipal water utilities, and irrigators. Different green water management options were analyzed and showed that considerable improvements could be obtained in terms of water security for both upstream as downstream stakeholders.



Based on the proof-of-concept phase it was concluded that regarding the biophysical analysis the following refinements are required during Phase II:

- A smaller focus area from Upper and Middle Tana to Upper Tana only.
- A higher spatial detail so that smaller areas could be assessed.
- Focus on more recent years.
- Improved accuracy and higher spatial (from 25 km to 1 km) and temporal (from month to day) resolution of rainfall data.
- Applying more recent streamflow validation data.
- Extensive emphasis on knowledge transfer.
- Using a more user-friendly modeling interface.

This report describes the development and results of this improved biophysical analysis, including all these bullet points.



## 2 Baseline information

For the pilot operational design of the Green Water Credits concept it is crucial to fully understand and quantify the up- and downstream interactions in terms of water flows and sediment transport. Consequently good data on the interfering variables of the current situation are needed and have to be analyzed with the appropriate tool. During the Proof of Concept phase different tools were assessed and the Soil and Water Assessment Tool (SWAT) resulted to be the most useful tool for this biophysical analysis, given the importance of studying the influence of land use on the water dynamics in the basin.

This chapter reviews the available datasets necessary for the building of a distributed hydrological model applied to the Upper Tana basin, using the Soil and Water Assessment Tool. Different datasets are compared and evaluated in order to make an appropriate dataset selection and obtain maximum accuracy in the quantification of the interactions relevant for the scope of Green Water Credits mechanism.

### 2.1 Basin delineation

#### 2.1.1 Data source

Digital Elevation data are obtained from the Shuttle Radar Data Topography Mission (SRTM) of the NASA's Space Shuttle Endeavour flight on 11-22 February 2000. SRTM data were processed from raw radar echoes into digital elevation models at the Jet Propulsion Laboratory (JPL) in California.

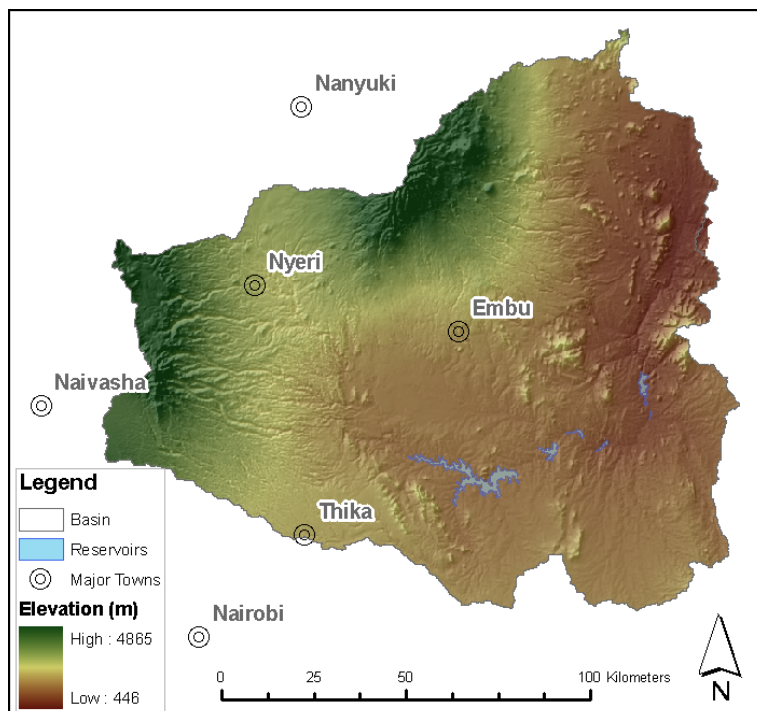


**Figure 2: The SRTM Digital Elevation Model at 250 m resolution**

SRTM data at 3 arc-second (90 meters) is currently available for global coverage between 60 degrees North and 56 degrees South latitude. The product consists of seamless raster data and



is available in geographic coordinates (latitude/longitude) and is horizontally and vertically referenced to the EGM96 Geoid (NASA 1998).

The SRTM-DEM data have been obtained using the USGS Seamless Data Distribution System (USGS 2004).

### 2.1.2 Methodology

The original SRTM-DEM data are provided at a resolution of 90 m. However, the basin size and the numerical limitations of SWAT required this dataset to be resampled to a spatial resolution of 250 m (Figure 6). The basin outlet was defined at the location of the to-be-built Low Grand Falls dam. Consequently, all the tributaries of the Aberdares mountain range and of Mount Kenya belonging to the basin are included in the analysis.

The DEM forms the base to delineate the catchment boundary, stream network and create sub basins. This is performed by the pre-processing module of SWAT and requires a so-called threshold area. This refers to a critical source area defining the minimum drainage area required to form the origin of a stream. The determination of an appropriate threshold area has to be in accordance with the desired level of detail.

An appropriate threshold area of 2,000 ha was found to provide a good balance between the level of detail and the computational constraints in the lower part of the basin. However, applying this threshold area resulted in very prolonged subbasins in the higher regions of the Aberdares and Mount Kenya (Figure 3). This implies a large difference between the minimum and maximum elevation within the subbasin, reaching differences of around 3000 meters within one single subbasin.

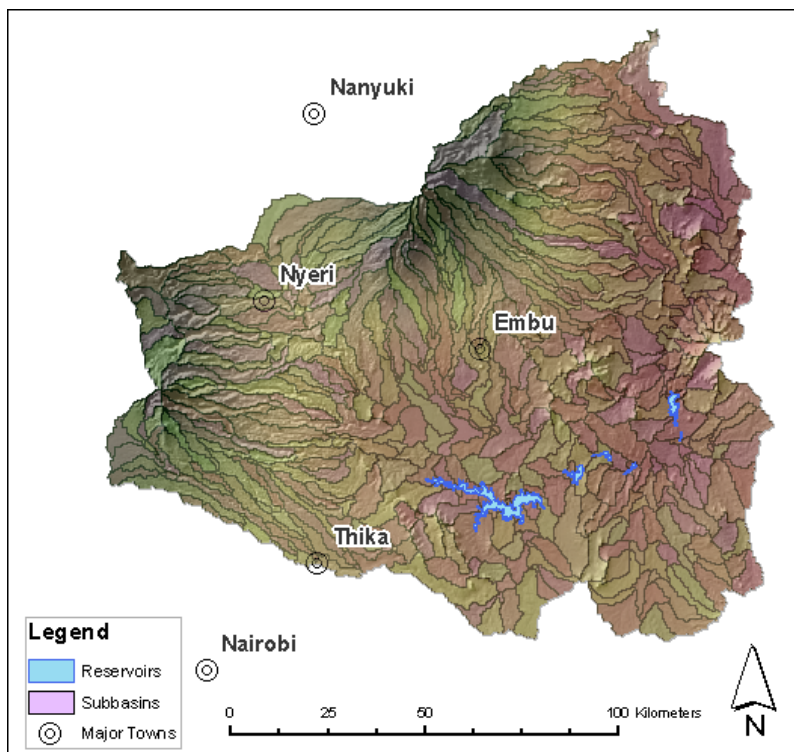
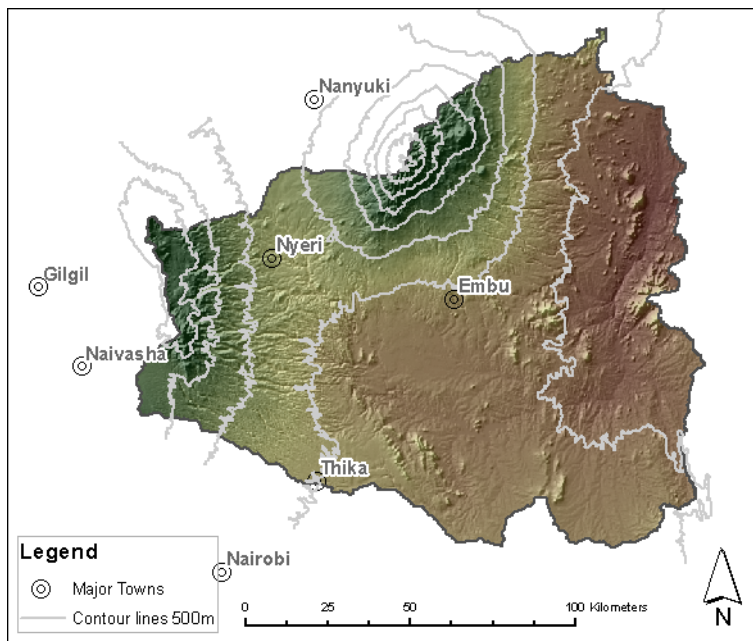


Figure 3: Subbasin delineation with a threshold area of 15.000 ha



Considering the importance of the orographic precipitation regime in the basin, it was necessary to implement a second delineation step for the higher mountain catchments. This will allow a correct implementation of the heterogeneous rainfall distribution in SWAT. This second delineation step divides the prolonged subbasins using elevation intervals of 500 meters. The SRTM dataset was used to extract the contour lines with this interval (Figure 4).

The process of subdividing the higher mountain subbasins was performed by adding watershed nodes in the prolonged original watersheds, using the contour lines as a reference. These nodes further subdivide and delineate the prolonged subbasins of the higher mountain areas. In spite of this procedure, a few prolonged subbasins with a large elevation range persisted. For this reason it was necessary to make a few manual additional subdivisions to obtain a correct and consistent subbasin distribution.



**Figure 4: Contour lines (500 m) used for the subdivision of the upstream subbasins**

### 2.1.3 Results

With the proposed modified delineation methodology the stream network (Figure 5) and subbasins were defined. This resulted in a subbasin distribution with a slightly denser distribution in the higher mountain areas (Figure 6) which will allow a correct simulation of the orographic precipitation regime. The result of the analysis showed that the total basin area is 17,420 km<sup>2</sup> and a total of 564 subbasins were delineated.

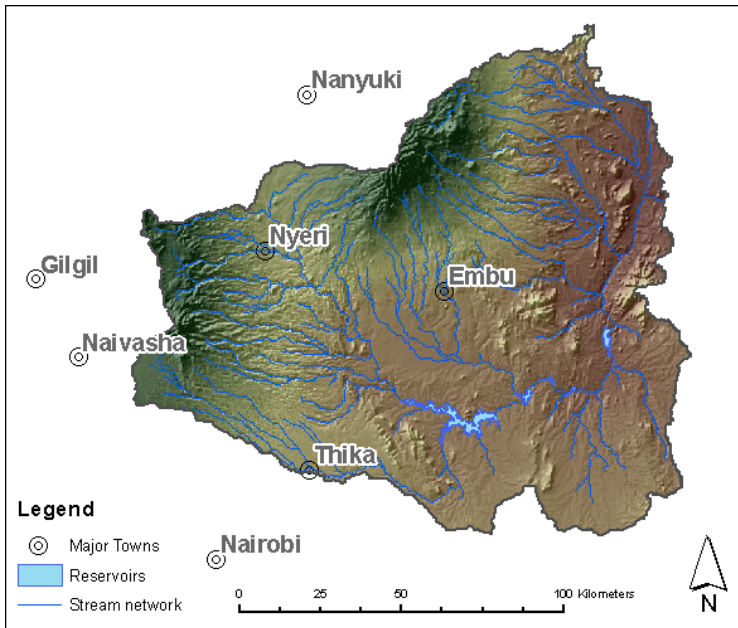


**Figure 5: The derived stream network**

The adjusted frequency distribution of the elevation range now shows that most of the subbasins have an elevation range of less than 500 meters (Figure 7) as this was the interval used to make the subdivisions using the contour lines. Within this elevation interval it is reasonable to assume that there are no important changes in the precipitation regime. Most of the subbasins with a large elevation difference were subdivided by this method, although still a few subbasins cover an elevation difference of around 1000 meters. These subbasins, however, correspond to the lower lying subbasins that contain irregularities in terrain morphology of which can be assumed that they are too small to alter the precipitation regime locally.

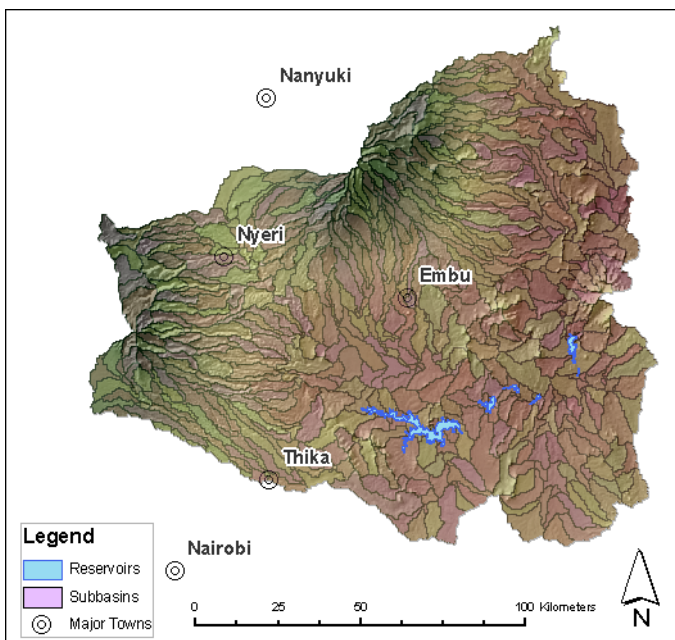


**Figure 6: The delineated subbasins using the modified delineation methodology**



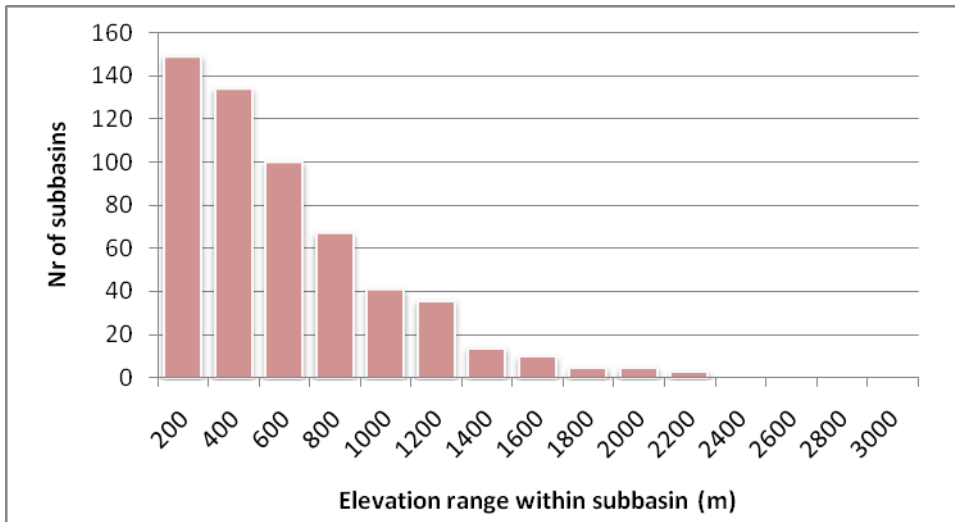


**Figure 7: Frequency distribution of the difference in elevation within each subbasin, without and with refinement using contour lines.**

## 2.2 Climate

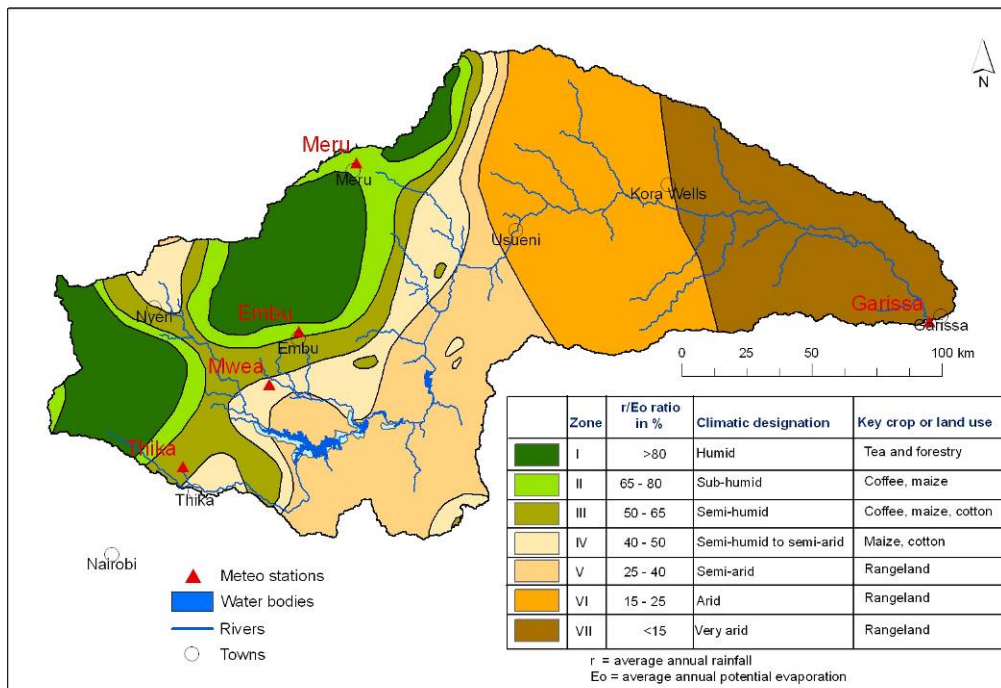
### 2.2.1 Climate conditions

The upper Tana basin has two wet seasons and two dry seasons as a result of the monsoon. From mid-March to June the heavy rain season, known as the *long rains*, brings approximately half of the annual rainfall in the basin. This is followed by the wetter of the two dry seasons which lasts until September. October to December bring the so-called *short rains* when the mountain receives approximately a third of its rainfall total. Finally the time between December to mid-March is the driest period of the precipitation regime.

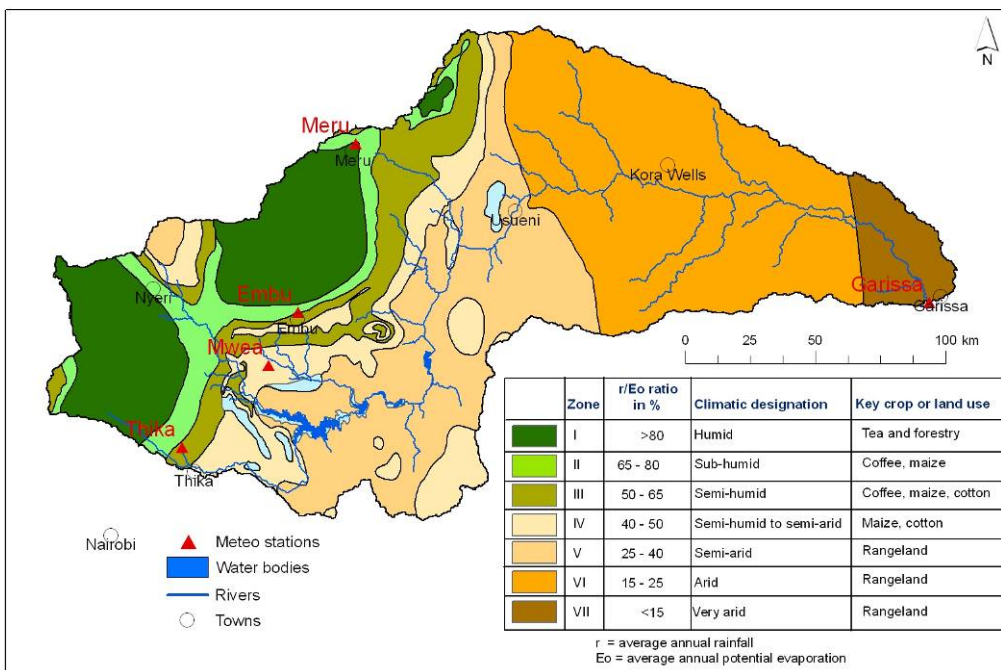
Figure 8 shows the main agro-climatic zones which are based on the balance between precipitation and evapotranspiration (Sombroek *et al.* 1982). The Upper and Middle Tana basin (outlet at Garissa) encompasses seven main climatic zones ranging from humid to very arid. Comparing this distribution with the contour lines of Figure 4 it becomes clear that there is a close correlation between elevation and climatic zones; in other words, the rainfall regime follows the elevation gradient.

Figure 9 presents the agro-ecological zones according to the Farm Management Handbook of Kenya (Jaetzold and Schmidt 1983). This map shows more detail than Figure 8, although the number and the boundaries of the main zones are very similar. This map characterizes the AEZ according to the main land use, e.g. humid tea zone, arid rangeland zone etc.





**Figure 8: Agro-climatic zones of the Upper and Middle Tana Basin**



**Figure 9: Agro-ecological zones of the Upper and Middle Tana basin**

### 2.2.2 Data needs

The SWAT model requires meteorological data to be available at a daily time step. The following variables are needed:

- accumulative daily rainfall
- minimum and maximum daily temperature





- solar radiation
- wind speed
- relative humidity

Several methods can be used to calculate the potential evapotranspiration. The most complete method available, which is the Penman-Monteith method, requires data on temperature, solar radiation, wind and humidity for the calculation of the spatially distributed potential evapotranspiration rates.

This watershed has a particular strong orography, which causes strong meteorological gradients within the basin. Mount Kenya and the Aberdares mountain range cause a strong orographic precipitation regime. This can be observed in Figure 10 showing the isohyets in the study area. Rainfall amounts in the upper mountains are about 2 times the amounts in the lower parts. This fact requires an appropriate distributed approach for the rainfall input in the hydrological model and this was taken into account during the delineation of the subbasins (as explained in paragraph 2.1.3).

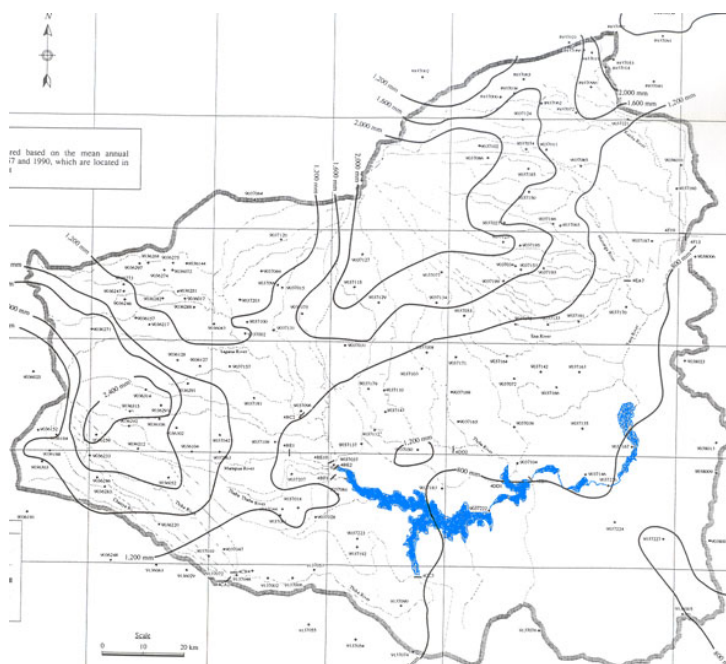


**Figure 10: Isohyetal map of the Rainfall distribution in the Upper Tana River Basin (Source: MWD 1992)**

### 2.2.3 Data sources

#### 2.2.3.1 Documents

An extensive inventory of historical data can be found in the Study on the National Water Master Plan (MWD, 1992). The accompanying databook contains data statistics and metadata on the meteorological and discharge information available until approximately 1985. Also some measurements are included on the suspended loads analyzed from samples taken around the year 1980.



The information on meteorological data concerns monthly statistics averaged over the full available data period. In some cases the time span of the dataset is very short, around 5 years. Also the discharge data given in this report are monthly averages over the whole data period.

### 2.2.3.2 Locally obtained station data

For the Proof of Concept phase of Green Water Credits local data were obtained of various meteorological stations in the basin. All the data have a monthly time basis. The following table gives a summary of their characteristics and Figure 11 represents their spatial distribution in the basin:

**Table 1: Characteristics of locally obtained meteorological stations**

Name	Elevation (m)	Start (year)	End (year)	Variables*
Chogoria forest station	1388	1960	2003	P
Embu	1494	1977	2005	T, MMSH
Karatina agricultural office	1784	1960	2003	P
Karatina hombe forest station	2159	1960	2003	P
Kerugoya castle forest station	2066	1960	2003	P
Kerugoya district water office	1598	1960	2003	P
Kitiri chief's camp, Embu	1157	1960	2003	P
Meru forest station	1604	1960	2003	P
Mwea irrigation agrometeorology station	1172	1960	2003	P
Mwea irrigation scheme (Tebera)	1234	1960	2003	P
Njukiini forest station, Embu	1388	1960	2003	P
Nyeri met station	1780	1978	2005	P, T, MMSH
Sagana fish culture farm	1234	1960	2003	P
Sagana state lodge	1850	1969	2003	P
Thika meteorological station	1480	1981	2005	T, MMSH

\* P=precipitation, T=minimum and maximum temperature, MMSH=Mean Monthly Sunshine Hours

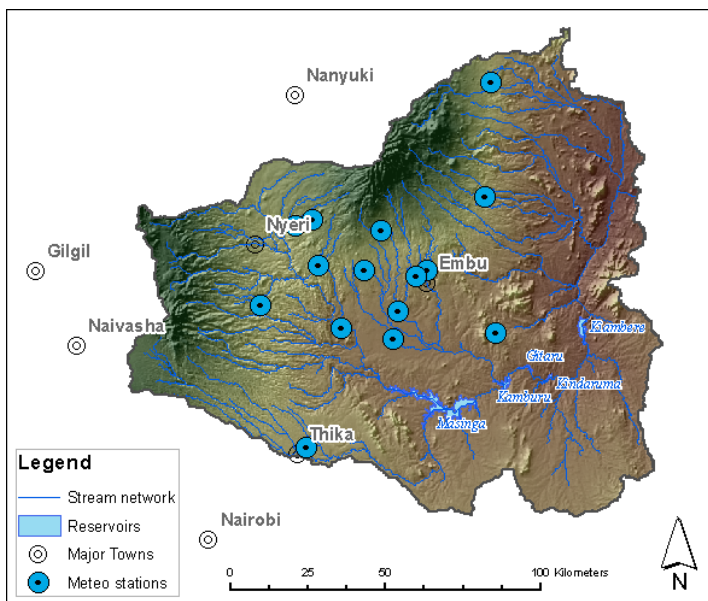


**Figure 11: Location of the stations with locally obtained data**



### 2.2.3.3 The Weather Underground database

The Weather Underground archive ([www.wunderground.com](http://www.wunderground.com)) has an extensive amount of data available for downloading of stations from all over the world. However, within the study basin only 1 station can be found, which is the station Meru, shown in the northeastern part of Figure 12. Besides, the stations present in Nairobi (south) and the station Nakuru (northwest) are relatively close to the basin.

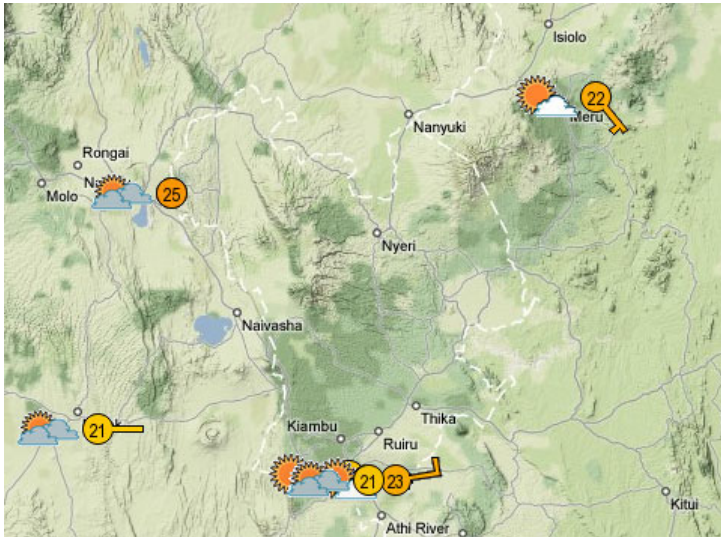


**Figure 12: Availability of stations in the Weather Underground archive**

### 2.2.3.4 The GSOD database

Meteorological data from weather stations all over the world can be found at the public domain Global Summary of the Day (GSOD) database archived by the National Climatic Data Center (NCDC). This database offers a substantial number of stations with long-term daily time series. The GSOD database submits all series (regardless of origin) to extensive automated quality control. Therefore, it can be considered a uniform and validated database where errors have been eliminated.

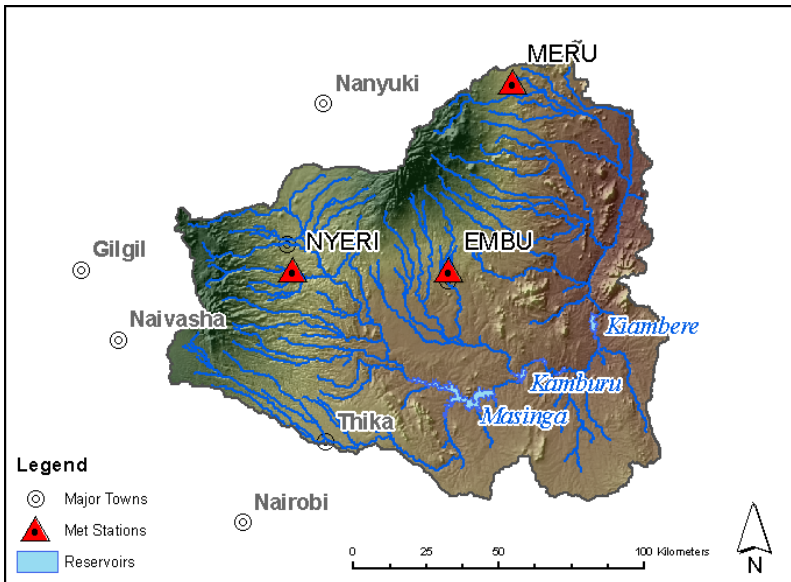


**Figure 13: Location of the active meteorological weather stations**

In the study basin there are three active stations of which the data can be downloaded (Figure 13). A shortcoming of these three weather stations is that their location is more or less in the same climatic zone. Table 2 shows the elevation of the stations, ranging from 1493 until 1759 m.a.s.l (Table 2). No active or inactive weather stations can be found in the lower semi-arid areas or in the humid high mountain areas.

**Table 2: Characteristics of meteorological stations**

Station name	Latitude	Longitude	Elevation	Data
MERU	0.08	37.65	1554	1914 - 2009
NYERI	-0.50	36.97	1759	1920 - 2009
EMBU	-0.50	37.45	1493	1908 - 2009

#### 2.2.3.5 The CRU dataset

The Climate Research Unit (CRU) data set of the University of East Anglia gathered the CRU TS 2.0 data-set that comprises 1200 monthly grids of observed climate, for the period 1901-2000, and covering the global land surface at 0.5 degree resolution. There are five climatic variables available: cloud cover, DTR, precipitation, temperature and vapour pressure.

The observed grids are based exclusively on meteorological measurements from individual stations and no remote sensing information was included. Coverage of the stations used for the interpolation of the grids was sparse on the African continent. Therefore, it was assumed that if there is no adjacent station information available the best estimate of a certain point in the grid is the long-term average value. The interpolation method used to create the continuous grids is called 'relaxation to the climatology'.

The fact that the interpolated grids are only based on scarce station information on the African continent makes this dataset less reliable for hydrological modeling of an area with large climatic differences as the Tana basin.



### 2.2.3.6 The FEWS network

One day estimates of precipitation for the African continent are prepared operationally at the Climate Prediction Center (CPC) for the United States Agency for International Development (USAID) as a part of the Famine Early Warning System Network (FEWS NET). The algorithm for the rainfall estimates uses Meteosat 7 geostationary satellite infrared data that are acquired in 30-minute intervals, and areas depicting cloud top temperatures of less than 235K are used to estimate convective rainfall. Two other satellite rainfall estimation instruments are incorporated into the algorithm, being the Special Sensor Microwave/Imager (SSM/I) on board Defense Meteorological Satellite Program satellites, and the Advanced Microwave Sounding Unit (AMSU). All satellite data are first combined using a maximum likelihood estimation method, and then GTS station data are used to remove bias. Warm cloud precipitation estimates are not included in the algorithm.

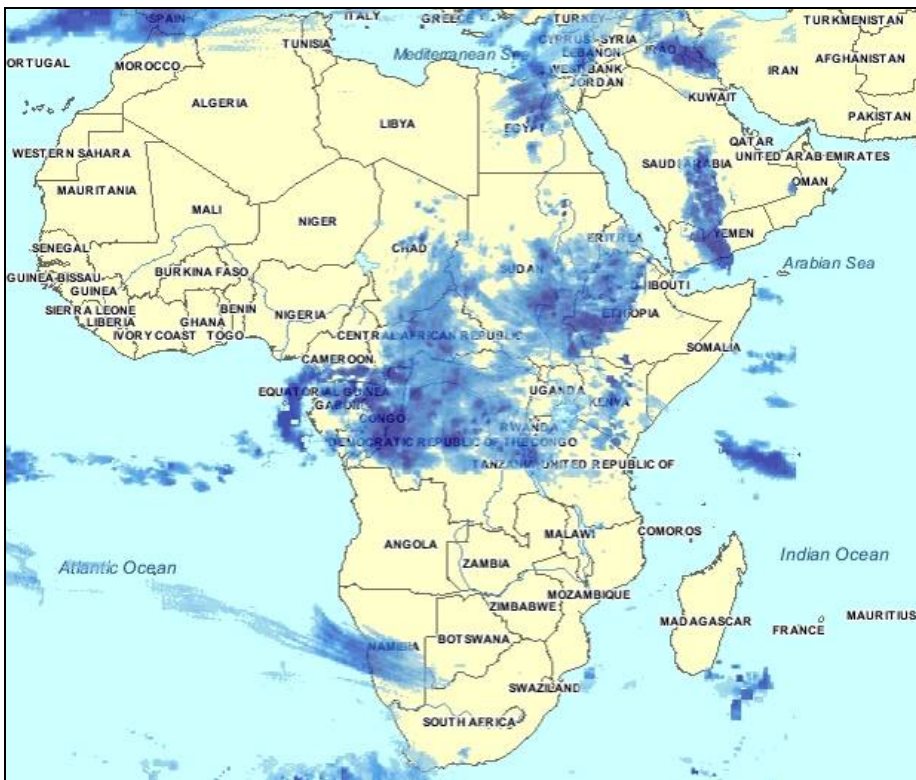


**Figure 14: Rainfall estimate obtained from the FEWS network (24/11/2000)**

CPC/FEWS Estimates are available from October 2000 until present with a spatial resolution of 0.1 degree. Figure 14 shows an example of the rainfall estimate covering whole Africa.

## 2.2.4 Dataset evaluation

### 2.2.4.1 Data Availability

The following Table 3 resumes the characteristics of the different available data sources. Especially the temporal and spatial resolution of the datasets are of importance for a consistent model implementation.



**Table 3: Characteristics of different meteorological data sources**

Name	Type	Format	Temporal resolution	Nr. stations* / Spatial resolution	Availability	Variables**
Presently available Local Data	Observed	Station	Monthly	8	1960 - 2003	P, Tmax, Tmin, MSHM
Weather Underground Archive	Observed	Station	Daily	1	- present	P, Tmax, Tmin, DEWPT, WNDVAV,
GSOD database	Observed	Station	Daily	3	- present	P, Tmax, Tmin, DEWPT, WNDVAV,
CRU interpolation grids	Interpolated with station data	Grid	Monthly	0.5°	- 2000	P, CC, DTR, T, VP
FEWS grid estimates	Estimated with RS	Grid	Daily	0.1°	2000 - present	P

\* The number of available stations present within the study basin

\*\* P=precipitation, Tmax=maximum temperature, Tmin= minimum temperature, T= temperature, MSHM=mean sunshine hours month, DEWPT=Dew point, WNDVAV=Average wind speed, CC=Cloud cover, DTR=Diurnal temperature range, VP=Vapour pressure

As can be seen from the previous table, only the FEWS precipitation estimates and the GSOD database provide daily data. For this reason, the following dataset evaluation was exclusively based on these datasets.

#### 2.2.4.2 Missing values

An important issue to deal with is the number of missing values and the methodology to fill them. A few years in the dataset from the GSOD database contain a considerable number of missing values while the estimates of the FEWS network do have a more constant coverage. Besides, most of the missing values found in the FEWS dataset are during the dry month of July in 2006, which means that these missing values are of minor importance. Table 4 shows the missing values found in both datasets.

**Table 4: Missing values in the estimated (FEWS) and observed datasets**

Year	FEWS grids	Embu station	Meru station	Nyeri station
2001		56	7	47
2002		48	10	40
2003	1	85	4	87
2004	1	208	26	132
2005		140	40	80
2006	15	60	22	30
2007	1	49	25	16
2008		72	59	23
2009		24	4	10



### 2.2.4.3 Evaluation of daily data

To be able to compare both datasets, time series were extracted from the daily FEWS grids for the location of the 3 weather stations. Consequently, the time series of the observed values from the GSOD database were compared with the estimates of the FEWS network. It was observed that there is a 1 day time lag between both datasets, which means that apparently the timestamp of one of both datasets contains a small error. This was corrected for the comparative analysis.

Figure 15 shows the daily values during a wet month for the Embu station. It is clear that there is a high correspondence between both datasets. Also the scatterplots in Figure 16 confirm that there is a strong correlation as the majority of the points is located around the imaginary  $x = y$  line. Some strong rainfall events either measured or estimated are not represented in the other dataset. These differences can be explained by either

1. Outliers in the observed data due to errors in the measurements
2. Erroneous estimates due to scale and resolution issues

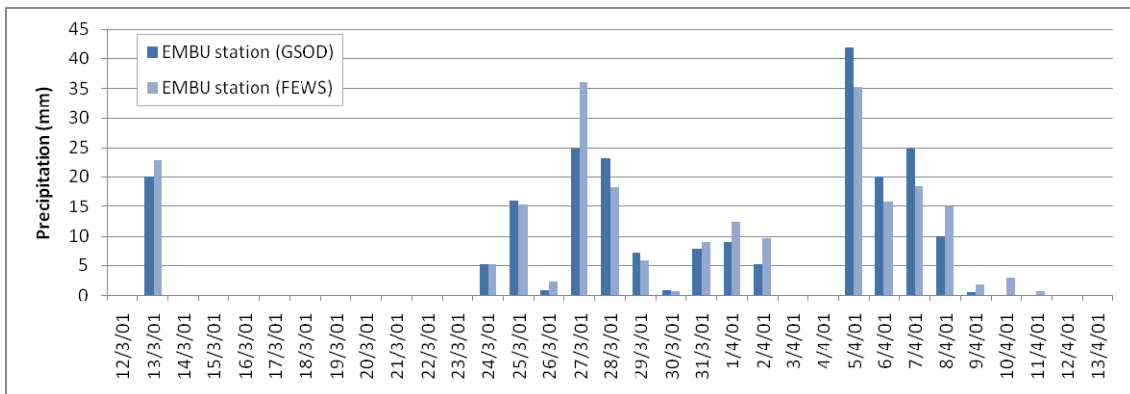


**Figure 15: Daily rainfall during March 2001 of the EMBU station according to the observations (GSOD) and the estimates (FEWS)**

The  $r^2$  correlation coefficient for the 3 stations ranges from 0.28 (Nyeri) until 0.47 (Meru). Especially in the Nyeri datasets discrepancies for the large rainfall events can be found. The correlation coefficient is strongly affected by these discrepancies and consequently the coefficient is relatively low for this station while in the scatterplot a very clear correlation can be observed (Figure 16), although the FEWS estimates slightly underestimate the actual values.

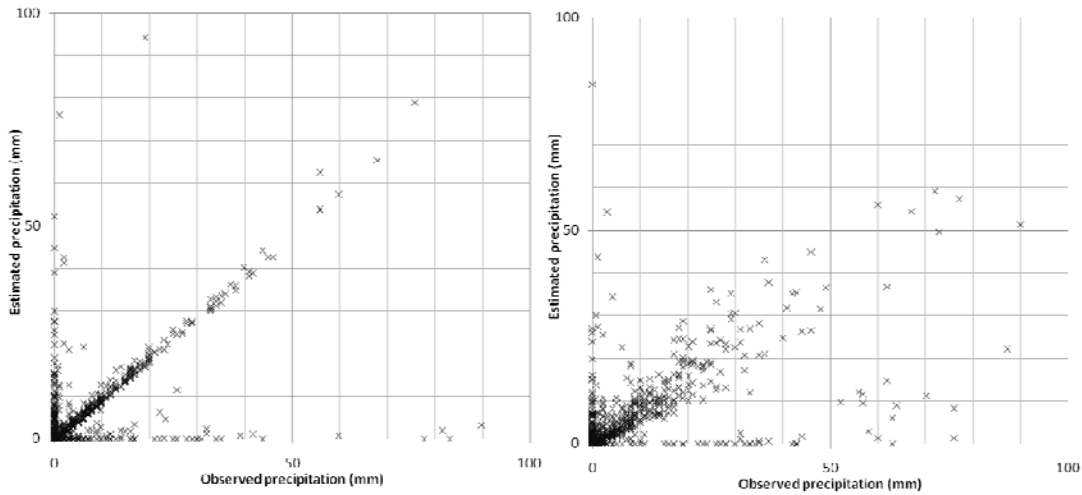


**Figure 16: Scatterplots of observations (GSOD) and the estimates (FEWS) of the Nyeri station (left) and the Embu station (right)**

The FEWS daily rainfall estimates are primarily based on observations of cloud top temperatures, which in turn are related to vertical motion and convection. Short rains due to convection and orographic precipitation might not always be detected by the FEWS algorithm. This type of rainfall occurs mostly in the wet season around the month April and the month November. The FEWS dataset showed that especially during these months discrepancies occur when heavy rainfall events are measured as shown in the GSOD dataset.

#### 2.2.4.4 Evaluation of monthly totals

The monthly accumulated totals were calculated using both datasets. In Figure 17 the observed and estimated monthly totals are shown in a scatterplot. It becomes clear that it depends on the weather station how well the FEWS estimates perform compared to the observations. On one hand, for the wet months the FEWS estimates seem to underestimate rainfall at Meru station. A slight overestimation is however observed for the dryer months at Embu. In general, the diagram shows a good correlation between both datasets as is confirmed by the fairly high  $r^2$  correlation coefficients. The general tendency is that the FEWS estimates underestimate the monthly rainfall amounts.





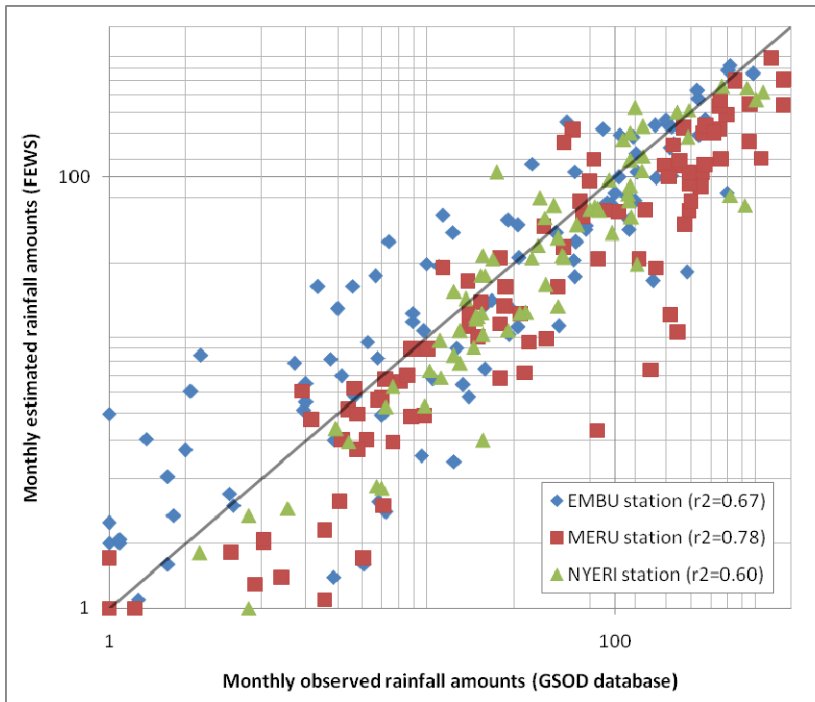


**Figure 17: Scatter plot of observed and estimated monthly accumulated rainfall**

Long-term monthly averages of the FEWS dataset were also compared to the long-term monthly averages from three stations. The long-term record of monthly totals for the three stations was obtained from the TanDaBa database that was set up during the proof of concept phase of Green Water Credits. It contains rainfall data from 1960 until 2005. The monthly averages of this time span were compared with the monthly averages from 2000 until 2009 from the FEWS dataset. Figure 18 compares the monthly average rainfall amounts measured at the stations, with the averages of the monthly accumulated FEWS estimates.

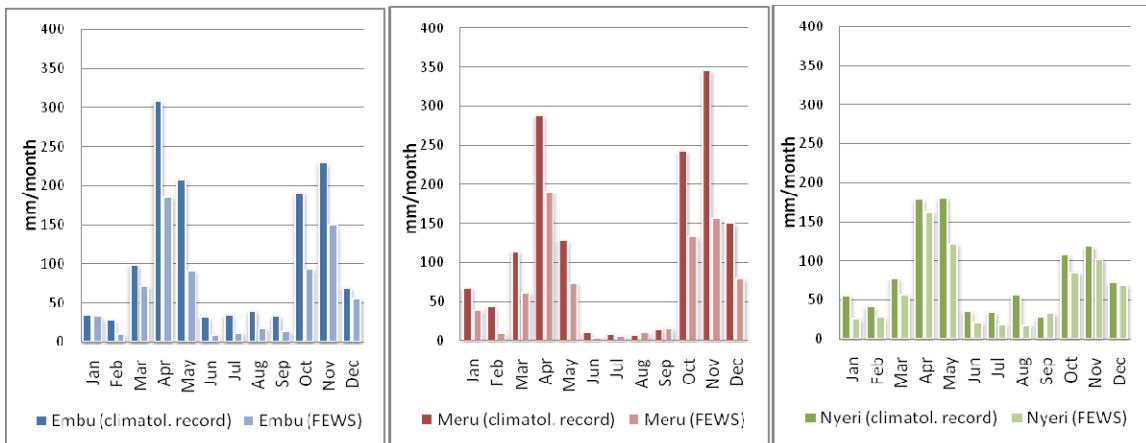


**Figure 18: Comparison of monthly averages measured at the 3 weather stations with the accumulated FEWS estimates.**

In general, both data sources show the same precipitation regime over the year, at each of the weather station locations. However, especially during the wet months the differences between the observed and estimated averages are clear. It confirms that the FEWS algorithm does not detect all the strong rainfall events and that for this reason the monthly averages are lower than



those from the climatological record. Also a careful look on the daily data shows that some local heavy rainfall events are not represented in the FEWS dataset.

This seasonal effect can also be observed by analyzing the residual mean defined as the average difference between the observed values from the weather stations and the estimated values of the FEWS grids. Figure 19 shows the residual mean for every month in the time series, to give insight in the difference between observation and estimate on a monthly basis. It can be observed that especially during the rainy months the differences are present. Moreover, the difference between both datasets is almost always negative, which means that on average the FEWS estimates have lower values as the observed GSOD dataset.

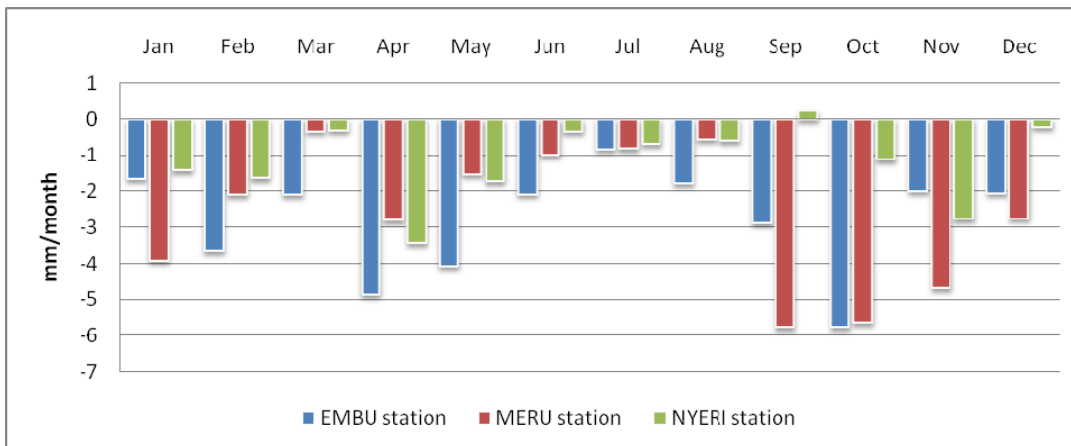


**Figure 19: Residual (estimate - observed) mean per month of the 3 stations**

Winds with an easterly component dominate the Kenyan tropics. The northeasterly monsoons are most prevalent from December to April while the southeasterly monsoon dominates from April to October (Gatebe et al. 1999). The monthly accumulated FEWS grids (Figure 20) show that the orographic precipitation caused by these winds is detected on the west side of Mount Kenya. Around the Aberdares mountain range this orographic effect is only lower as can be observed from the following figure.



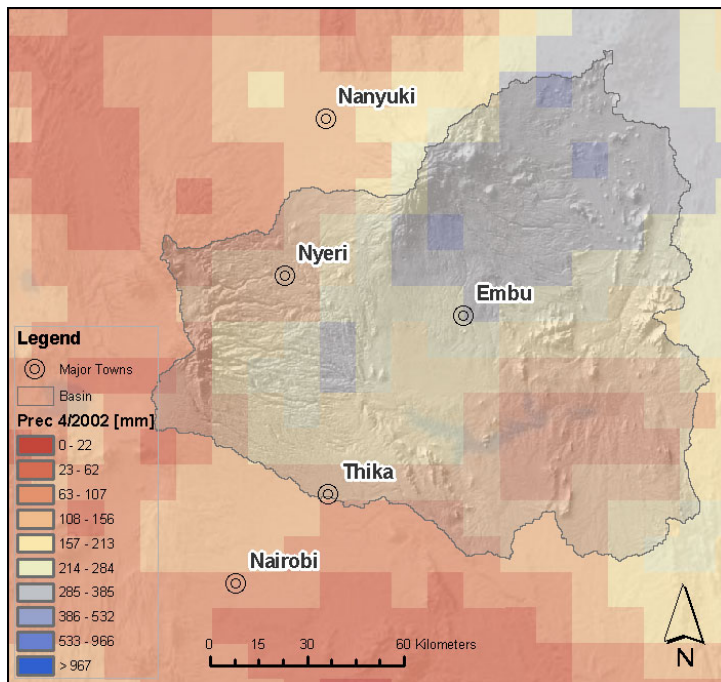


**Figure 20: Monthly total of April 2002 from the FEWS rainfall estimations**

#### 2.2.4.5 Evaluation of yearly totals

A comparison between FEWS and GSOD annual totals is made as well. The daily datasets were used to obtain the yearly accumulated total rainfall amounts for each of the three weather stations and for the corresponding pixels from the FEWS gridded estimates. The years that contained too many missing values were filtered out depending on whether the missing values were recorded during a wet or a dry period in the year. Figure 21 shows the results for both datasets for the years 2001, 2002 and 2006 – 2008.

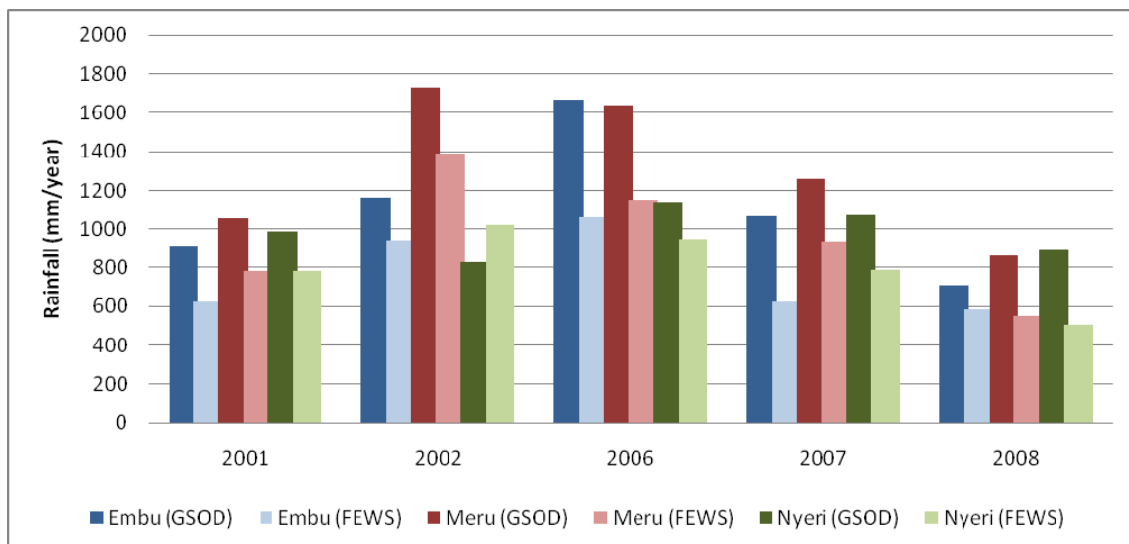


**Figure 21: Observed (GSOD) and estimated (FEWS) yearly total rainfall amounts of the Meru station**

As can be seen in the previous figure, in almost all cases the yearly totals of the FEWS estimates are below the ones recorded at the weather station. For this reason it was decided to apply a correction factor to the FEWS estimates in order to make the yearly totals in good



correspondence with the records at the weather stations. Accordingly, the daily rainfall amounts were incremented by 25% over the entire FEWS record.

Although the yearly accumulated totals show a significant bias between both datasets, it has to be noted that the FEWS grids detect correctly the annual spatial rainfall pattern. Figure 22 shows the accumulated grid for the year 2002. A gradient in rainfall amounts from the northeastern to the southwestern part of the basin can also be detected in the yearly totals in Figure 21 for this particular year.

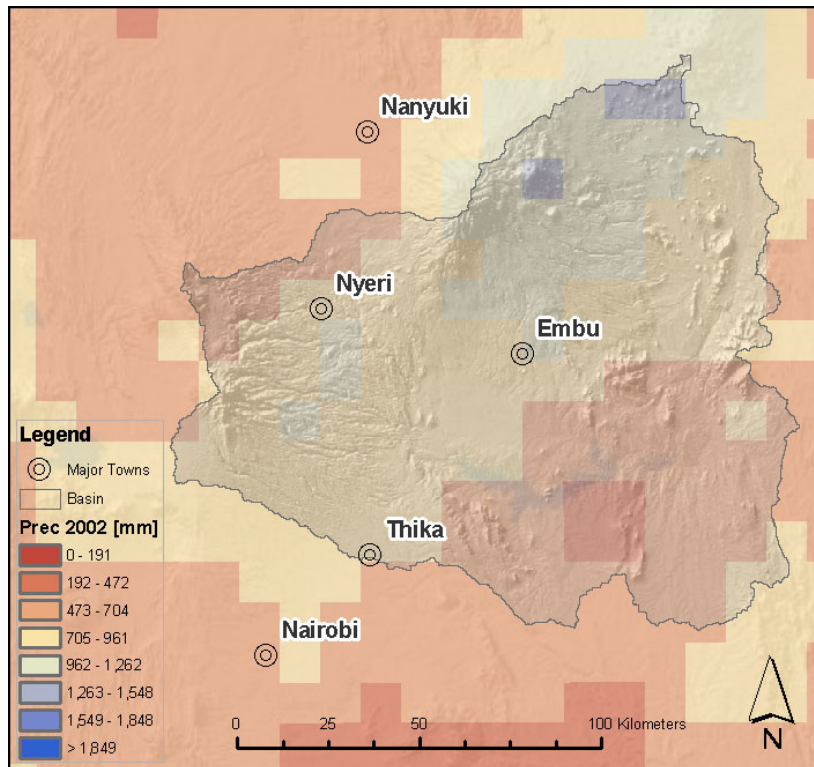


**Figure 22: Total rainfall of 2002 in mm, accumulated with the FEWS rainfall estimations**

### 2.2.5 Conclusion

The precipitation estimates from the FEWS dataset have two major advantages: firstly, they are available on a daily time basis, giving a continuous coverage in time. And secondly, the dataset gives information on the spatial patterns within the basin, with a fairly good resolution. The station data of the GSOD database contain quite a lot of missing values that would have to be filled using statistical methods.

The gauged spatial patterns are well reproduced by the FEWS dataset. The comparative analysis showed that a good correlation between the gauged and the satellite-derived product. This correlation implies that the FEWS dataset can be adjusted by a (seasonally invariant) factor. This assures a better correlation with the rainfall amounts. A similar conclusion was made comparing the FEWS dataset with gauged estimates by Asadullah et al. (2008). Also in this study, the FEWS dataset resulted to underestimate the gauged amounts by about 25%. For Green Water Credits, the dataset was adjusted by a factor 1.25, leading to an excellent correspondence with the gauged dataset.



The rest of the required data for the SWAT model as temperature, solar radiation, wind velocity and relative humidity were obtained from the stations from the GSOD database. The temperature lapse rate was set to  $-6^{\circ}\text{C}/\text{km}$ . These meteorological data are available on a daily time scale. Therefore, there is sufficient information to apply the Penman-Monteith method in the model to determine the potential evapotranspiration rates, leading to better estimates of this negative term of the basin water balance.

## **2.3 Land cover**

### *2.3.1 Data sources*

#### 2.3.1.1 The Africover dataset

The GWC Phase I studies used the best available maps, based on the FAO Africover project (FAO 2000) which designates land use/land cover for points on an approximately 2400 x 4800 m irregular grid. The effective scale is about 1: 250 000. The land cover has been produced from visual interpretation of digitally enhanced LANDSAT TM images (Bands 4,3,2) acquired mainly in the year 1999. The land cover classes have been developed using the FAO/UNEP international standard LCCS classification system.

#### 2.3.1.2 The Globcover dataset

GlobCover is an ESA initiative in partnership with JRC, EEA, FAO, UNEP, GOCF-GOLD and IGBP. The GlobCover project has developed a service capable of delivering global composite and land cover maps using as input observations from the 300m MERIS sensor on board the ENVISAT satellite mission. The GlobCover service has been demonstrated over a period of 19 months [December 2004 - June 2006], for which a set of MERIS Full Resolution (FR) composites (bi-monthly and annual) and a Global Land Cover map are being produced.

The GlobCover composites are derived from a set of processing made on the MERIS FR images such as cloud detection, atmospheric correction, geolocalisation and re-mapping. The GlobCover Land Cover map is compatible with the UN Land Cover Classification System (LCCS).

The use of medium resolution data brings a considerable improvement in comparison with other global land cover products at lower spatial resolution as for example the GLC2000 dataset. However, the quality of the Globcover product is highly dependent on the reference land cover database used for the labelling process and on the number of valid observations available as input. When the reference dataset is of higher spatial resolution with a high thematic detail, the Globcover product also shows a high accuracy. On the other hand, the number of valid observations is a restrictive factor. The spatial coverage of the MERIS data clearly determines the quality of the temporal mosaics and therefore, of the land cover map.

### *2.3.2 Dataset evaluation*

The Africover and Globcover dataset were produced using different methods and different sources of remote sensing information. A major difference is that the classification of the Africover dataset was based on visual interpretation of the satellite imagery, while the Globcover dataset used an automated classification approach using local reference datasets. In order to evaluate which of the two datasets is optimal for the hydrological model, both datasets were analyzed and compared with recent high resolution satellite imagery.



Agricultural areas are generally difficult to map using satellite information because of the high sub-pixel heterogeneity with different crop cycles. Also many areas have inter-annual variability with crop rotation and fallow grounds. Besides, in dry areas there is a high spectral similarity with grassland, which makes the classification even more complex.

The Africover dataset is known to have a reasonable correspondence with national and subnational agricultural statistics. However, the Globcover dataset was produced using more recent data than the Africover dataset. Thus, to assess the consistency of both datasets, it is important to verify accuracy of the mapped areas using recent remote sensing information.

Figure 23 shows a detail of an area with rice, maize and mixed irrigated areas, close to the Masinga Dam. As can be observed, the delimited features have not been altered significantly in the time between the Africover mapping (1999) and the more recent imagery (2005). Some rice fields seem to be out of use in the recent image, however, this seems to be a temporary state.

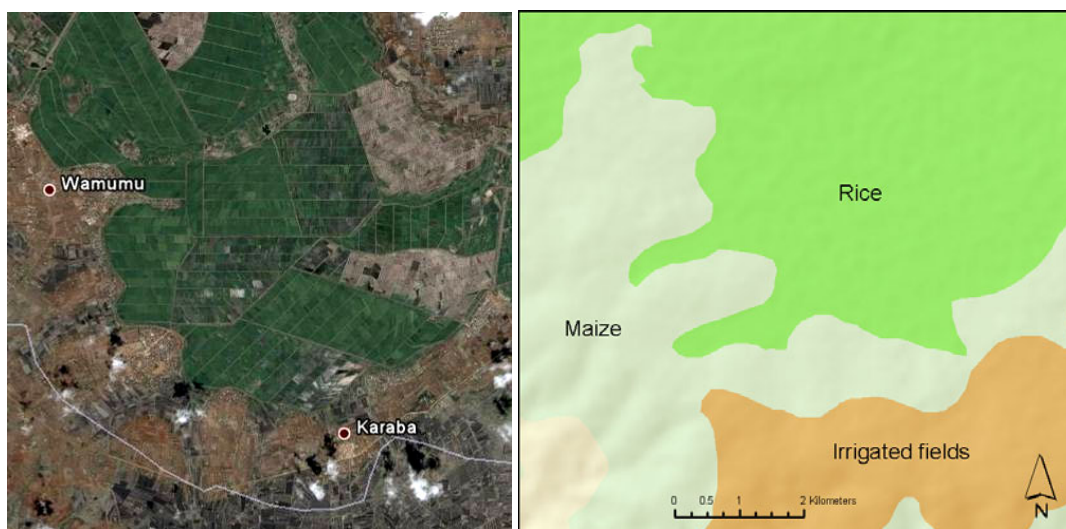


**Figure 23: Evaluation of different mapped cultivated areas of the Africover dataset with recent satellite imagery (source: Google Earth)**

On the other hand, Figure 24 shows the areas mapped as being cultivated north of the Masinga Dam. Here it is clear that the cultivated areas have been extended between the time of production of the Africover dataset (1999) and the satellite imagery (2005).





**Figure 24: Detail of mapped agricultural areas according to the Africover dataset (in green) with recent satellite imagery (source: Google Earth)**

Similar inconsistencies can be observed near the footslopes of Mount Kenya, however, in this case it seems more likely that these areas were misclassified. The Africover dataset shows large areas that have been classified as “Open trees with closed to open shrubs”. Satellite imagery of 2005/2006 shows that these areas are being cultivated almost completely (Figure 25). In this case, the Globcover dataset seems to be more consistent as it shows that part of these areas are occupied with agricultural activities.



**Figure 25: Detail of recent remote sensing imagery, classified in the Africover dataset as “open trees with closed to open shrubs” (source: Google Earth)**

However, in the Globcover dataset, the forest areas are continuously misclassified. Only a small part of the forested areas around Mount Kenya is correctly classified. A possible explanation is that the GLOBcover dataset is known to show thematic errors in rugged terrain due to mountain shadows.

It is also observed that the distinction between irrigated and flooded lands is very difficult in several regions, leading to an underestimation of cultivated areas. Especially when comparing the acreages of the irrigated areas, some considerable differences can be observed. Figure 26 shows the difference between both datasets around the Masinga Dam. The Globcover dataset only classified a few pixels as irrigated, while the Africover dataset shows far larger areas with this land use type.

Actually, a large part of the irrigated areas of the Africover dataset are not even classified as croplands according to the Globcover dataset. Recent satellite imagery confirms that the areas were correctly classified by the Africover dataset and that the Globcover dataset tends to underestimate this class.

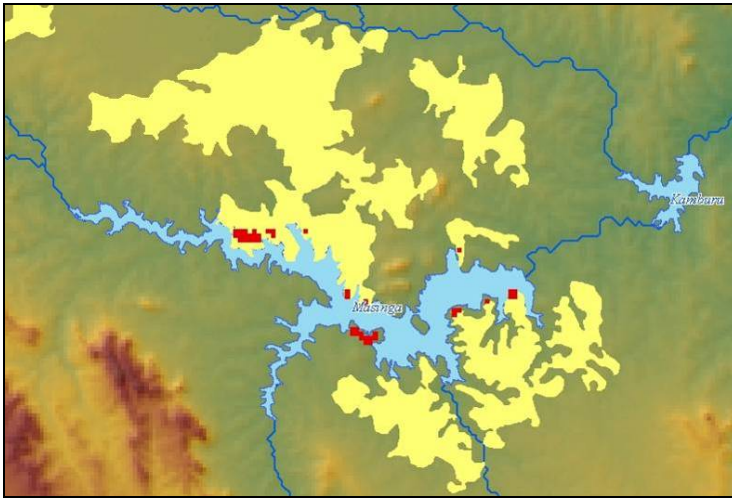


**Figure 26: Units classified as irrigated area, (Africover – yellow; Globcover – red) around the Masinga Dam**

Finally, it's noteworthy that, from the end users point of view, the Globcover land cover map contains a significant amount of mosaic classes, which limits the thematic sharpness of the Globcover product and its relevancy for hydrological modeling. For example, the Globcover dataset shows that the mountainous areas of the Aberdare Range are classified as a mosaic of vegetation and croplands. However, recent satellite imagery shows clearly that these areas are mainly forest and that no agricultural activities take place. Another major drawback of the Globcover dataset for hydrological modeling is that it is not crop specific. This would make it necessary to use more generic land use classes in the SWAT model.

### 2.3.3 Conclusion

Although the Globcover dataset was based on more recent information, the dataset evaluation showed clearly that the Africover dataset has much higher accuracy. The comparison of the mapped areas with recent satellite imagery showed that the delimited features have not been altered significantly since the production of the dataset, taking into account the working scale of the study. Therefore, it was decided to use the Africover dataset for the land cover input for the biophysical analysis using the model SWAT. However, it has to be noted that based on the visual comparison with the satellite imagery a number of polygons were corrected. According to the original dataset these polygons had a dominating natural land cover but the imagery showed that the agricultural activities in those areas are more significant, especially in terms of hydrology. Also the agricultural classification of some of the high mountain peak slopes of the Aberdares and Mount Kenya had to be corrected. Figure 27 shows the spatial distribution of the land covers as is used in the SWAT model.





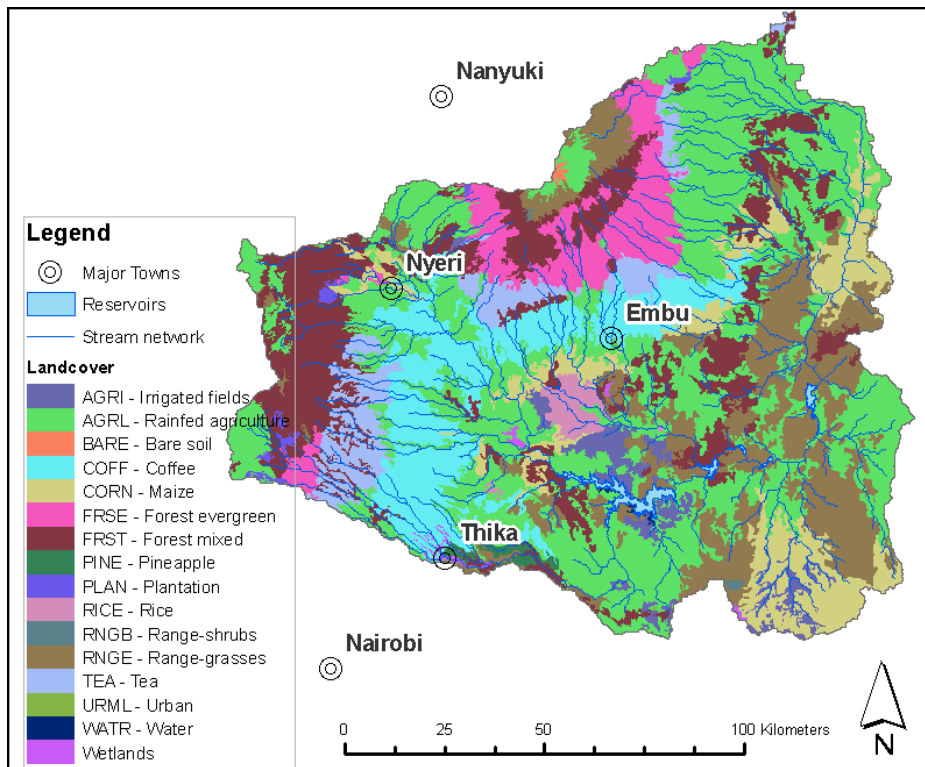


**Figure 27: Landcover map as used in the SWAT model, main source: Africover dataset, corrected by comparison with recent satellite imagery**

## 2.4 Soils

### 2.4.1 Data sources

#### 2.4.1.1 The KenSOTER database

The KenSOTER database at scale of 1:1 million (KSS 1996), holds data on landform, parent material and soils in a standardized digital format (van Engelen and Wen 1995). This database was updated by Kenya Soil Survey and ISRIC-World Soil Information (Batjes and Gicheru 2004). This 2004 version was expanded for GWC with additional profile data with measured water retention values of the Upper Tana catchment. The current KENSOTER database contains now data of 340 soil profiles, of which 68 of the Upper Tana, we will refer to it as the KenSOTER-version 2 database (KSS and ISRIC 2007).

The dominant soil types of the Upper Tana catchment are presented in Figure 28 and show a relationship with elevation. The higher slopes of Mt Kenya and the Aberdares are dominated by volcanic ash soils (Andosols). The middle foot slopes have mainly deep well structured nutrient rich clay soils (Nitisols). The lower foot slopes are dominated by very deep strongly leached poor clay soils (Ferralsols) and by less leached soils (Cambisols and Luvisols). At lower elevations, roughly below 1000m, Cambisols and sodic-alkaline soils (Solonetz) are the dominant soils (KSS 1996; Sombroek, Braun and van der Pouw 1982).

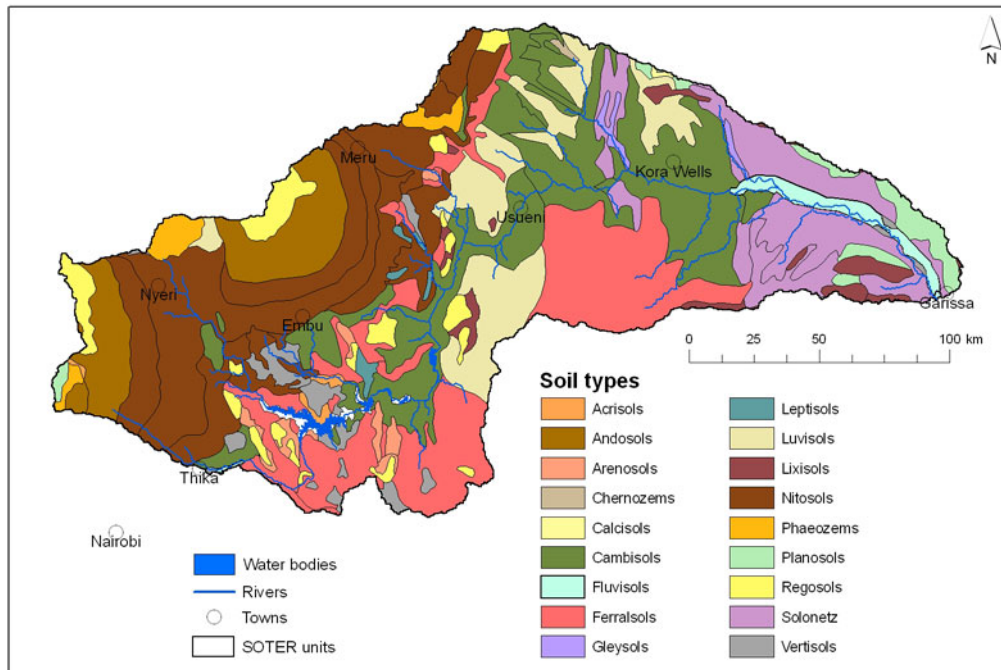


**Figure 28: Dominant soil types of the Upper Tana catchment (KenSOTER-version 2)**

Effective rootable depth and Available Water Content<sup>1</sup> are key soil hydrological properties determining the water balance, which are used in SWAT (Table 5). The geographic distribution and the differences are shown in Figure 29 and Figure 30. Comparing soil types in the Upper Tana it appears there is a factor 5 to 10 difference between lowest and highest values of Total Available Water Content.

**Table 5: Average soil moisture characteristics of dominant soils in the Upper Tana catchment**

Dominant soil (and phase)	Effective rooting depth (cm)	Moisture at saturation (%) <sup>(a)</sup>	Moisture at Field Capacity (%)	Moisture at Wilting Point (%)	Available Water Content <sup>(b)</sup> (%)	Total Available Water <sup>(c)</sup> (mm)
Acrisols	113	56	24	16	9	98
Andosols	100	60	40	24	16	172
Arenosols	100	53	16	3	13	130
Chernozems	75	55	37	21	16	120
Calcisols	40	41	16	10	6	24
Cambisols	53	48	28	14	14	74
Fluvisols	93	44	17	4	13	120
Ferralsols	90	53	26	17	9	82
Gleysols	45	56	37	21	16	72
Leptosols	10	53	21	12	9	7
Luvisols	80	47	25	13	12	95
Lixisols	88	47	16	11	5	43
Nitisols	104	53	31	22	9	98
Phaeozems	80	56	38	26	12	98

<sup>1</sup> Available Water Content is the amount of moisture held between pF2.3 and pF4.2



Planosols	25	50	35	22	13	33
Regosols	37	48	19	9	10	33
Solonetz	28	45	28	13	15	42
Vertisols	80	50	46	22	24	191

(a) Volume percentages; (b) Available water or plant extractable water; (c) Total available water = Available Water Content over Effective rooting depth.

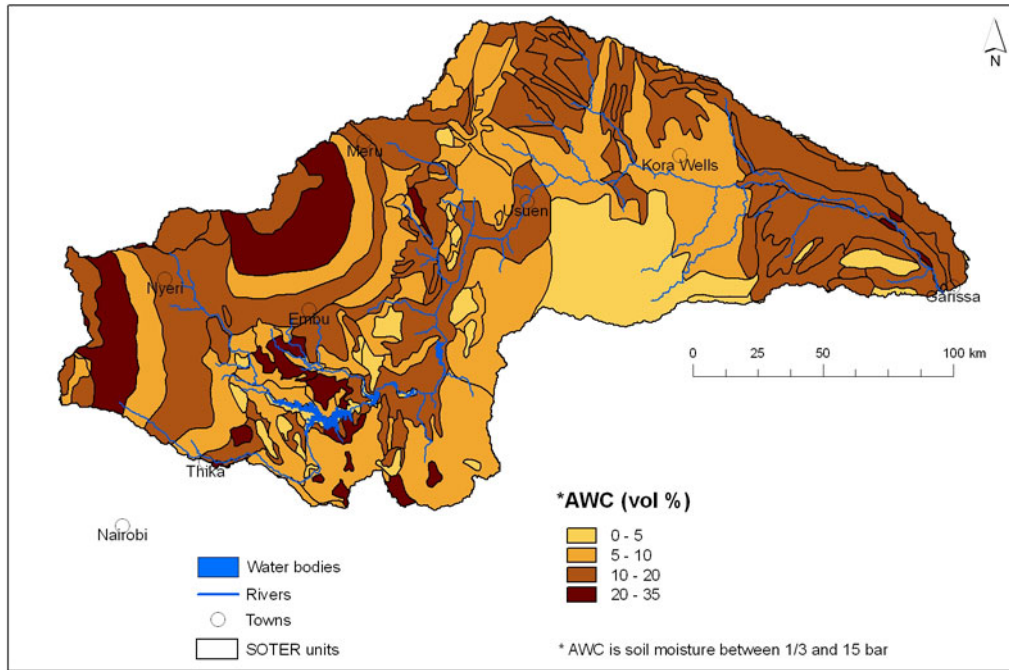


**Figure 29: Available Water Capacity of dominant soils of the Upper and Middle Tana catchment (KenSOTER-version 2)**

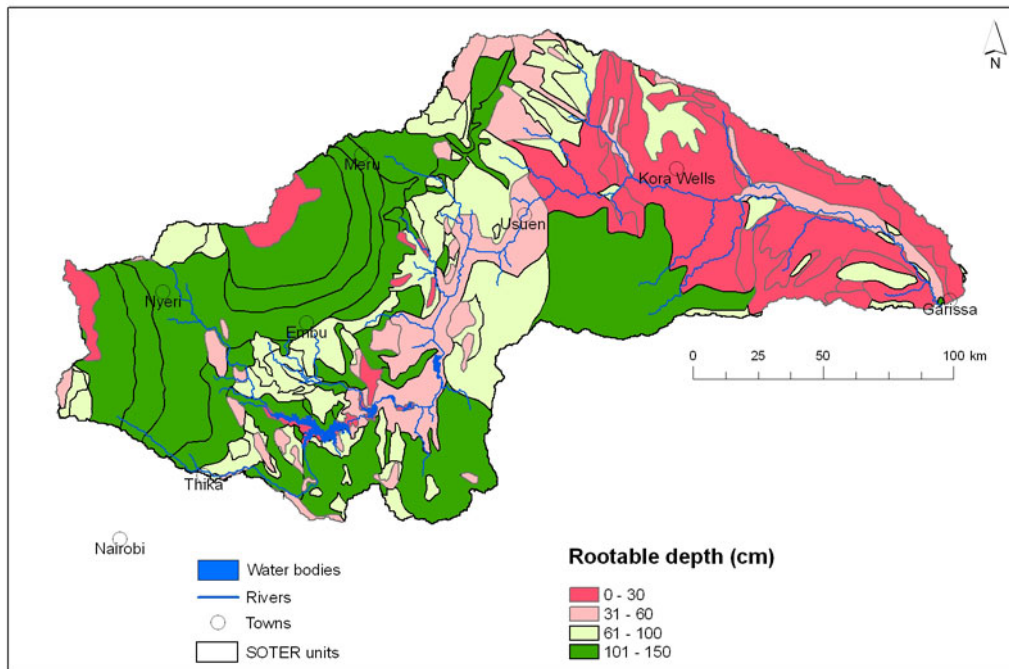


**Figure 30: Rootable depth of dominant soils of the Upper and Middle Tana catchment (KenSOTER-version 2)**



#### 2.4.1.2 Harmonized KENSOTER

The harmonized KENSOTER database is a secondary dataset with median attribute values. Missing entries are based on pedotransfer rules (van Engelen *et al.* 2005). Following these taxotransfer rules (Batjes 2003), the median attribute values have been estimated using attribute data and aggregate these over five fixed depth intervals, all on basis of texture group and soil unit classification (Batjes 1995). Soil classification follows the Revised Legend of the Soil Map of the World (FAO 1988).

The harmonized KENSOTER database includes the total available water capacity of the soil, which data can be directly used in SWAT. A comparison of the two databases showed that the soil moisture contents given by the harmonized KenSOTER database are higher than those of the measured data in the KenSOTER-version 2 database. The rootable soil depth is directly extracted from the harmonized KenSOTER database. In a few cases the rootable depths of the harmonized KENSOTER is somewhat different of KenSOTER-version 2, because of the use of different criteria.

The harmonized KENSOTER database contains most of the information necessary for the SWAT model. Therefore, it is convenient to use it as for the model input on soil characteristics, although some of the properties were derived and not fully consistent with the measured values.

#### 2.4.1.3 Pedo-transfer functions

An important characteristics not provided in KenSOTER database is the saturated hydraulic conductivity. A well-developed technique to overcome this problem is to use so-called pedo-transfer functions (PTF). A wide range of pedo-transfer functions have been developed and applied successfully over the last decades over various scales (e.g. field scale in (Droogers *et al.* 2001); basin scale at (Droogers and Kite 2001).

Sobierja *et al.* (2001) concluded from a detailed analysis that most PTFs were not very reliable and that the impact on runoff estimates could be considerable. The PTF that generated conductivity values close to measured ones was the Jabro equation (Jabro 1992):

$$K_{\text{sat}} = \exp(11.86 - 0.81 \log(\text{st}) - 1.09 \log(\text{cl}) - 4.64 \text{BD})$$

$K_{\text{sat}}$  is saturated hydraulic conductivity ( $\text{cm h}^{-1}$ )  
st is silt content (%)  
cl is clay content (%)

This equation was used to derive  $K_{\text{sat}}$  values from the KENSOTER database.

#### 2.4.2 Conclusion

SWAT requires detailed spatially distributed information on soil characteristics and related soil parameters. The information available in the harmonized KENSOTER database resulted to be adequate for use in the SWAT model. The saturated hydraulic conductivity was obtained using the described methodology by means of pedo-transfer functions.



## 2.5 Streamflow

### 2.5.1 Data source

Discharge data of a couple of streamflow gauges were available in the study area. Figure 31 shows the locations of gauging stations in the Upper Tana. Figure 31 and Table 6 provide an overview of the gauging stations data that have been obtained and processed. Data were made available by Kenyan Soil Survey, University of Nairobi and some additional data from the Global Runoff Discharge Database. The most complete series of observed stream flow data is from 1962-1977 (see Table 6).

### 2.5.2 Dataset evaluation

Data quality was poor, with missing records, unknown units and locations, conflicting names, etc. An example is station 4CC05 which is the inflow from Thika River in Masinga. A total of 15 years (1966-1980) of daily data were available. Of the total 5479 records 1340 were missing which corresponds to almost 25%.

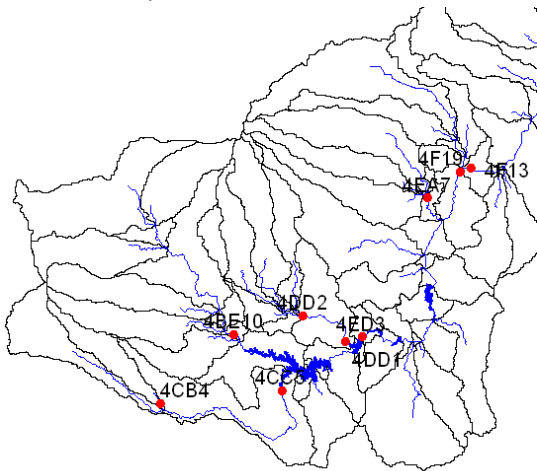


**Figure 31. Location of gauging stations for which data have been obtained.**

Data accuracy can also be hampered by the source the data was obtained from. One example is station Garissa, the outlet point of Middle Tana, where daily data were obtained from two sources (University of Nairobi and Global River Discharge Database). Data from UoN were daily records from 1941 to 1993 and data from GRDD covered 1934 to 1975, monthly. Figure 32 shows the difference between these two data sources for the overlapping period of 1941 to 1975. The scatter plot in the Figure indicates that quite some differences exist between the two datasets. The time plot however reveals that patterns are quite comparable and especially peak and low flows are comparable for the two datasets.

For stream flow station at Grand Falls, known as 4F13, two records of data were obtained from two different data sources as well (Figure 33). For these two datasets also some differences occur, but looking at the time plot these differences were restricted to some periods in the sixties and seventies.

Besides data from gauging stations, reservoir data on inflow and outflow were available from various sources (University of Nairobi and KenGen). For Masinga inflow as well as outflow data were available, while for the other reservoirs (Kamburu, Gitaru, Kindaruma, Kiambere) only inflow and levels were obtained.

Flow data is available from either stream gauges (Table 6) or from reservoir measurements (Table 7). The location of the gauges can be observed in Figure 31.

**Table 6. Availability of flow data from stream gauges.**

Code	River	Location	Interval	Period	Source
4BE10	Sagana		Daily	1980-1994	UoN
4CB04	Thika		Daily	1945-1997	UoN
4CC05	Thika		Daily	1966-1980	UoN
4DD01	Thiba		Daily	1948-2006	UoN
4DD02	Thiba		Daily	1966-1993	UoN
4EA07	Mutonga		Daily	1966-1990	UoN
4ED03	Tana	Kamburu	Daily	1951-1972	UoN
4F13	Tana	GrandFalls	Daily	1962-1995	UoN
4F19	Kazita		Daily	1966-1994	UoN
4G01	Tana	Garissa	Daily	1941-1993	UoN
GAR	Tana	Garissa	Monthly	1934-1975	GRDD
GRF	Tana	GrandFalls	Monthly	1962-1977	GRDD

\*UoN=University of Nairobi, GRDD=Global Runoff Discharge Data

**Table 7. Availability of reservoir related variables**

Reservoir	Time basis	Period	Source	Variables*
Masinga	Monthly	1982-2005	UoN	Qin, Qout, h
Kamburu	Monthly	1988-2005	UoN	Qin, h
Gitaru	Monthly	1988-2005	UoN	Qin, h
Kindaruma	Monthly	1988-2005	UoN	Qin, h
Kiambere	Monthly	1988-2005	UoN	Qin, h

\*Qin=Inflow, Qout=Outflow, h=level

### 2.5.3 Conclusion

There is only one gauge available with daily data of the last decade, the data of the other gauges are from before 1995 (see also Table 6). Also, recent data is available on the inflow of the Masinga Dam. The model should be calibrated with recent information to correctly simulate the current conditions in the basin. Given that this biophysical analysis is a basin scale assessment, the calibration with daily records of two gauging stations can be justified. However, to carry out a better validation of the model, it would be necessary to include more daily and recent timeseries on streamflow of the major branches in the basin.



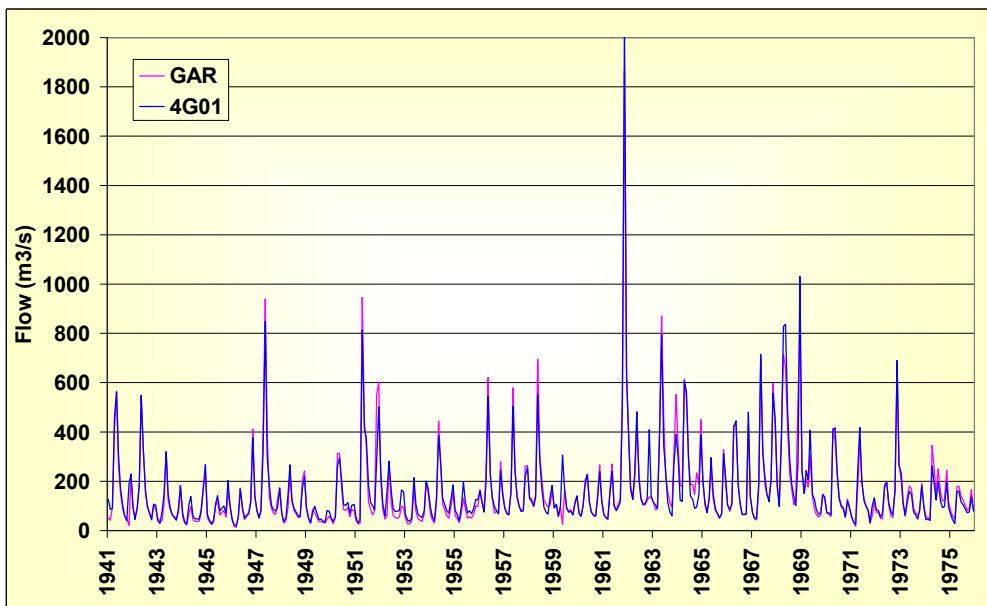
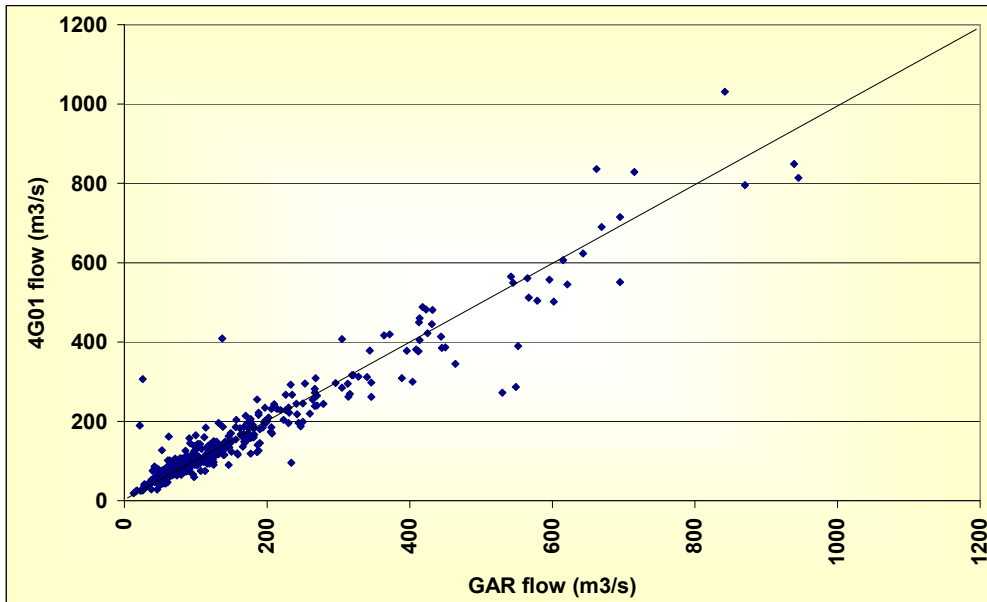


Figure 32. Comparison between similar data from two sources at Garissa. GAR originates from Global Runoff Discharge Data and 4G01 from University of Nairobi.



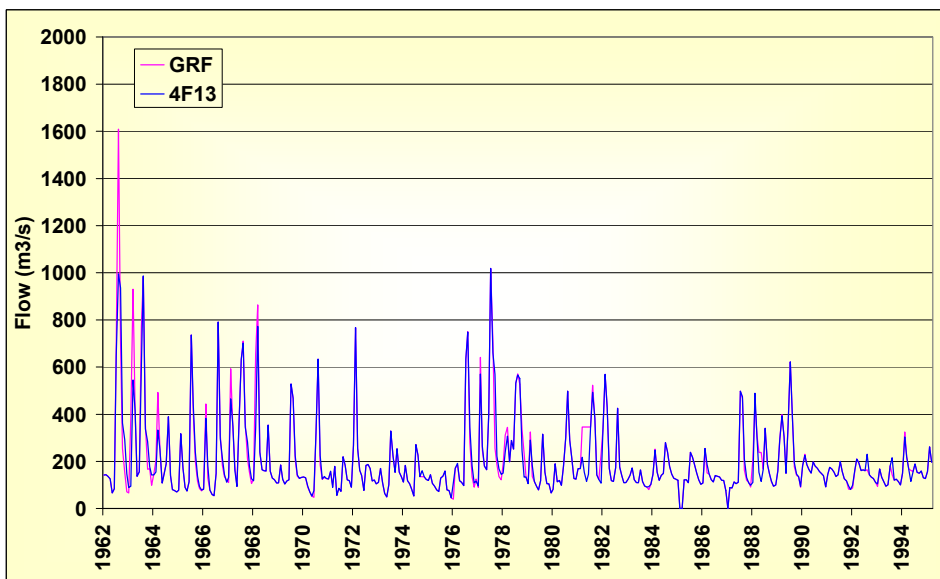
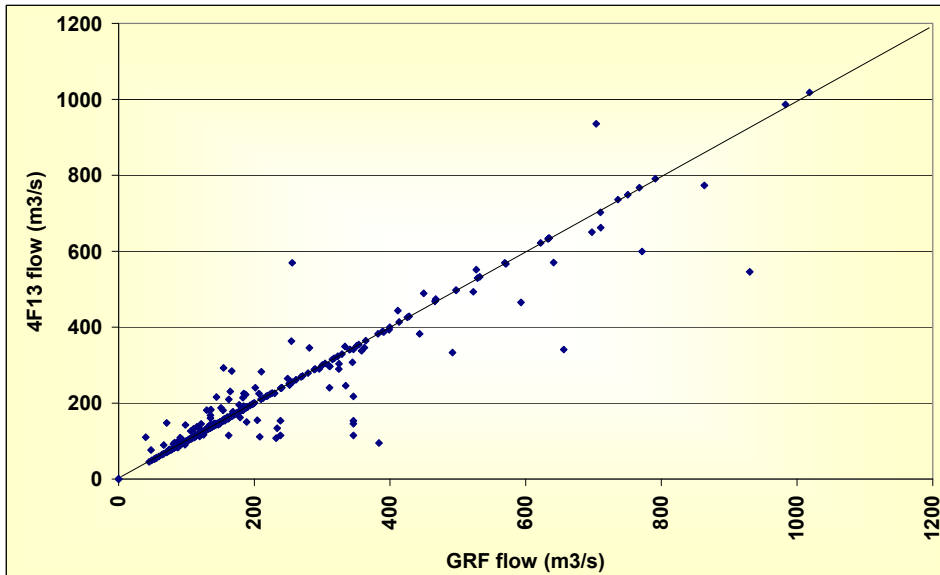


Figure 33. Comparison between similar data from two sources at Grand Falls. GRF originates from Global Runoff Discharge Data and 4F13 from University of Nairobi.





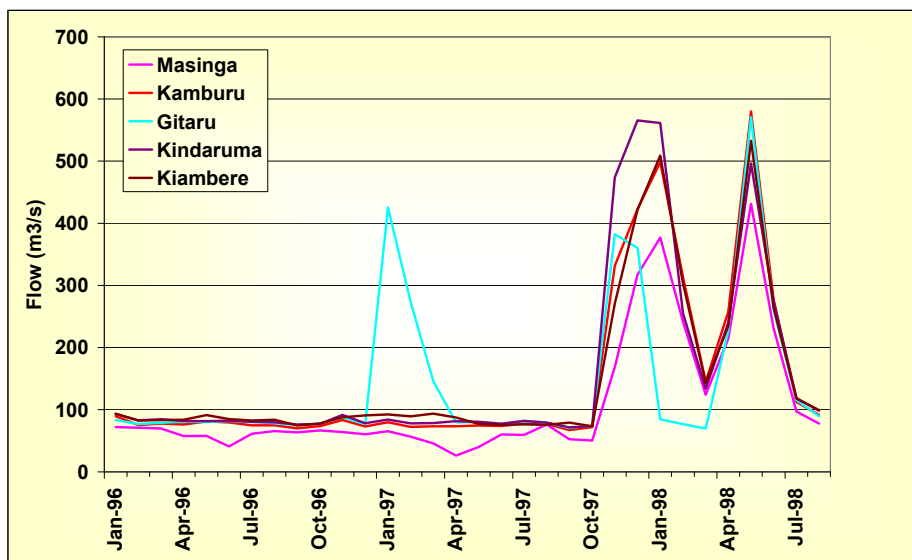


Figure 34. Outflow from main reservoirs in Tana.

## 2.6 Reservoirs

There are several reservoirs along the stream network of the basin related to hydropower plants. Some of them are so-called mini hydro stations and can be neglected in terms of routing as they do not alter significantly the river flows on a basin scale. However, there are 5 reservoirs that were included in the network schematization, which are: Masinga, Kamburu, Gitaru, Kindaruma and Kiambere (Figure 35). Besides, there are several planned reservoirs, downstream of these 5 main reservoirs. The planned Mutonga and the Low Grand Falls Dam are within the study basin.

The following reservoir characteristics were used for the flow routing in the hydrological model:

Table 8. Reservoir characteristics

Name	Unit	Masinga	Kamburu	Kindaruma	Gitaru	Kiambere
year of completion		1980	1974	1968	1978	1987
height of dam	m	69.5	56.0	24.3	30.0	112.0
capacity	MCM	1.560E+03	1.500E+02	1.600E+04	2.000E+01	5.850E+02
area	MCM	120,000	15,000	250	310	25,000
emergency spillway surface area	ha	1.440E+04	1.800E+03	3.000E+01	3.720E+01	3.000E+03
emergency spillway volume	m <sup>3</sup>	1.872E+03	1.800E+02	1.920E+01	2.400E+01	7.020E+02



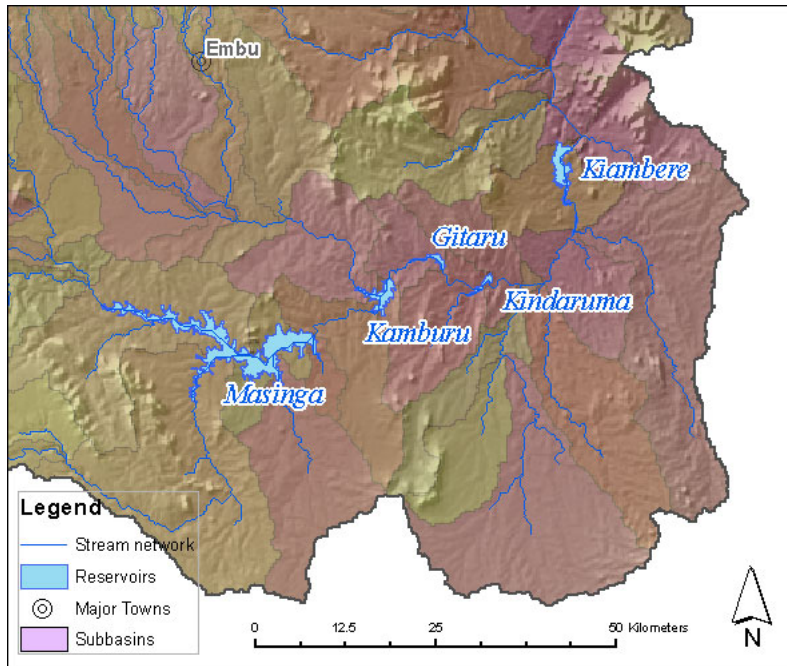


**Figure 35: The 5 main reservoirs included in the basin delimitation**



## 3 Baseline model analysis

### 3.1 Introduction

The Proof of Concept phase of Green Water Credits showed that the Soil and Water Assessment Tool (SWAT) was an appropriate tool to study and quantify the up- and downstream interactions in the basin, as well as the influence of land use and management on the water resources and sediment transport in the basin. For the current operational design phase a more accurate model was set up using the best available data sources, discussed in Chapter 2.

The model was set up with data from the last 10 years (2000 until 2009) in order to obtain insight in the current basin situation and interactions. This is an improvement compared to the Proof of Concept phase, when historical datasets were used for the basin assessment.

The main goal of this assessment is quantifying the impact of Green Water Credits management practices and identifying potential pilot areas from a biophysical point of view. This impact on the water and sediment balances in the basin depends on the water it receives through precipitation. For this reason, it is useful to assess the impact both during a dry as a wet year. to focus on the wettest and driest year of the 10-year timeseries in order to obtain insight in the effectiveness of management options during both extremes.

From the last ten years, the year 2005 represents the last year of a drought period that started in 2004 (Figure 36). On the other hand, the year 2006 can be considered an extraordinary wet year with about 2 times more rainfall than in 2005. These two years were used to quantify how the different Green Water Credits management options affect the green and blue water resources in the basin.

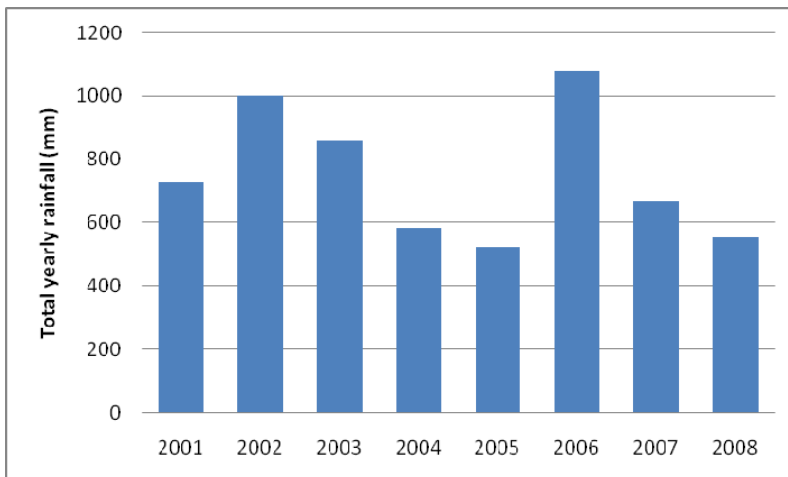


Figure 36: Total yearly basin rainfall (FEWS precipitation estimates)



## 3.2 Model set up

### 3.2.1 Distributed model input

The evaluation of the available data sources on precipitation (Chapter 2.2) indicated that the use of the FEWS dataset implies a considerable improvement compared to the use of point data from the weather stations, as was done during the Proof of Concept phase. Therefore, this dataset was used as the forcing weather model input, after a bias correction with the observed weather station data. Other meteorological data required by the model as temperature, wind, radiation, etc were obtained from the measured timeseries at the 3 available weather stations in the basin. For the daily temperature throughout the basin a lapse rate was used of  $-6^{\circ}\text{C}/\text{km}$ .

The FEWS dataset gives a reliable estimate of the spatial distribution of the daily precipitation amounts throughout the basin. The methodology used to delineate the subbasins allowed to correctly incorporate this information allowing a fully distributed rainfall-runoff modeling approach. The daily rainfall grids were prepared for the model input and the different daily rainfall timeseries were assigned to each subbasin in the model. For the following figures the daily values were summed showing the total rainfall per subbasin for the dry (2005) and the wet year (2006).

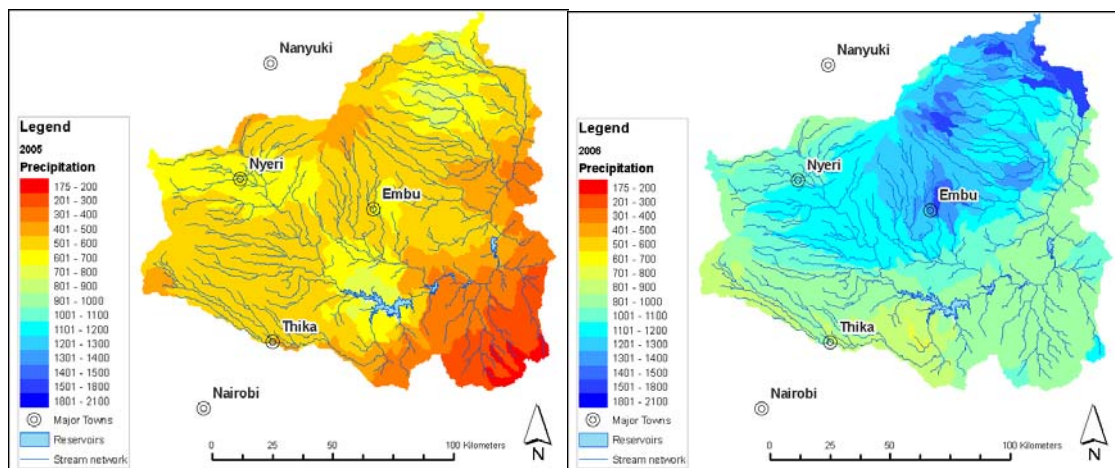


**Figure 37. Total precipitation for 2005 (left) and 2006 (right)**

### 3.2.2 Hydrological response units

For the spatial discretization of the subbasins, SWAT uses the concept of Hydrological Response Units (HRU) (Neitsch *et al.* 2002): portions of a sub basin that possess unique land use/management/soil attributes. In other words, an HRU is the total area in the sub basin with a particular land use, management and soil combination. While individual fields with a specific land use, management and soil may be scattered throughout a sub basin, these areas are lumped together to form one HRU. HRUs are used in SWAT runs since they simplify a run by lumping all similar soil and land use areas into a single response unit. The size of a HRU depends on the size of the total area under consideration.

Implicit in the concept of the HRU is the assumption that there is no interaction between HRUs in one sub basin. Loadings (runoff with sediment, nutrients, etc. transported by the runoff) from each HRU are calculated separately and then summed together to determine the total loadings from the sub basin. If the interaction of one land use area with another is important, rather than defining those land use areas as HRUs they should be defined as sub basins. It is only at the sub basin level that spatial relationships can be specified.



The benefit of HRUs is the increase in accuracy it adds to the prediction of loadings from the sub basin. The growth and development of plants can differ greatly among species. When the diversity in plant cover within a sub basin is accounted for, the net amount of runoff entering the main channel from the sub basin will be much more accurate.

In practice the HRUs are defined by overlaying three data layers: (i) sub basins, (ii) land cover (section 2.3), and (iii) soils (section 2.4). Due to computational constraints it is necessary to limit the total number of HRUs and filter out the minor land use and soil classes within each subbasin. For this analysis, a threshold of 10% for both layers was used. This means that if a certain land use and soil combination covers less than 10% in a certain subbasin, this HRU was filtered out. This way only the dominating units in terms of hydrological response within each subbasin are analyzed. A total of 2226 HRUs were determined using this procedure (Figure 38) which means a substantial improvement to the Proof of Concept model when 874 HRUs were defined, distributed over a larger basin (outlet Garissa).

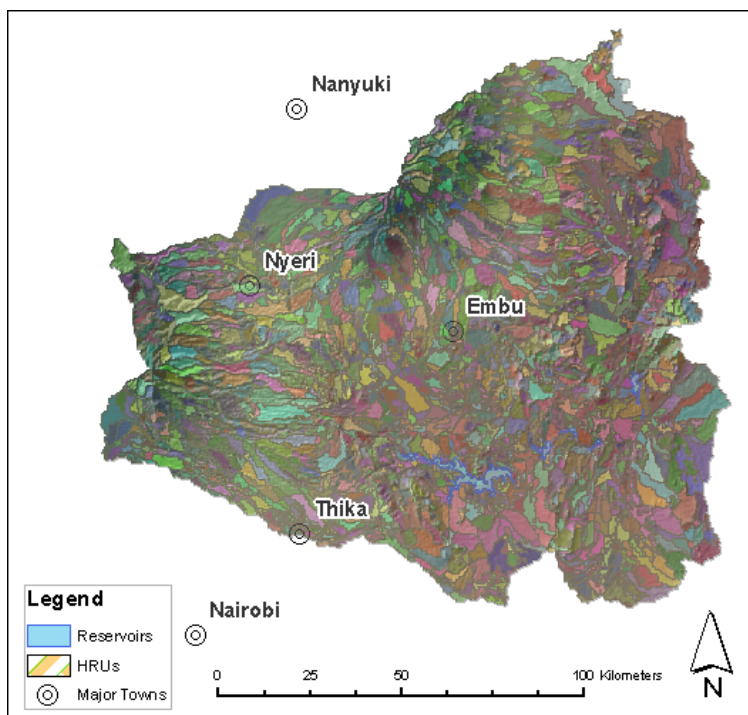


**Figure 38. The defined hydrological response units (HRUs).**

### 3.3 Calibration and model performance

The FEWS precipitation estimates were available from the year 2000 (October) until 2009 (April). Measured riverflow data were available until 2005 for two very relevant points in the basin. Additional calibration including more gauged points is scheduled to take place in a following-up study. For pilot operation of Green Water Credits, the key focus is to assess the impact of the GWC practices on the water and sediment fluxes in the basin, quantifying the differences between the studied scenarios and the current management situation (i.e. baseline scenario). In this sense, it is crucial to note that conclusions drawn from scenario analysis are much more reliable than absolute model predictions (relative vs. absolute model accuracy, e.g. Droogers et al. 2008).



To determine the calibration parameters, first a sensitivity analysis was carried out using the parameters shown in Table 9. These five parameters were altered within realistic boundary conditions, showing that the model output was most responsive to the soil available water capacity and the groundwater delay time. The second parameter determines the time lag between the moment the water leaves the soil storage and the moment it becomes available in the aquifer storage. It is difficult to infer this parameter from measurable soil and hydro-geological characteristics, especially at the basin scale. Also the soil available water capacity is a parameter which is known to be highly heterogeneous.

**Table 9. Parameters used for sensitivity analysis**

SWAT Code	Unit	Variable
Alpha_BF	Days	Baseflow alpha factor
GW_REVAP	-	Groundwater "revap" coefficient
SOL_AWC	mm H <sub>2</sub> O/mm soil	Available water capacity of the soil layer
GW_DELAY	Days	Groundwater delay time
SOL_K	mm/hr	Saturated hydraulic conductivity

The soil available water capacity and the groundwater delay time were used to calibrate the model. It was assumed that the a priori estimates of these parameters represent the spatial distribution pattern but that the relative magnitudes of the parameters in each field need to be adjusted up or down via a single multiplier  $\alpha$ . This is a common method to calibrate distributed hydrological models (e.g. Vieux et al. 2004). The following table shows the values of  $\alpha$  used for the calibration:

**Table 10. Boundary values and calibrated value of multiplier used for calibration**

Parameter	$\alpha$ lower limit	$\alpha$ upper limit	$\alpha$ final
GW_REVAP	0.03	1.5	0.3
SOL_AWC	0.3	1.5	1

The calibration was done using the daily observations at the two gauges, each of them at a key location within the basin. The two gauges are located upstream of the reservoirs, which guarantees that streamflow reaching the gauges is not influenced by reservoir operations. Moreover, they allow the calibration of the two major parts of the basin. The data available on the inflow of the Masinga reservoir joins the Maragua and Sagana subbasins of the Aberdares mountain range. The second gauge (code 4DD01) in the Thika river covers an important part of the Mount Kenya subbasins draining into the Kamburu reservoir (Figure 39).



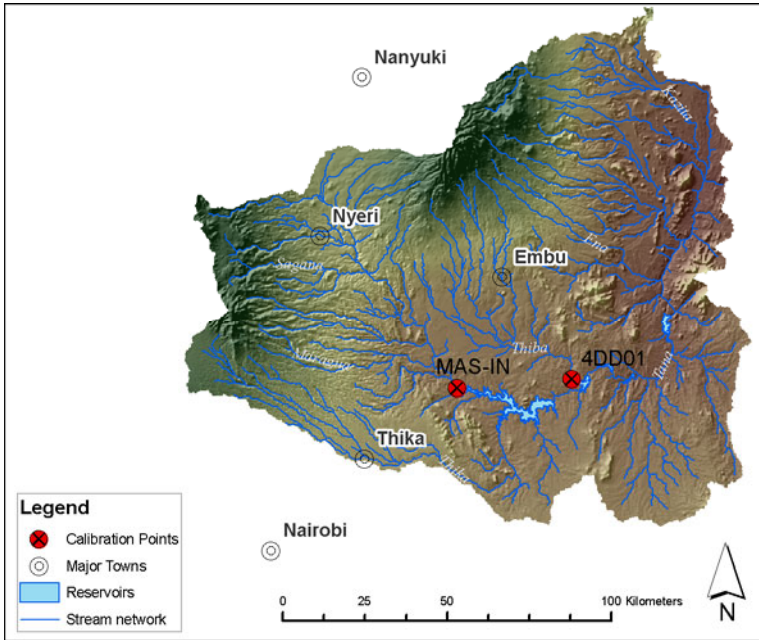


**Figure 39: Location of the calibration points in the basin**

The model calibration with the two parameters was done using three performance coefficients and visual comparison of the observed and simulated discharges. The correspondence between both records was assessed using the Pearson product-moment correlation coefficient, the Normalized Root Mean Square (RMS) and the Nash-Sutcliffe model efficiency coefficient (Table 11).

The Normalized Root Mean Squared is the RMS divided by the maximum difference in the observed streamflow values, and is expressed by the following equation:

$$NormalizedRMS = \frac{RMS}{(X_{obs})_{max} - (X_{obs})_{min}}$$

The Normalized RMS is expressed as a percentage, and is a more representative measure of the fit than the standard RMS, as it accounts for the scale of the potential range of data values. For example, an RMS value of 1.5 will indicate a poor calibration for a model with a range of observed values between 10 and 20, but it will indicate an excellent calibration for a model with a range of observed values between 100 and 200. The Normalized RMS value for the first model would be 15%, while the Normalized RMS for the second model would be 1.5%.

The Nash-Sutcliffe model efficiency coefficient, the third measure to assess the performance of the SWAT model, is defined as follows:

$$E = 1 - \frac{\sum_{t=1}^T (Q_o^t - Q_m^t)^2}{\sum_{t=1}^T (Q_o^t - Q_o)^2}$$

where  $Q_o$  is observed discharge, and  $Q_m$  is modeled discharge.  $Q_o^t$  is observed discharge at time  $t$ .

Nash–Sutcliffe efficiencies can range from  $-\infty$  to 1. An efficiency of 1 ( $E = 1$ ) corresponds to a perfect match of modeled discharge to the observed data. An efficiency of 0 ( $E = 0$ ) indicates that the model predictions are as accurate as the mean of the observed data, whereas an efficiency less than zero ( $E < 0$ ) occurs when the observed mean is a better predictor than the model.

The following table shows the three performance coefficients before and after calibration. As could be seen in Table 10, the a priori estimates of the soil available water capacity were not altered ( $\alpha=1$ ), as the parameter sets did not improve the model performance significantly. All the calibrated values of the three coefficients improve compared to the initial non-calibrated model. The normalized RMSE indicates a relative error of around 10% and the Nash Sutcliffe coefficient shows a fairly good match of modeled discharge to the observed data.

**Table 11. Performance coefficients for the calibration points**

	Gauge 4DD01*		Inflow Masinga*	
	Initial	Calibrated	Initial	Calibrated
Normalized RMSE	15%	14%	12%	9%
Pearson correlation coefficient	0.77	0.86	0.85	0.92
Nash Sutcliffe coefficient	0.53	0.59	0.67	0.80

\* Rainfall period of November 2004 was omitted in the calculation for mentioned reasons

Observed and simulated monthly discharges from the two gauging stations can be seen in Figure 40 and Figure 41 (first year was used for model warming-up and is not represented). Also these figures confirm that the simulated model discharges correspond well with the observed monthly flow data. Overall, both low flows as high peak flows are well simulated by the model, although low flows seem to be slightly underestimated in some periods. A major striking discrepancy can be observed during the month November 2004. This month shows a large difference between observed and simulated streamflow, at both points. A comparison of daily precipitation estimates (FEWS) with the gauged values at the weather stations showed that particularly during this month the estimates failed to capture some strong rainfall events. As a result, this discrepancy can be interpreted as an irrelevant error in the model input rather than an error in the model itself. In general, a very good correspondence was observed between both rainfall datasets (see previous chapter).

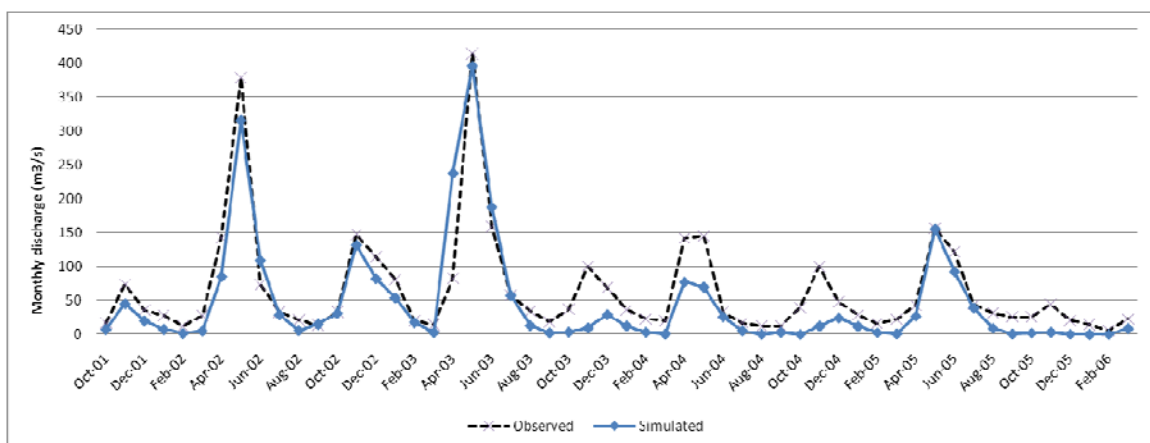


**Figure 40: Simulated and observed inflow of the Masinga Reservoir**





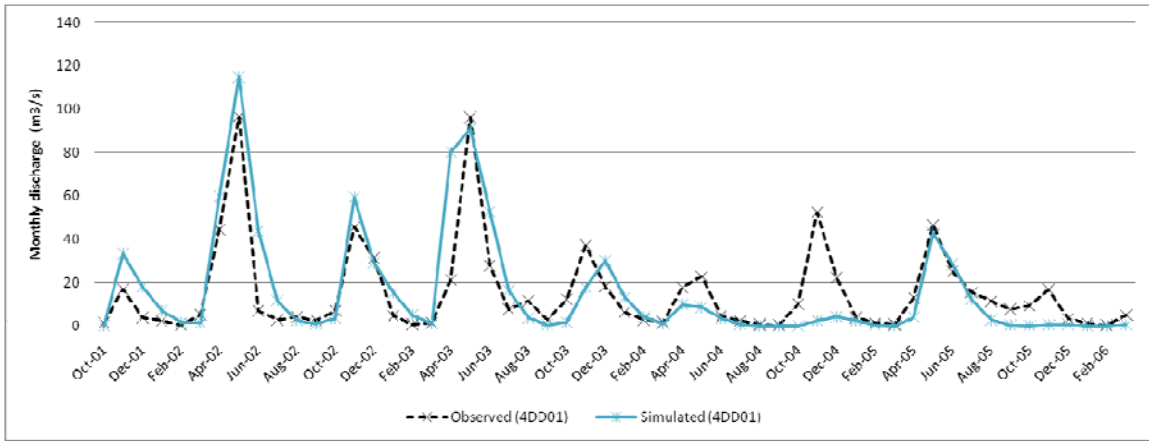


**Figure 41: Simulated and observed inflow of the gauge 4DD01 (Thiba river, Kamburu Reservoir)**

### 3.4 Crop-based assessment

To explore what the most relevant land use classes regarding Green Water Credits are, results were aggregated for each land use class. The most relevant items plotted are:

- The total amount of water consumed by vegetation (crop transpiration) and water lost by soil evaporation (Figure 42).
- T-fraction: percentage of total evapotranspiration used for crop transpiration (Green Water). This factor indicates the effectiveness of the vegetation to use the Green Water source (Figure 43).
- Blue Water: water entering the streams by surface runoff and returnflow (i.e. groundwater discharge) that can be used for generating hydropower or being reused by downstream users (Figure 44).
- Erosion: total actual sediment loss (Figure 45).

Evapotranspiration is the sum of water consumed by the plants to grow (crop transpiration) and the water lost through evaporation, mainly from the soil surface (evaporation also occurs by rainfall interception but this process was not included in the analysis). Soil evaporation can be considered an actual unbeneficial loss of water from the system. The water gained by reducing soil evaporation can be either used for crop transpiration or can be infiltrated and serve for groundwater recharge.



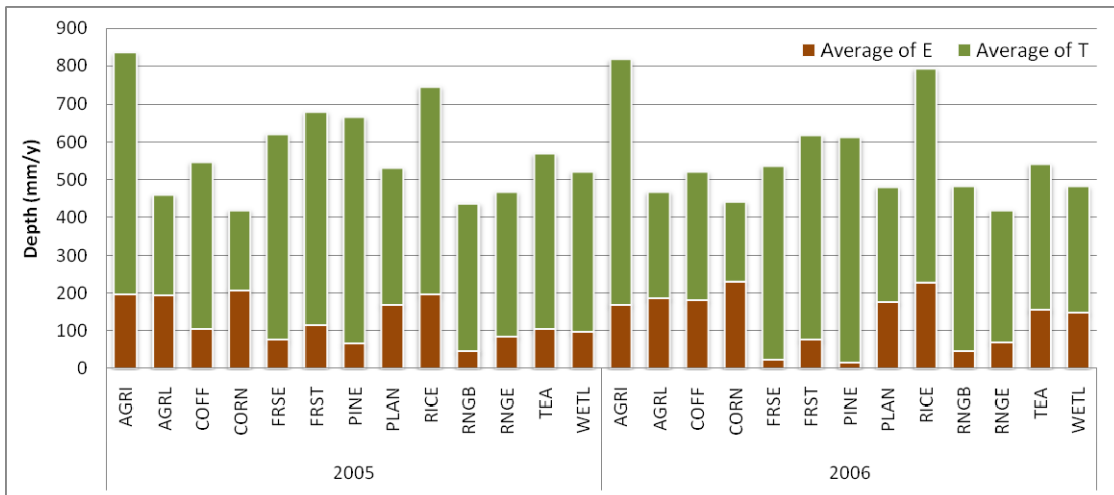


**Figure 42: Evapotranspiration split in crop transpiration (T) and soil evaporation (E) per crop for the dry year (2005) and the wet year (2006) (for meaning of codes, see Figure 27).**

The crops with potential for the implementation of Green Water Credits management practices are those that are cultivated in the upstream areas. Secondly, the crops of interest should also show the potential to reduce the amount of soil evaporation and reduce erosion. Figure 42 and Figure 43 give insight in which part of total evapotranspiration is used beneficially for the crops and which part is lost through soil evaporation. From these figures can be concluded that the main agricultural crops that show potential for the implementation of GWC practices are:

- CORN: maize
- COFF: coffee
- AGRL: non specified agricultural crops

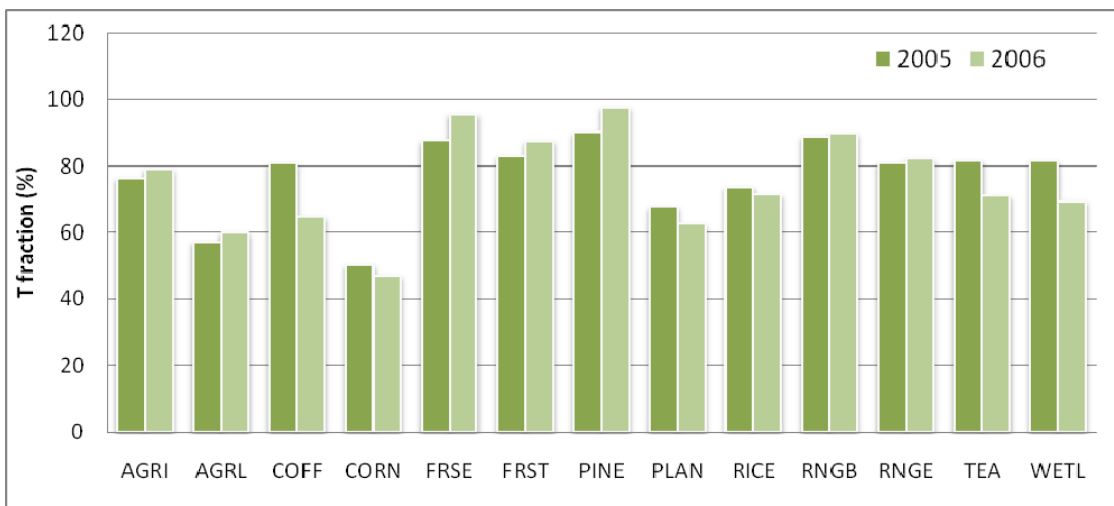


**Figure 43: Percentage of total evapotranspiration used for crop transpiration for the dry year (2005) and the wet year (2006).**

Figure 44 shows the large differences in Blue Water coming from each of the crop cultivated areas between the dry year and the wet year. These differences are mainly caused by the balance between surface runoff and groundwater discharge. During the dry year, basically all the Blue Water comes from groundwater discharge, while during the wet year the main source for Blue Water is surface runoff. It becomes clear that there is a great potential to improve this



balance on a crop scale by implementing GWC practices. Stimulating groundwater recharge will reduce the large differences between the dry and the wet year and make the Blue Water a better manageable water source for downstream users. Moreover, an increase over groundwater recharge will reduce erosion substantially.

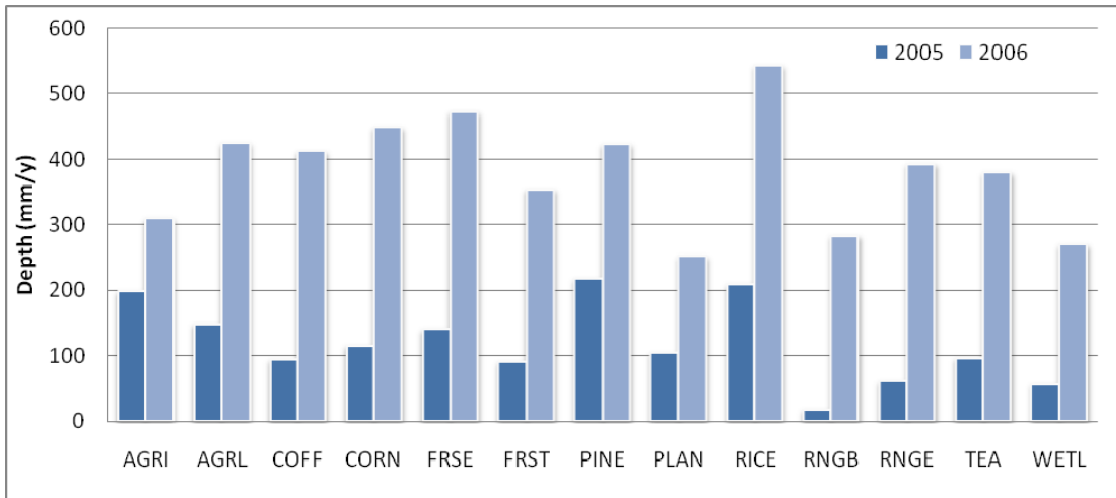


**Figure 44: Water entering the streams by surface runoff and drainage (Blue Water) for the dry year (2005) and the wet year (2006).**

As can be seen from Figure 45, the selected crops for GWC are also those that show the highest sediment loss rates, especially during the wet year. The implementation of GWC might be able to reduce erosion significantly, as is confirmed by the scenario analysis in the following chapter.

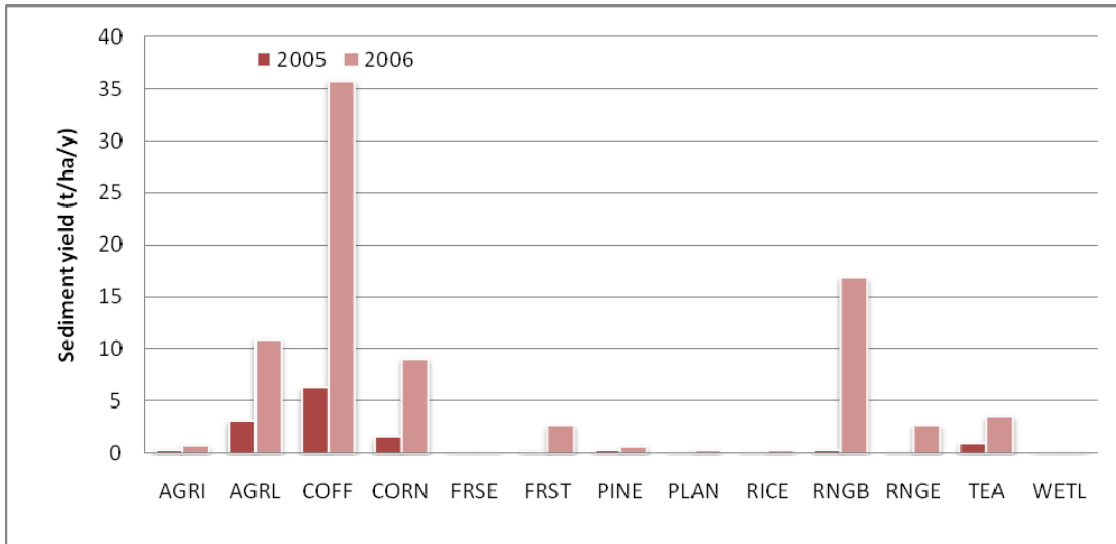


**Figure 45: Total actual sediment loss per crop for the dry year (2005) and the wet year (2006).**

### 3.5 Temporal responses

Blue Water, of interest for the downstream water users, is mainly the sum of surface runoff and groundwater discharge (also called return flow or baseflow). Surface runoff has an immediate response to rainfall events while groundwater discharge shows a more delayed and gradual



response to the rainfall events. This is an effect of the natural water reservoir of the soil and aquifer.

The differences in response of both Blue Water sources can be clearly observed in Figure 46. The surface runoff shows peak values in the same month as the peak rainfall value, while the groundwater discharge tends to show the maximum value a month after the highest rainfall. The percolated water needs a certain travel time before it enters the aquifer storage. This storage releases its water gradually, depending on its geo-hydrological characteristics.

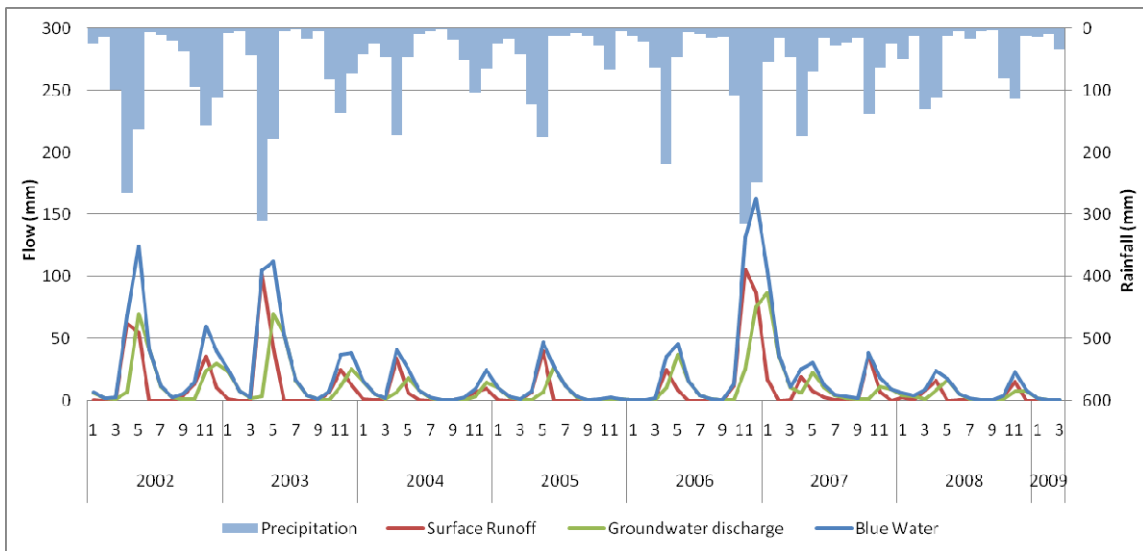


**Figure 46: Total basin precipitation and Blue Water, being the sum of surface runoff and groundwater discharge.**

Surface runoff, on the other hand, generates high peak flows which are only manageable through the reservoirs to a certain extent. This means that due to capacity limitations and especially during wet years water of strong rainfall events cannot be stored and has to be released from the reservoirs without giving the water any beneficial use. This is actually confirmed by the measured data on reservoir outflow. Consequently, the Blue Water source becomes more predictable and manageable when direct runoff is reduced while at the same time stimulating groundwater discharge by enhancing infiltration and aquifer recharge.

The potential of the natural storage in the reservoir is clearly illustrated when having a close look on the differences between the dry and the wet year of the basin scale water balance (Figure 47). The figure shows that the size and sign of the balance terms depends on the amount of incoming precipitation. During the dry year (2005) outflow is limited and more or less equal to the change in basin storage. In other words, most of the outflow during this year came from groundwater discharge and reservoir releases and thus from water stored during previous years. On the other hand, during the wet year 2006, precipitation is the only positive 'incoming' component of the water balance, and the storage compartments are refilled, due to groundwater recharge and the recovery of man-made reservoir storage capacity. This demonstrates that enhancing groundwater recharge during wet periods leads to more groundwater discharge during drought periods and thus more Blue Water when surface runoff is limited.



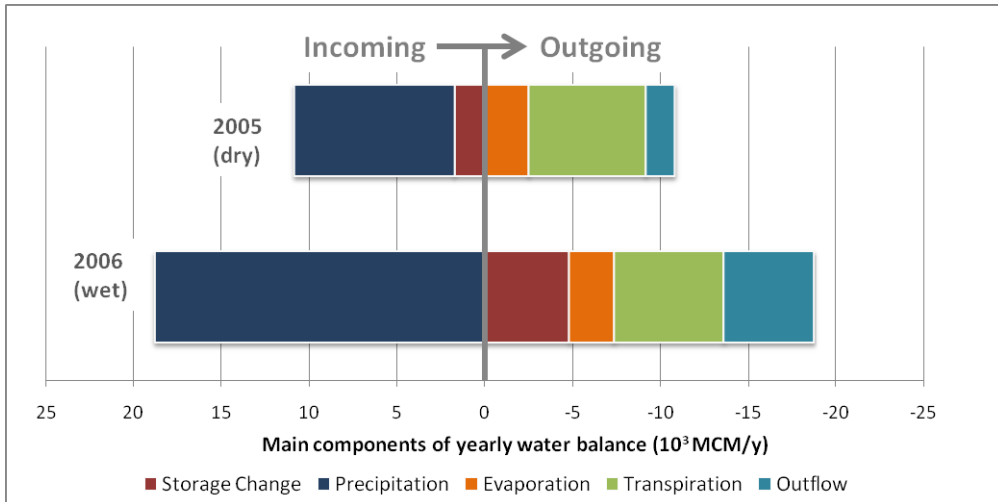


**Figure 47: Main components of water balance of 2005 (dry) and 2006 (wet)**

The previous figure highlights the role of storage in the water balance of the basin. It is clear that the soil and aquifer reservoirs have a potential to improve the management of water resources in the basin as they assure a more continuous and reliable flow regime. Green Water Credits management options aim at maximizing the potential of these natural reservoirs.

### 3.6 Heterogeneity and spatial distribution

The distributed modeling approach that was chosen for the design phase of Green Water Credits gives the ability to assess Green and Blue water options at a high spatial resolution. This allows assessing how the potential sites for Green Water Credits are spatially distributed. The following maps are plotted here for the relatively dry (2005) and a relatively wet (2006) year:

- Actual evapotranspiration: total amount of water consumed by vegetation (crop transpiration) and water lost by soil evaporation (soil evaporation).
- Actual transpiration: total amount of water that is used by vegetation (agricultural as well as natural vegetation) to produce biomass. This can be considered as Green Water.
- Actual soil evaporation: total amount of water that is lost by soils. This includes bare soils, but also areas partly covered by vegetation. This soil evaporation can be considered as a non-beneficial loss as it does not serve any function.
- T-fraction: percentage of total evapotranspiration used for crop transpiration (Green Water). This factor indicates the effectiveness of the vegetation to use the Green Water source.
- Blue Water: water entering the streams by surface runoff and drainage that can be used for generating hydropower or being reused by downstream users.
- Groundwater recharge: water that contributes to the groundwater recharge. Only water that enters the deep groundwater is included. Water entering the shallow groundwater which will contribute to drainage is included in the previous item (Blue Water).
- Erosion: total actual sediment loss.



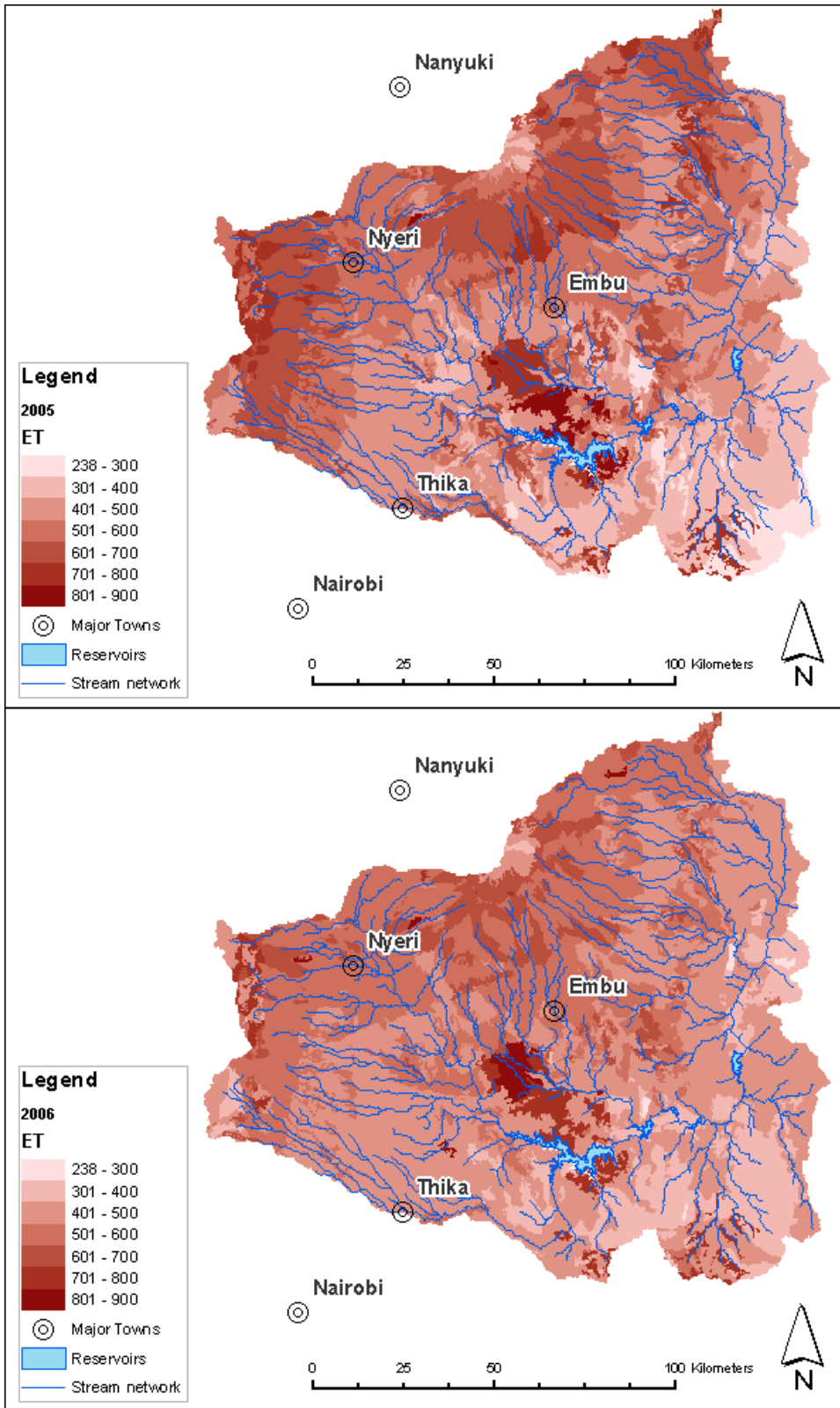


**Figure 48. Actual evapotranspiration for 2005 (dry) and 2006 (wet) in mm.**



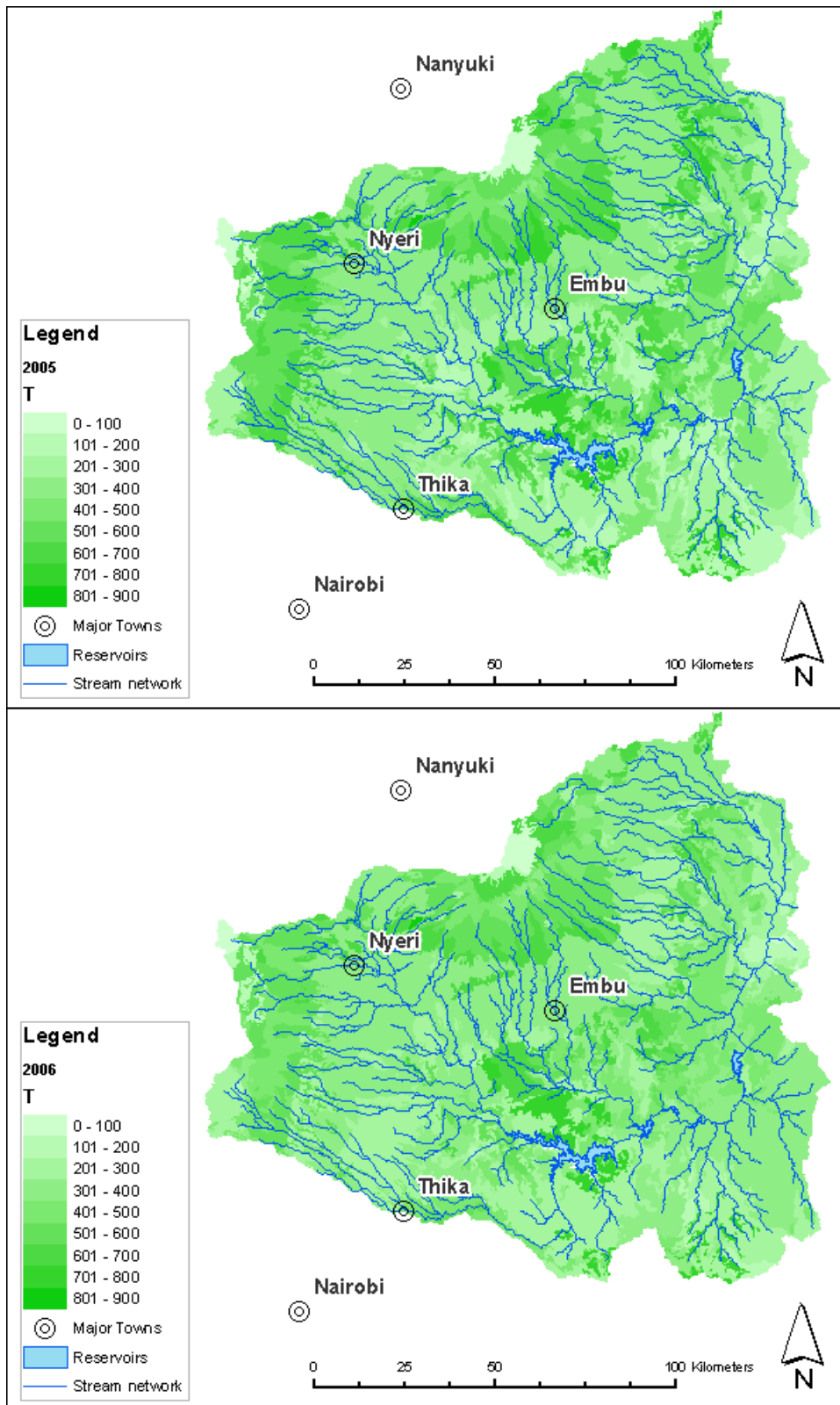


**Figure 49. Actual transpiration for 2005 (dry) and 2006 (wet) in mm.**



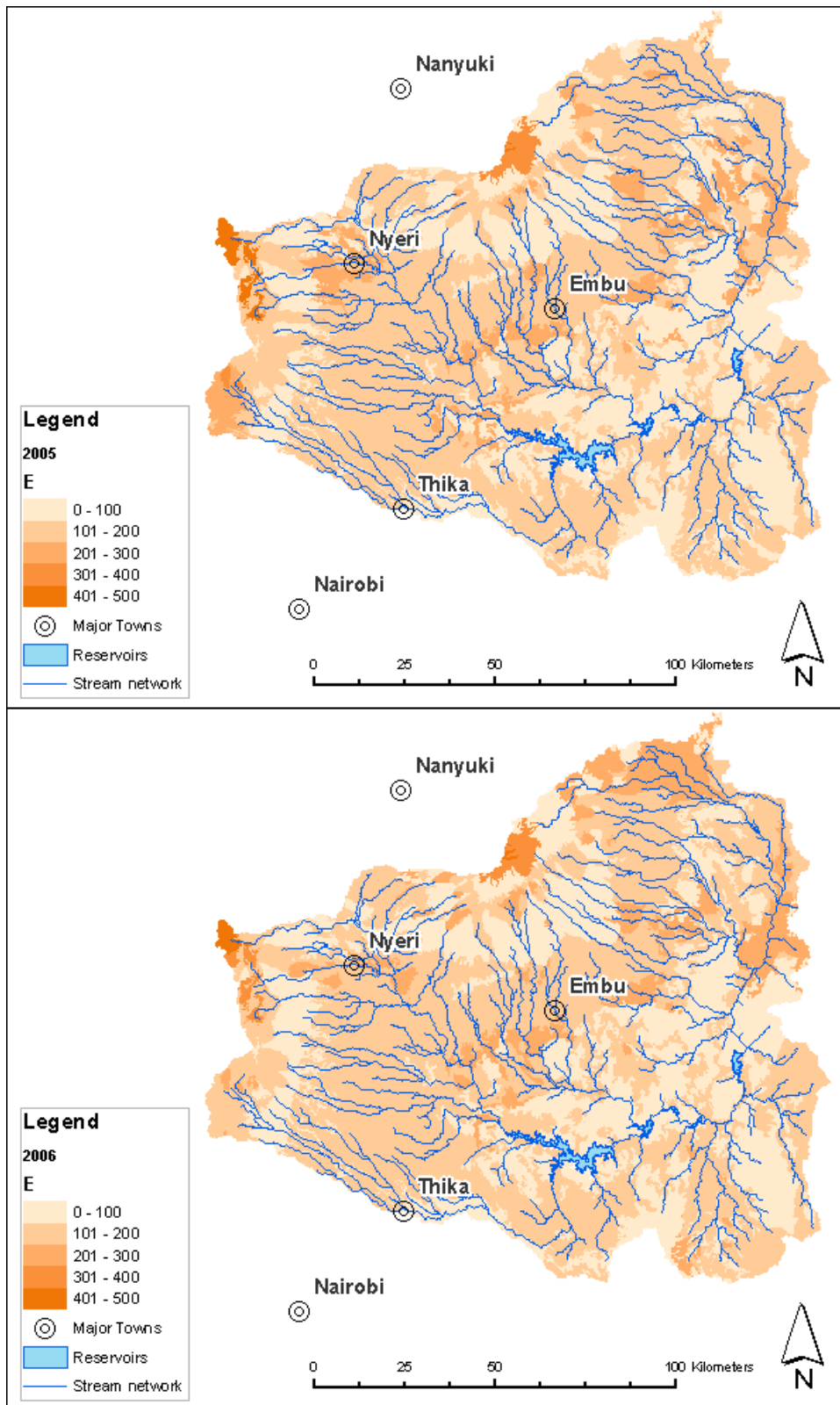


**Figure 50. Actual soil evaporation for 2005 (dry) and 2006 (wet) in mm.**





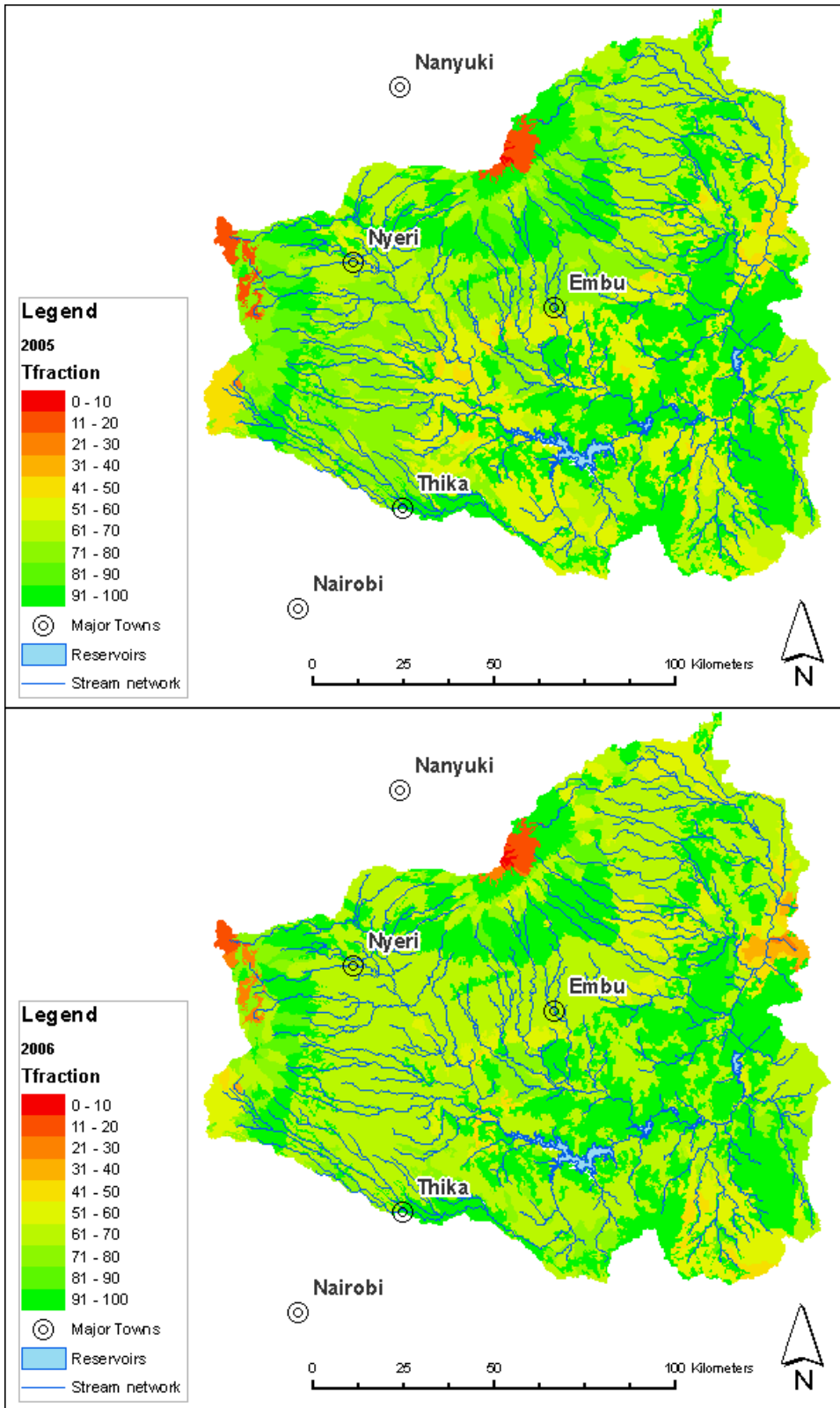


**Figure 51. Percentage of total actual evapotranspiration used for Green Water for 2005 (dry) and 2006 (wet)**



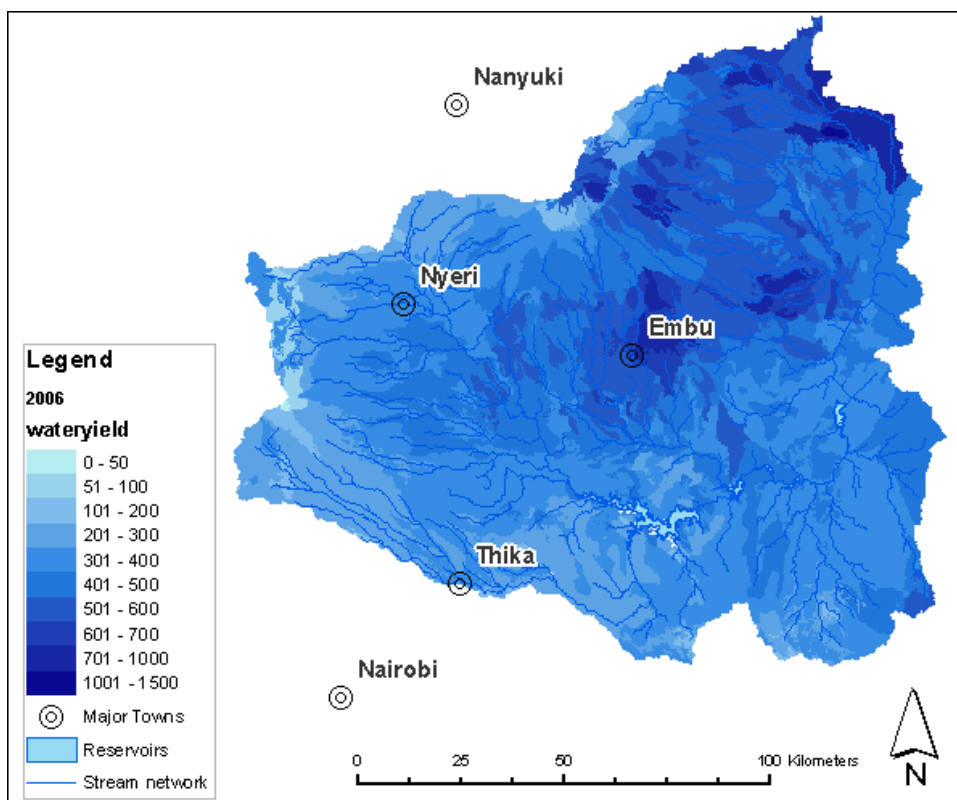
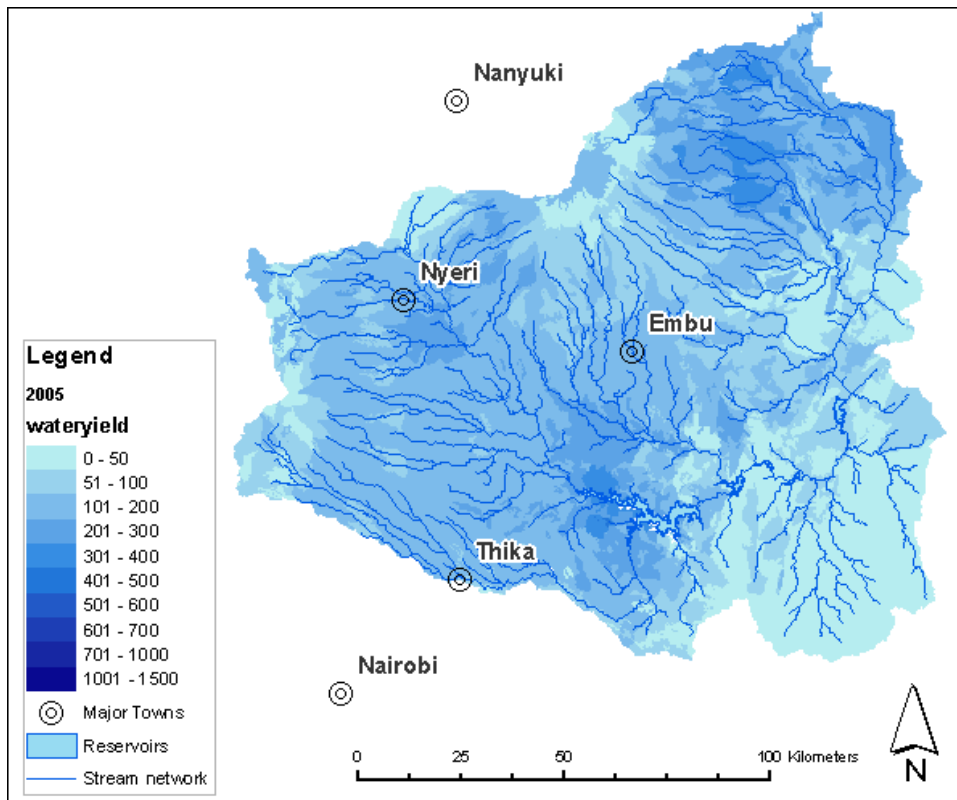


**Figure 52. Blue Water (water entering the streams by surface runoff and baseflow) for 2005 (dry) and 2006 (wet) in mm.**



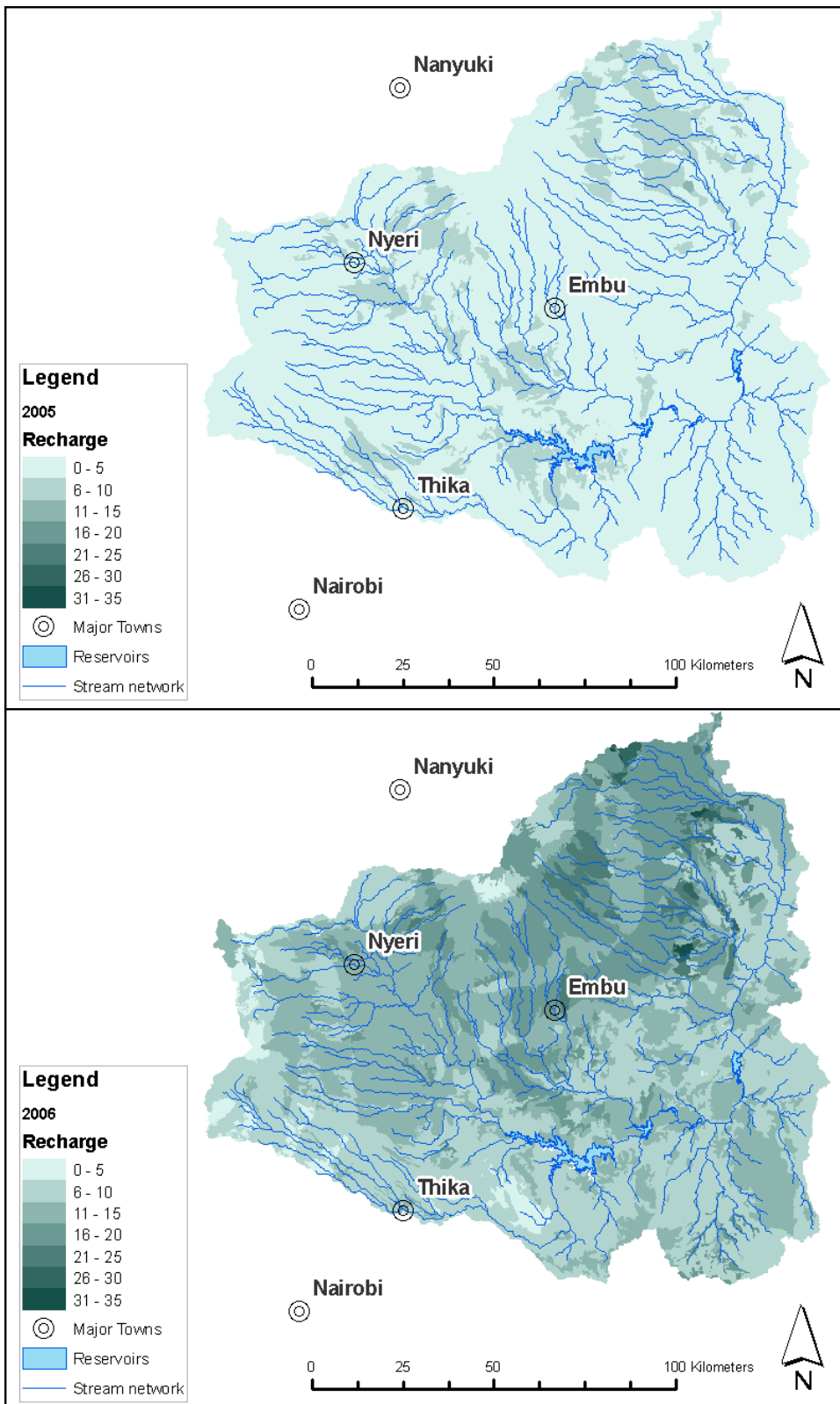


Figure 53. Deep groundwater recharge for 2005 (dry) and 2006 (wet) in mm.

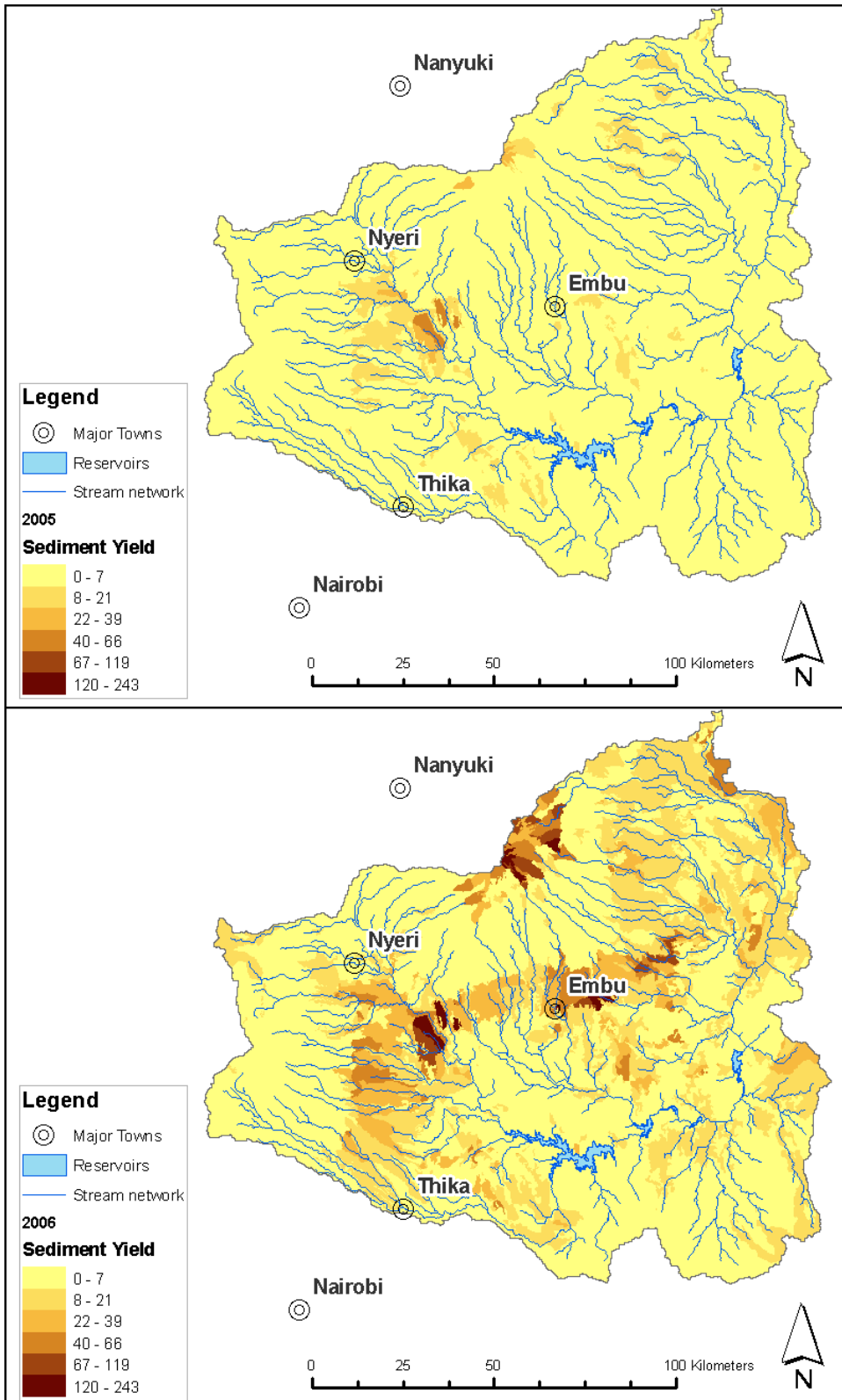


Figure 54. Erosion for a dry year (2005, top) and a wet year (2006, bottom) in ton/ha/yr



# 4 Options for Green Water Credits

## 4.1 Potential benefits

Water is a conservative resource, in other words, it cannot be created. However, the Proof of Concept phase of Green Water Credits showed that green water resources can be much increased and downstream delivery of blue water better regulated by increasing infiltration at the soil surface – cutting destructive runoff and banking this water in the soil – and by reducing unproductive evaporation. By arresting runoff, these practices conserve the soil, increase groundwater recharge and stream base flow. Soil and groundwater are free reservoirs that hold orders of magnitude more water than all existing or conceivable man-made reservoirs. So Green Water Credits has potential benefits for both green water as blue water users:

1. Potential benefits for **upstream land** users:
  - a. More productive rain-fed cropping, so higher crop water productivity and less non-productive evaporation from soil surface.
  - b. Better water infiltration and retention in soil
  - c. Reduce loss of soil nutrients by soil erosion during high intensity rainfall events
2. Potential benefits for **downstream water** users
  - a. Augment supply of 'blue' water to reservoirs
  - b. Augment groundwater infiltration upstream to reduce peak flows (that in some cases cannot be captured in the reservoirs) and to stimulate a more continuous supplying flow regime during the dry months
  - c. Reduce sediment input into reservoirs to preserve capacity

GWC is about meeting the objectives of **both** up- and downstream stakeholders **at the same time**. It has to be noted that meeting the objectives separately would lead to other solutions (fertilizers, sediment traps, artificial groundwater recharge, etc). However, Green Water Credits aims at a sustainable mechanism to be implemented by stimulating the interaction between up- and downstream stakeholders.

Upstream land and water management practices determine the green and blue water and sediment flows both in the upstream as to the downstream areas of the basin. In other words, downstream users depend on their supply highly on the management practices used in the upstream areas. This chapter assesses and quantifies this interaction between land management practices and the blue water and sediment flows to the downstream reservoirs. This will lead to the identification of target areas where the implementation Green Water Credits is most effective and will lead to significant gains for upstream farmers and downstream water uses as for example hydropower.

## 4.2 Proposed Green Water Credit management practices

The proof-of-concept of Green Water Credits showed that the following management practices have a potential to benefit both upstream as downstream stakeholders:

- permanent vegetative contour strips
- mulching
- tied ridges



With the developed biophysical analysis tool (SWAT), the influences and possible trade-offs of these practices could be studied and quantified. The following paragraphs give a more detailed explanation on these practices.

#### 4.2.1 *Permanent vegetative contour strips*

Strip cropping is a practice in which contoured strips of sod are alternated with equal-width strips of row crop or small grain. Strips of grass or other permanent vegetation in a contoured field help trap sediment and nutrients. Because the buffer strips are established on the contour, runoff flows slower and evenly across the grass strip, reducing sheet and rill erosion. The vegetation can also provide habitat for small birds and animals. Permanent vegetative contour strips are in fact an inexpensive substitute for terraces.



**Figure 55. Example of permanent vegetative contour strips (source: NRCS)**

#### 4.2.2 *Mulching*

Mulching requires residues produced within the cropping area and/or residues collected from elsewhere and transported to the cropping area. These residues are then applied in the field, spreading them on top of the soil. They protect the soil from erosion, reduce compaction from the impact of heavy rains, conserve soil moisture and maintain a more stable soil temperature. Besides there are several secondary benefits as for example the prevention of weed growth.



**Figure 56. Example of tree loppings used as a mulch in the Quesungual system (Honduras) to reduce the loss of rainwater through runoff and evaporation (source: FAO)**



### 4.2.3 Tied ridges

This technique consists of soil ridges of varying width and height, average being 30cm width and 20 cm height. At regular intervals, crossties are built between the ridges. The ties are about two-thirds the height of the ridges, so that if overflowing occurs, it will be along the furrow and not down the slope.

Farmers find tied ridges hard yet efficient in harvesting water and conserving soil. Crops planted on the ridges grow faster than those in plots without ridges. A disadvantage is the heavy labour input, although levels of maintenance are considerably lower than the initial construction work.

Tied ridges help to minimize problems of drought power and labour shortage in land preparation. There are positive effects on soil erosion in the area.



**Figure 57. Example of graded contour ridges with cross ties lower than the main ridges to retain water between the cross ties, but allow excess rainwater to flow between the ridges rather than spill over or break the main ridges (source: FAO)**

## 4.3 Technical background

To assess how these practices affect the water and sediment flows in the basin, each of them is implemented in the model with the accompanying model parameter adjustments. The model parameters that represent these GWC options are the soil evaporation compensation coefficient (ESCO), the support practice factor for soil loss ( $P_{usle}$ ) and the runoff curve number (CN2), each of them being described in the following paragraphs.

### 4.3.1 Soil evaporation

The soil evaporation compensation factor (ESCO) is a coefficient that has been incorporated to modify the depth distribution used to meet the soil evaporative demand. This factor accounts for the effect of capillary action, crusting and cracks, but also of other evaporation limiting or enhancing soil adjustments. ESCO must be between 0.01 and 1.0. As the value for ESCO is reduced, the model is able to extract more of the evaporative demand from lower levels (Figure 58).

The default value for ESCO is 0.95. From the sensitivity analysis carried out during the Proof of Concept phase of Green Water Credits it was showed that ESCO can have a substantial impact on soil evaporation. Changing the default from 0.95 to 0.80 means an increase in soil evaporation of about 10%. On the other hand soil evaporation can be reduced by 10% when changing the coefficient from 0.95 to 0.99.

Several studies showed that besides the positive effect on erosion, mulching is able to reduce soil evaporation significantly, in some cases up to 40% (Chen et al. 2007; Tolk et al. 1999). These results have been used to define the parameter changes for the mulching scenario.

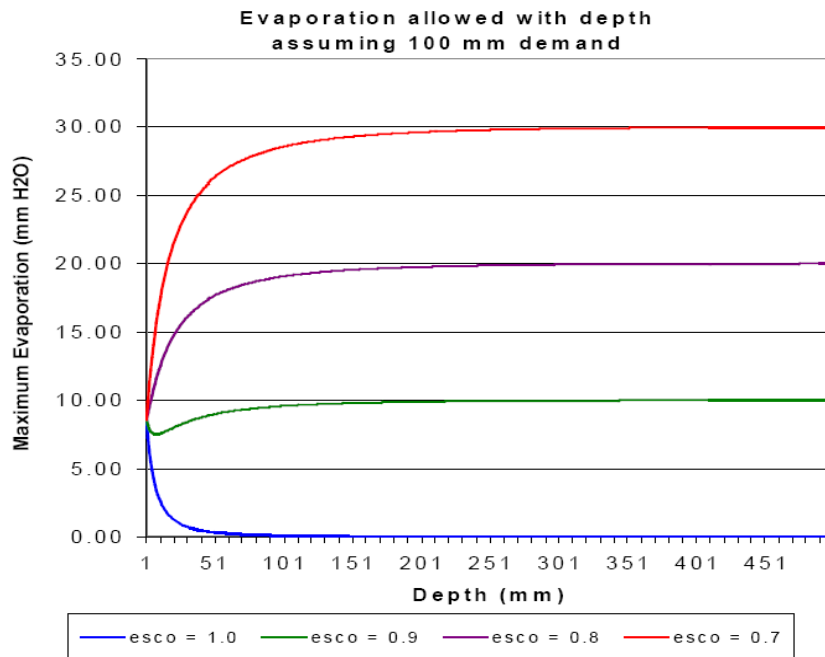


**Figure 58: Impact of soil evaporation compensation factor ESCO on depth of evaporation extraction**

#### 4.3.2 Soil Erosion

Erosion and sediment yield are estimated for each HRU with the Modified Universal Soil Loss Equation (MUSLE)(Williams and Berndt 1977). While the USLE uses rainfall as an indicator of erosive energy, MUSLE uses the amount of runoff to simulate erosion and sediment yield.

The modified universal soil loss equation (Williams 1995) is:

$$sed = 11.8 * (Q_{surf} * q_{peak} * area_{hru})^{0.56} * K_{USLE} * C_{USLE} * P_{USLE} * LS_{USLE} * CFRG$$

where  $sed$  is the sediment yield on a given day (metric tons),  $Q_{surf}$  is the surface runoff volume (mm H2O/ha),  $q_{peak}$  is the peak runoff rate (m3/s),  $area_{hru}$  is the area of the HRU (ha),  $K_{USLE}$  is the USLE soil erodibility factor (0.013 metric ton m2 hr/(m3-metric ton cm)),  $C_{USLE}$  is the USLE cover and management factor,  $P_{USLE}$  is the USLE support practice factor,  $LS_{USLE}$  is the USLE topographic factor and  $CFRG$  is the coarse fragment factor. The crop management factor is recalculated every day that runoff occurs. It is a function of above-ground biomass, residue on the soil surface, and the minimum C factor for the plant.





## **P<sub>USLE</sub>**

The support practice factor,  $P_{USLE}$ , is defined as the ratio of soil loss with a specific support practice to the corresponding loss with up-and-down slope culture. Support practices include contour tillage, strip cropping on the contour, and terrace systems. Stabilized waterways for the disposal of excess rainfall are a necessary part of each of these practices. Contour tillage and planting provides almost complete protection against erosion from storms of low to moderate intensity, but little or no protection against occasional severe storms that cause extensive breakovers of contoured rows.

The following tables from scientific literature serve as guidelines for the definition of the scenarios and for future implementation of the management practices. Table 12 shows different values for  $P_{USLE}$  and slope-length limits for contour support practices. It is confirmed that contouring and the use of vegetative strips is most effective on slopes from 1 to 8 percent.

**Table 12. P factor for different management practices, as was studied in the United States (Wischmeier and Smith, 1978)**

Practice	Slope	Maximum length (m)	P
Contour tillage	1 to 8%	122 to 61	0.5
	9 to 12%	36	0.6
	13 to 16%	24	0.7
	17 to 20%	18	0.8
	21 to 25%	15	0.9
Contour tillage between grass strips	1 to 8%	40 to 30	0.25 (r) 0.50
	9 to 16%	24	0.30 (r) 0.60
	17 to 25%	15	0.40 (r) 0.90

Table 13 shows the results of a study that was applied to the African situation. In this case mulching with straw led to an extremely high reduction in erosion.

**Table 13. P factor for different management practices, as was studied for West Africa (Roose, 1977)**

Management practice	P
tied contour ridging	0.2 to 0.1
erosion control strips 2 to 4 m wide	0.3 to 0.1
straw mulch, over 6 t/ha	0.01
Curasol mulch, 60 g/l/m <sup>2</sup> (depending on slope and crop)	0.5 to 0.2
temporary pasture or cover plant (depending on cover)	0.5 to 0.01
low earth bunds protected by stones or rows of perennial grass or low dry stone walls every 80 cm + contour tillage + hoeing + fertilization	0.1 to 0.05

The sensitivity analysis carried out during the Proof of Concept phase of Green Water Credits confirmed that  $P_{USLE}$  has a substantial impact on soil erosion. In fact, there is a linear relationship between the coefficient and erosion rate (ton/ha), as can be seen also from the previous soil loss equation. Those results and the boundary limits defined in the previous tables were used to define the scenarios for mulching and for the vegetative strip contours.



**Table 14. Runoff curve numbers according to different types of land covers (USDA-SCS, 1972)**

Land Use Type	Conservation Practice	Hydrologic Condition	Hydrologic Group			
			A	B	C	D
Row Crops	None(0)	Poor	72	81	88	91
		Good	67	78	85	89
	Contour (1), Strip (2) or Terrace (4)	Poor	70	79	84	88
		Good	65	75	82	86
		Poor	66	74	80	82
		Good	62	71	78	81
Small Grain	None(0)	Poor	65	76	84	88
		Good	63	75	83	87
	Contour (1), Strip (2) or Terrace (4)	Poor	63	74	82	85
		Good	61	73	81	84
		Poor	61	72	79	82
		Good	59	70	78	81
Close Seeded Legume	None (0)	Poor	66	77	85	89
		Good	58	72	81	85
	Contour (1), Strip (2) or Terrace (4)	Poor	64	75	83	85
		Good	55	69	78	83
		Poor	63	73	80	83
		Good	51	67	76	80
Pasture or Range	None (0)	Poor	68	79	86	89
		Fair	49	69	79	84
		Good	39	61	74	80
	Contour, Strip or Terrace or combination of two or more	Poor	47	67	81	88
		Fair	25	59	75	83
		Good	6	35	70	79
Meadow (not used)	None (0)	Poor	45	66	77	83
		Fair	36	60	73	79
		Good	25	55	70	77
Fallow	All	All	77	86	91	94
Brom Grass	All	All	49	69	79	84
Other	All	All	86	86	86	86

#### 4.3.3 Runoff Curve Number

Surface runoff occurs whenever the rate of water application to the ground surface exceeds the rate of infiltration. When water is initially applied to a dry soil, the application rate and infiltration rates may be similar. However, the infiltration rate will decrease as the soil becomes wetter. When the application rate is higher than the infiltration rate, surface depressions begin to fill. If the application rate continues to be higher than the infiltration rate once all surface depressions have filled, surface runoff will commence. In SWAT the SCS runoff equation is used (USDA-



SCS 1972). This model was developed to provide a consistent basis for estimating the amounts of runoff under varying land use and soil types (Rallison and Miller 1981).

The SCS curve number is a function of the soil's permeability, land use and antecedent soil water conditions. Typical curve numbers for an average moisture condition (condition II) are listed in the following table for various land covers and soil types (USDA-SCS 1986). These values are appropriate for a 5% slope.

The parameter changes for each of the scenarios were defined based on the sensitivity analysis performed during the Proof of Concept phase of Green Water Credits, and using the above table as the principal guideline. More details on the definition of the scenario parameters can be found in the following chapter.

#### 4.4 Scenario definition

For each of the three proposed GWC management options (scenarios), the appropriate parameters are adjusted according to the following scheme. The SWAT model was used to evaluate these scenarios and results were compared to the business as usual situation. It was assumed for these three management options that they would be implemented on the land covers shown in Table 15.

**Table 15. Parameter changes for each of the scenarios**

Management Practice	Land use	ESCO		P <sub>usle</sub>		CN2	
		Baseline	Scenario	Baseline	Scenario	Baseline	Scenario
permanent	maize			1.0	0.7	77	70
vegetative	coffee			1.0	0.7	77	65
contour	tea			1.0	0.7	77	65
strips	agric gen.			1.0	0.9	77	70
mulching	maize	0.95	0.99	1.0	0.8		
	coffee	0.95	0.99	1.0	0.8		
	tea	0.95	0.99	1.0	0.8		
	agric gen.	0.95	0.97	1.0	0.9		
tied ridges	maize					77	62
	agric gen.					77	62

The analysis is carried out by comparing the scenario output of a dry (2005) and a wet year (2006) with the reference 'baseline' situation of the same year (Figure 36). The comparison is done using a number of indicators, graphics and maps, calculating the differences (absolute or percentage) between the baseline situation and scenario.

#### 4.5 Scenario analysis

The three GWC management practices as discussed in the previous section have been implemented in SWAT, using the parameters as shown in Table 15. The dry and the wet year were selected for analysis and the differences in key indicators, water balance terms and spatial distribution were calculated and interpreted. The following sections discuss these results, separated in (1) key indicators, (2) crop-specific, and (3) the spatial distribution using maps.



#### 4.5.1 Key indicators

In order to compare the three different soil and water management scenarios a set of indicators have been introduced showing the impact of each of the basin wide implemented practices. Table 16 introduces these indicators with their values as obtained using the Upper Tana SWAT model for the baseline situation and the 3 different scenarios. Numbers reflect averages over the entire Upper Tana. The balance component 'Outflow' corresponds to the yearly total outflow at the proposed Low Grand Falls dam, the study basin outlet. The 'Storage Change' state variable refers to the amount of water that flowed into (negative values) or out of (positive values) the basin storage compartments. Water is stored in the basin by the natural reservoirs (the aquifer and soil storage) together with the man-made reservoirs.

**Table 16. Values of the key indicators for the baseline situation and the 3 scenarios**

Key indicators	Baseline data		Contour Strips		Mulching		Tied Ridges	
	2005	2006	2005	2006	2005	2006	2005	2006
Inflow Masinga (MCM/y)	860	2,144	857	1,999	879	2,171	852	2,012
Sediments Inflow Masinga (10 <sup>3</sup> ton/y)	1,219	4,130	908	3,165	1,227	4,142	892	3,247
Outflow Kiambere (MCM/y)	1,036	2,326	1,025	2,216	1,072	2,362	1,030	2,201
Outflow Low Grand Falls (MCM/y)	1,657	5,137	1,650	4,922	1,709	5,195	1,664	4,860
Crop Transpiration (mm/y)	382	360	383	360	387	363	383	361
Soil Evaporation (mm/y)	145	146	145	146	137	138	145	146
Groundwater Recharge (mm/y)	57	229	69	260	59	232	73	267
Sediment loss (ton/ha/y)	2	10	1	6	2	9	1	8
Precipitation (MCM/y)	9,099	18,759	9,099	18,759	9,099	18,759	9,099	18,759
Transpiration (MCM/y)	-6,650	-6,264	-6,661	-6,271	-6,738	-6,316	-6,661	-6,273
Evaporation (MCM/y)	-2,517	-2,533	-2,522	-2,540	-2,391	-2,399	-2,524	-2,542
Outflow (MCM/y)	-1,657	-5,137	-1,650	-4,922	-1,709	-5,195	-1,664	-4,860
Storage Change (MCM/y)	1,725	-4,826	1,734	-5,025	1,739	-4,849	1,750	-5,083

For the baseline situation, inflows in Masinga range from 860 million cubic meters (MCM) in a dry year to 2144 MCM in a wet year. The maximum storage capacity of the Masinga reservoir is 1560 MCM, which means that during a wet year the entire water volume held in the reservoir is renewed. However, during a dry year, only about 60% of the maximum capacity of this first main reservoir (Masinga) enters as inflow.

Sediment inflows into the Masinga reservoir are considerable. During the wet year 2006, the total sediment inflow was more than 4 million tons of sediments. This corresponds to about 2% of the total dead storage volume of the reservoir. Besides, the Upper Tana model calculated the total sediment inflow from 2001 until 2008 into this reservoir at about 16 million ton. This value corresponds to 9% of the original dead storage volume. This confirms that the sediment inflow



into the reservoirs forms a serious threat to the reservoir water holding capacity. It becomes evident that significant gains can be obtained when the upstream sediment loss rates are reduced by implementing Green Water Credits management practices.

The impact of the Green Water Credits practices on the key indicators can be read from the same Table 16, but an easier interpretable comparison (absolute and relative) is done in Table 17 and in Figure 59. The table shows to which degree the key indicators changed for each of the scenarios compared to the baseline situation.

**Table 17. Absolute and relative changes (green = increase, red = reduction) of the key indicators for the 3 scenarios compared to the baseline situation**

Key indicators	Contour Strips				Mulching				Tied Ridges			
	2005		2006		2005		2006		2005		2006	
Inflow Masinga (MCM/y)	-3	0%	-145	-7%	19	2%	27	1%	-8	-1%	-132	-6%
Sediments Inflow Masinga (10 <sup>3</sup> ton/y)	-311	-26%	-965	-23%	8	1%	12	0%	-327	-27%	-883	-21%
Outflow Kiambere (MCM/y)	-12	-1%	-110	-5%	35	3%	36	2%	-6	-1%	-125	-5%
Outflow Low Grand Falls (MCM/y)	-7	0%	-215	-4%	52	3%	58	1%	7	0%	-277	-5%
Crop Transpiration (mm/y)	1	0%	0	0%	5	1%	3	1%	1	0%	1	0%
Soil Evaporation (mm/y)	0	0%	0	0%	-7	-5%	-8	-5%	0	0%	1	0%
Groundwater Recharge (mm/y)	12	21%	31	14%	2	3%	3	1%	16	27%	38	17%
Sediment loss (ton/ha/y)	-1	-45%	-4	-39%	0	-12%	-1	-13%	-1	-32%	-2	-21%
Precipitation (MCM/y)	0	0%	0	0%	0	0%	0	0%	0	0%	0	0%
Transpiration (MCM/y)	11	0%	8	0%	88	1%	52	1%	11	0%	10	0%
Evaporation (MCM/y)	5	0%	7	0%	-127	-5%	-134	-5%	7	0%	9	0%
Outflow (MCM/y)	-7	0%	-215	-4%	52	3%	58	1%	7	0%	-277	-5%
Storage Change (MCM/y)	9	1%	-200	-4%	14	-1%	-24	0%	25	1%	-258	-5%

The following conclusions can be drawn from the previous table:

- Implementation of vegetative contour strips or tied ridges at a basin scale leads to a significant reduction of the sediment inflow into the reservoirs. In the wet year almost a million tons less if practice is implemented basin wide.
- Groundwater recharge will increase, both during dry as wet years, stimulating a more continuous water supply through groundwater discharge.
- During the wet year, total inflow in the Masinga reservoir is reduced because of groundwater recharge. This means that during a wet year, water storage in the natural aquifer reservoir is enhanced, making more water available for dry years.
- The use of vegetative contour strips and tied ridges do not alter the water balance significantly during the dry year 2005. For the wet year, basin outflow is slightly reduced and the same amount of water is made available for following years as relatively less water is flowing out of the basin storage compartments (indicated by a negative storage change).



- The mulching scenario causes a considerable reduction in the amount of water evaporated from the soil surface, both during a dry as a wet year. This additional water available is redistributed by crop transpiration and blue water sources, as shown by the increase in the key indicators Inflow Masinga and Groundwater Recharge and basin outflow and storage.
- During the dry year 2005 about 75% of the rainfall is used beneficially to support crop growth, and almost all the rest is lost by non-beneficial soil evaporation. During the wet year, basin scale transpiration and evaporation reached similar values and the additional precipitation levels out with the outflow and storage component.

In fact, the mulching scenario leads to a general improvement of all the key indicators, although some of the changes are not that noteworthy as for the other scenarios. It is remarkable that although the sediment loss diminishes with about 12%, a small increase of sediment inflow can be observed during the dry year. This can be explained by the increase in water inflow into the reservoir, which means that more sediment could be transported. This is the only management practice that leads to a significant decrease in non-beneficial soil evaporation making more water available for the other water balance terms.

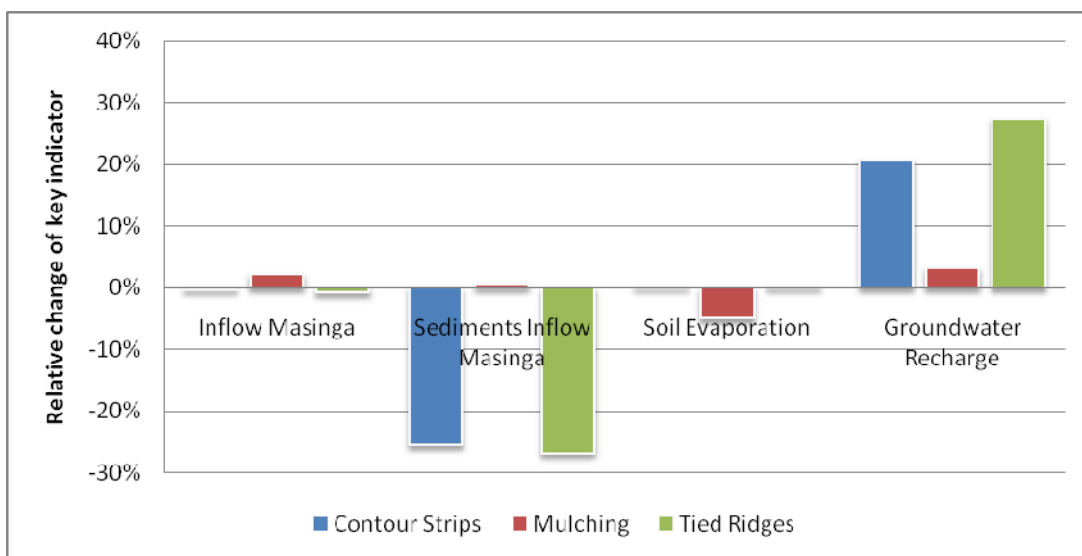


**Figure 59: Relative changes of some of the key indicators for the 3 scenarios compared to the baseline situation (2005, dry)**

It has to be noted that at a basin scale, the implementation of tied ridges gives very similar results as the scenario with vegetative contour strips. About the same reduction can be observed in sediment losses and reservoir inflow, and there is a similar basin wide improvement of groundwater recharge. However, the tied ridges were only applied to the maize crops and the generic agricultural land use class, and not to the coffee and tea crops (Table 15). The spatial analysis (Section 4.5.3) shows other major differences between both practices.

#### 4.5.2 Crop-based evaluation

The SWAT analysis tool allows carrying out a crop-specific assessment of the management practices' impact on the crop water balance. The crop water balance of the baseline 'business as usual' situation is shown in Figure 60. As can be seen, for the dry year surface runoff and groundwater recharge have a minor share in the water balance. Most of the water potentially available for the plant is used for crop growth through transpiration. On the other hand, during a



wet year, about the same amount of water used for crop growth leaves the plots through surface runoff. Moreover, a considerable amount of water infiltrates and percolates to the aquifer.

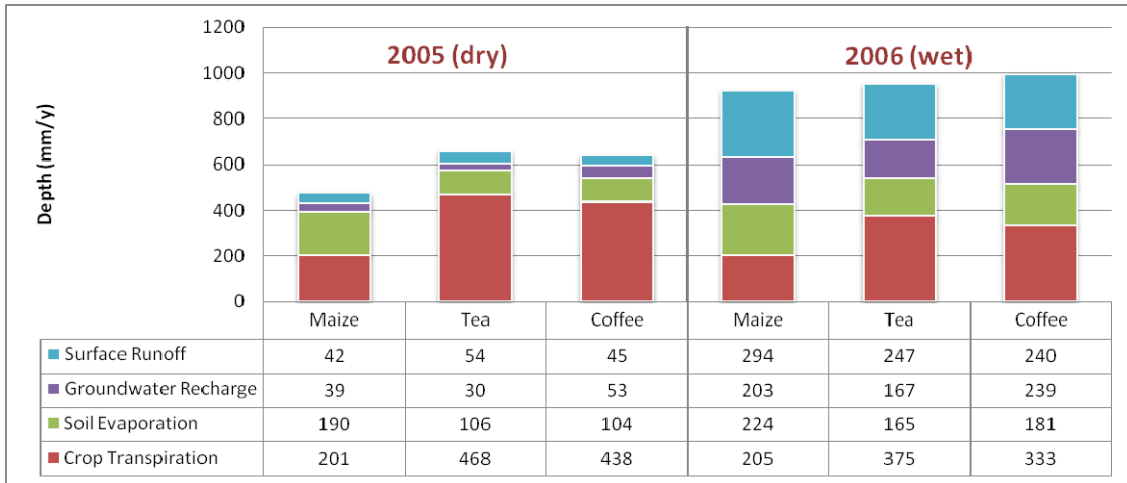


**Figure 60: 'Business as usual' water balance of the 3 major cultivated crops for the two reference years**

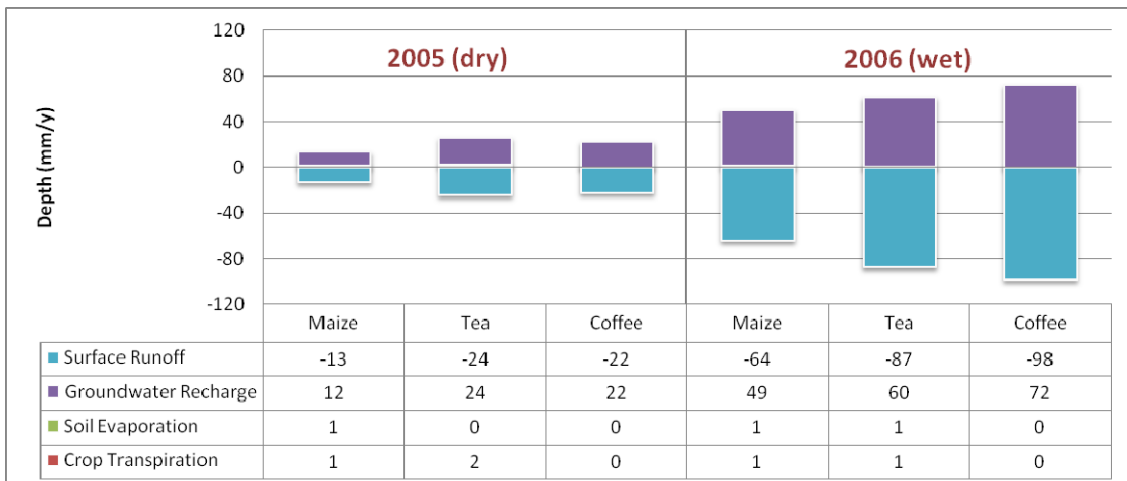


**Figure 61: Changes of the crop water balances for the 'vegetative contour strips' scenario compared to the baseline scenario**

During the wet year 2006 much more water is lost by soil evaporation than during the dry year, due to the higher soil water content. Transpiration rates are similar, although slightly lower in the wet year due to differences in radiation and temperature.

The crop water balances were compared with the baseline situation, and the absolute differences between the terms are represented in the following figures for each of the GWC management scenarios.

Figure 61 shows that even during dry years the use of vegetative contour strips causes a reduction in surface runoff (and erosion) and an increase of groundwater recharge. This additional water stored in the aquifer becomes then available for returnflow or baseflow. This was confirmed by the basin water balance in Table 17, indicating that this management practice does not lead to a reduction in basin outflow or reservoir inflow during a dry year.



The implementation of the mulching practice with the 3 main crops principally leads to changes of the evapotranspiration water balance terms (Figure 62). Productive crop transpiration is increased and soil evaporation is significantly reduced. This effect is similar both in the dry as in the wet year. Moreover, a slight increase in surface runoff and groundwater recharge can be observed, which means a minimal improvement of 'blue water' availability.

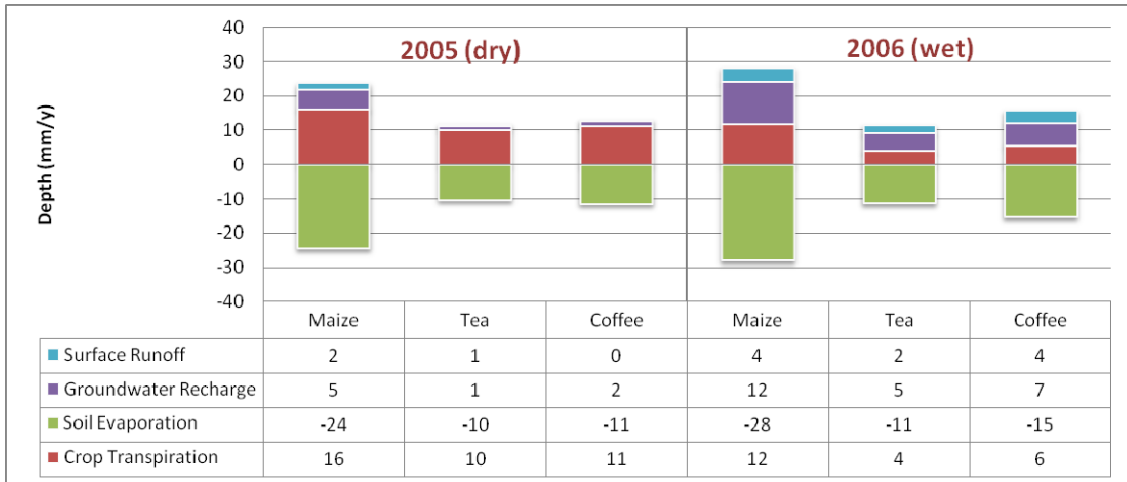


**Figure 62: Changes of the crop water balances for the 'mulching' scenario compared to the baseline scenario**

The implementation of 'tied ridges' was only applied to the maize and the generic agricultural land use class. Figure 63 shows a significant reduction in surface runoff and a similar increase in groundwater recharge. The evapotranspiration terms are not affected by this practice.

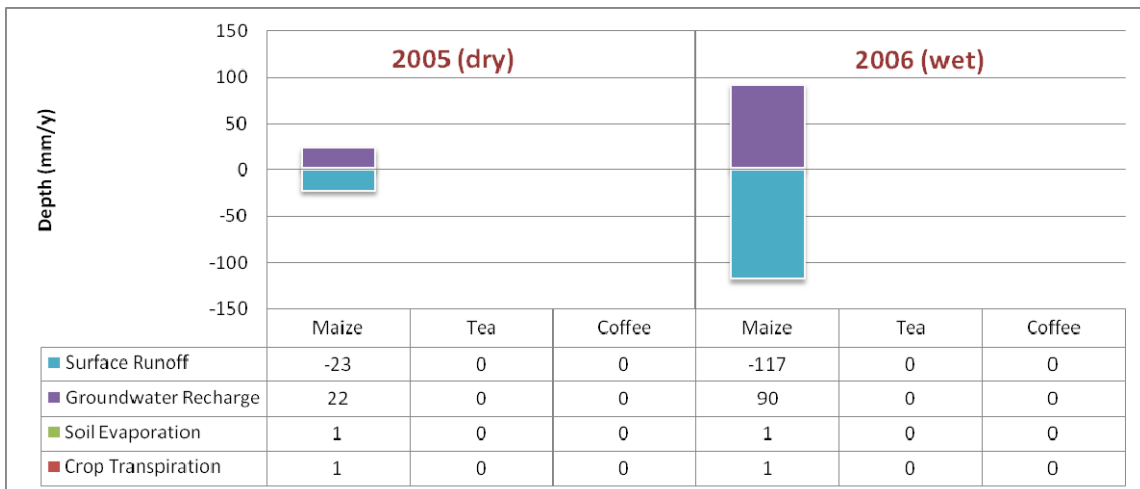


**Figure 63: Changes of the crop water balances for the 'tied ridges' scenario compared to the baseline scenario**

#### 4.5.3 Spatial analysis

The Upper Tana basin is heterogeneous in terms of climate, soil and topographical conditions. The effectiveness of the GWC management practices depends on these site characteristics. Therefore, a spatial analysis and comparison of the scenarios are necessary to provide knowledge on their spatial distribution and hydrological impact. This should give insight in where and under which conditions a certain practice contributes to the GWC objectives. This analysis is carried out on the scale of the finest modeling unit, the so-called Hydrological Response Unit





(HRU). Each of these units has a unique combination of climate conditions, soil, land use and topographical conditions.

Especially during years with high intensity rainfall events erosion rates can be very high, resulting in high sediment inflow into the reservoirs. The yearly sediment loss can be up to 4 times higher than during a dry year (Table 16). Figure 64 shows the relative reduction obtained by the contour strips and tied ridges scenario during the wet year. It has to be noted that the tied ridges scenario did not include any changes on the coffee and tea cultivated fields. As can be expected, the highest reductions are observed in the higher, steep slope areas, where the appliance of one of the practices leads to a reduction of about 50%. These are also areas where average rainfall intensity tends to be higher than in the lower part of the basin.

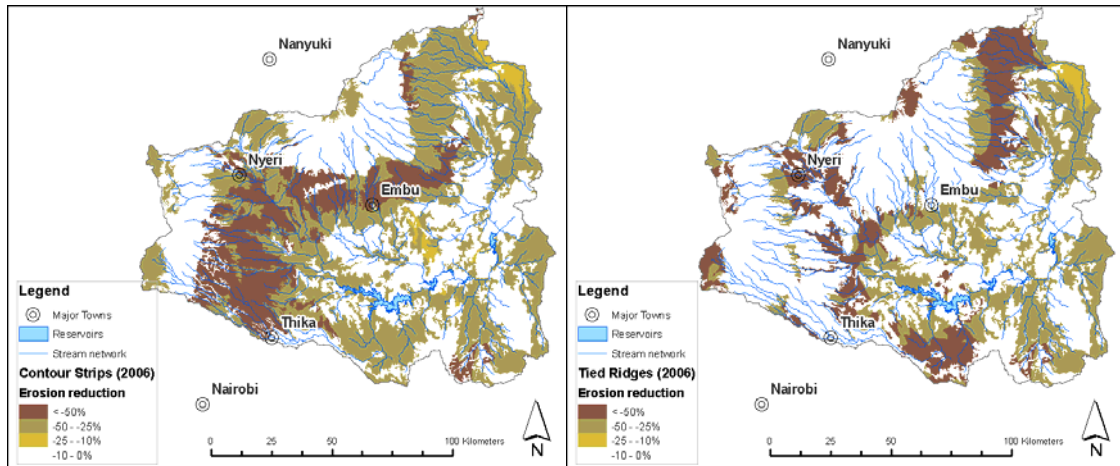


**Figure 64: Spatial distribution of relative erosion reduction for the contour strips (left) and tied ridges (right) scenarios for the wet year.**

The yearly loss of water through soil evaporation has a high dependency on the meteorological conditions of that year. Figure 47 showed that during a dry and relatively hot year (2005) a relatively large part (about 25%) of the incoming precipitation is lost through soil evaporation while during a wet year this loss has a minor share in the total water balance. This means that it is of special interest to reduce the soil evaporation during a dry year. The effectiveness of a certain practice, however, depends on the site conditions. Figure 65 shows that mulching reduces soil evaporation, but during the dry year this practice is more effective than during the wet year. Besides, this difference is accentuated in certain areas, as can be seen comparing the spatial distribution of the simulated reduction.

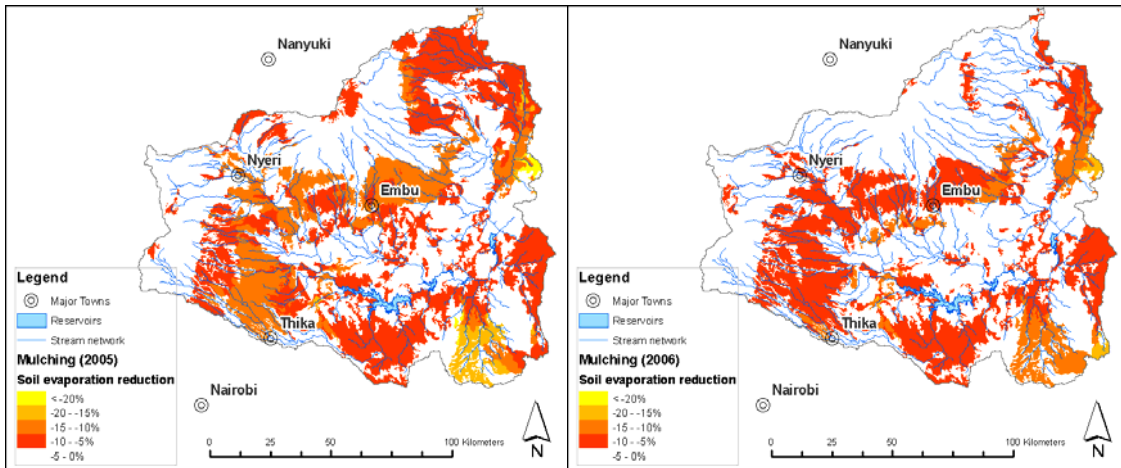


**Figure 65: Spatial distribution of relative reduction of soil evaporation for the mulching scenario for a dry year (left) and a wet year (right).**

One of the main GWC objectives is to assure and enhance a more continuous flow regime during the year for better flood control and enhanced reservoir supply. GWC practices lead to less runoff and therefore to less instantaneous water supply to the reservoirs. Therefore, it is of crucial importance to assess that a reduction in runoff also leads to a comparable increase in groundwater recharge. This guarantees that the water becomes available through groundwater discharge, forming a more reliable and continuous water supply.

Figure 66 shows both 'blue water' competing variables: groundwater recharge (left) and runoff reduction (right) for the contour strips scenario. It is interesting to compare whether a reduction in runoff in a certain area is accompanied with a parallel increase in groundwater recharge. In fact, in the lower basin parts, a reduction of 10 to 25% in runoff comes with an increase of 25 to 50% in groundwater recharge. In the higher upstream areas, however, the percentages of relative change are similar between both variables. The following section makes use of these observations, by taking into account within one single classification different beneficial impacts of GWC practices to identify potential target areas.

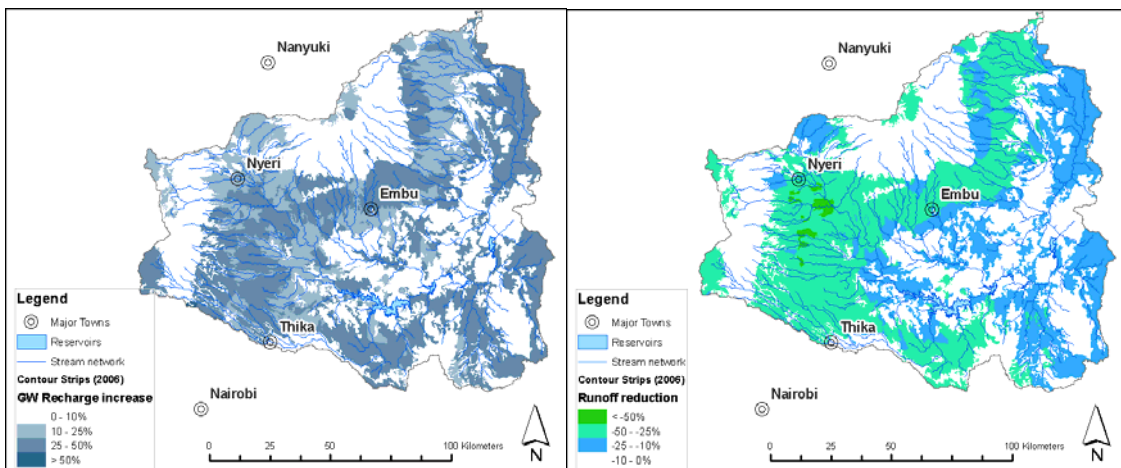


**Figure 66: Spatial distribution of relative increase in groundwater recharge (left) and reduction of runoff (right) for the contour strips scenario for a wet year.**



## 4.6 Results

### 4.6.1 Most effective practices

For the implementation phase of Green Water Credits it is crucial to decide based on quantitative and socio-economical criteria which of the practices have to be given priority to. However, as we have seen in the spatial analysis, each of the practices has different impacts depending on the site characteristics. Using the spatial distribution of the impact on the different variables as groundwater recharge and erosion reduction, it is possible to compare the effectiveness of each of the practices. Applying this approach it will be possible to assess which of the practices has the most impact.

Figure 67 (left) shows which of the practices leads to the highest increase of crop transpiration, location specific. In general, the mulching scenario gave best results in most of the HRUs, both in the higher, wetter and cooler areas as in the dryer areas. However, the use of vegetative contour stripes in the higher regions can also lead to a comparable increase of crop transpiration. Thirdly, in a few regions applying tied ridges leads to a higher relative increase of transpiration as the use of mulch.

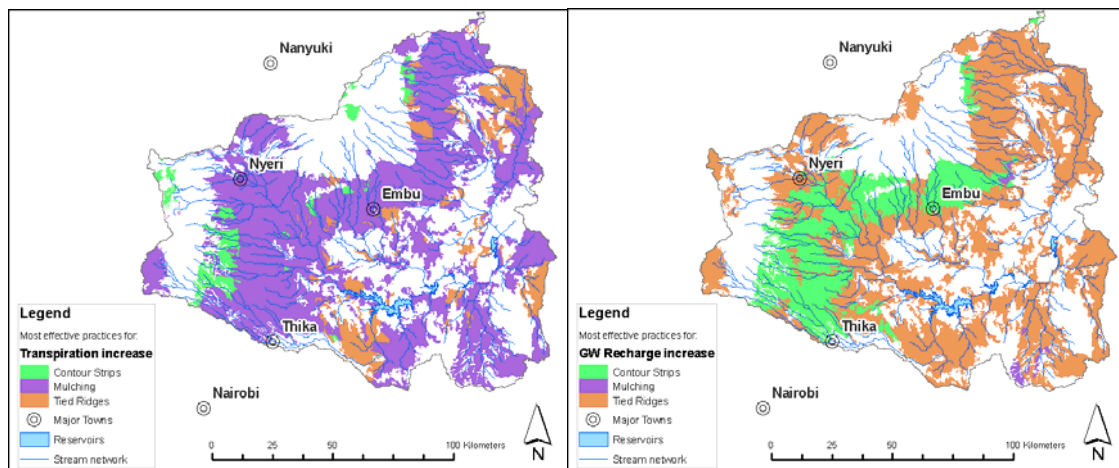


**Figure 67: Spatial distribution of most effective practices with a positive impact on crop transpiration (left) and groundwater recharge (right) for a dry year (2005).**

Also a comparison of the practices' impact on groundwater recharge highlights the importance of a spatially distributed comparison of the practices' impact. Figure 67 (right) shows which of the scenarios leads to the highest increase in groundwater recharge compared with the baseline situation. In general the application of tied ridges on the maize and non-specified agricultural fields is most effective in the majority of the HRUs. However, on a few sites mulching has a slightly higher positive impact on this indicator, although only during a dry year. Vegetative contour stripes turn out to be more effective in the tea and coffee cultivated areas, both for the dry as for the wet year.

The effectiveness of GWC measures depends on the yearly rainfall regime as shown in Figure 68. The left picture shows the spatial distribution of the most effective practices for reducing erosion, for a dry year (2005) for a wet year (2006). One of the conclusions that can be drawn is that the more precipitation falls, the more effective is the application of vegetative contour stripes. Also the previous analysis showed that GWC practices are most effective and beneficial during

wet years. Accordingly, the identification of potential target areas for pilot operation was done using the impact assessment of the wet year 2006.

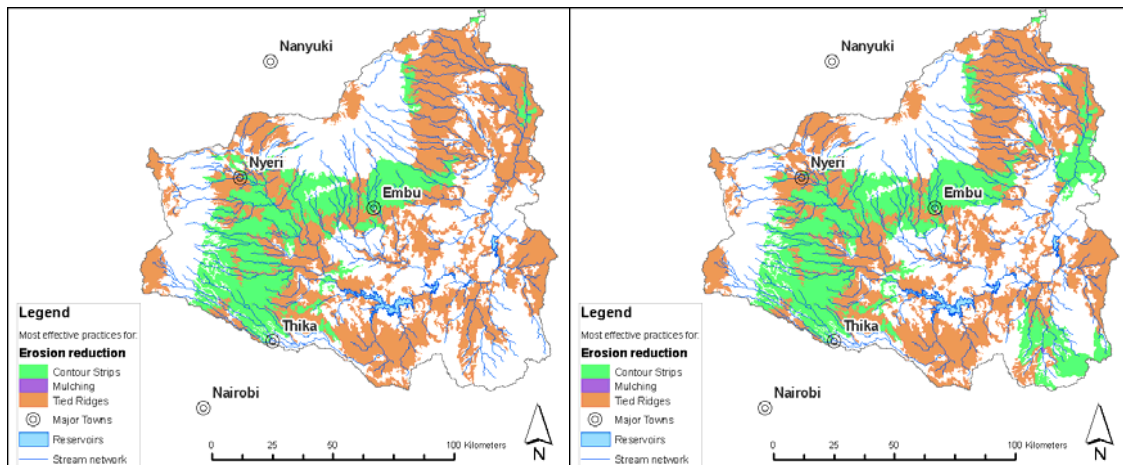


**Figure 68: Spatial distribution of most effective practices reducing erosion for a dry year (left) and a wet year (right).**

#### 4.6.2 Potential target area identification

The scenario analysis was based on basin wide implementation of management practices on all agricultural lands. One of the objectives of the current design phase of Green Water Credits is to define the potential target areas where the practices can be best implemented. The selection of target areas will depend on this hydrological and biophysical analysis but also on socio-economic and institutional factors. This chapter makes a first selection of potential sites based on the previously discussed scenario results for the biophysical aspects only.

For the selection of target areas, the following indicators were chosen to represent overall impact of GWC:

1. Reduction in soil erosion
2. Increase in groundwater recharge
3. Increase in crop transpiration
4. Reduction of soil evaporation

As discussed before, the impact of Green Water Credits practices is highest during wet periods. Erosion can be reduced significantly, groundwater recharge can be enhanced, storing more water in aquifers for drought periods and the evapotranspiration can be optimized. If the most effective practice is chosen for implementation, Figure 69 shows the spatial distribution of the relative changes that can be obtained.



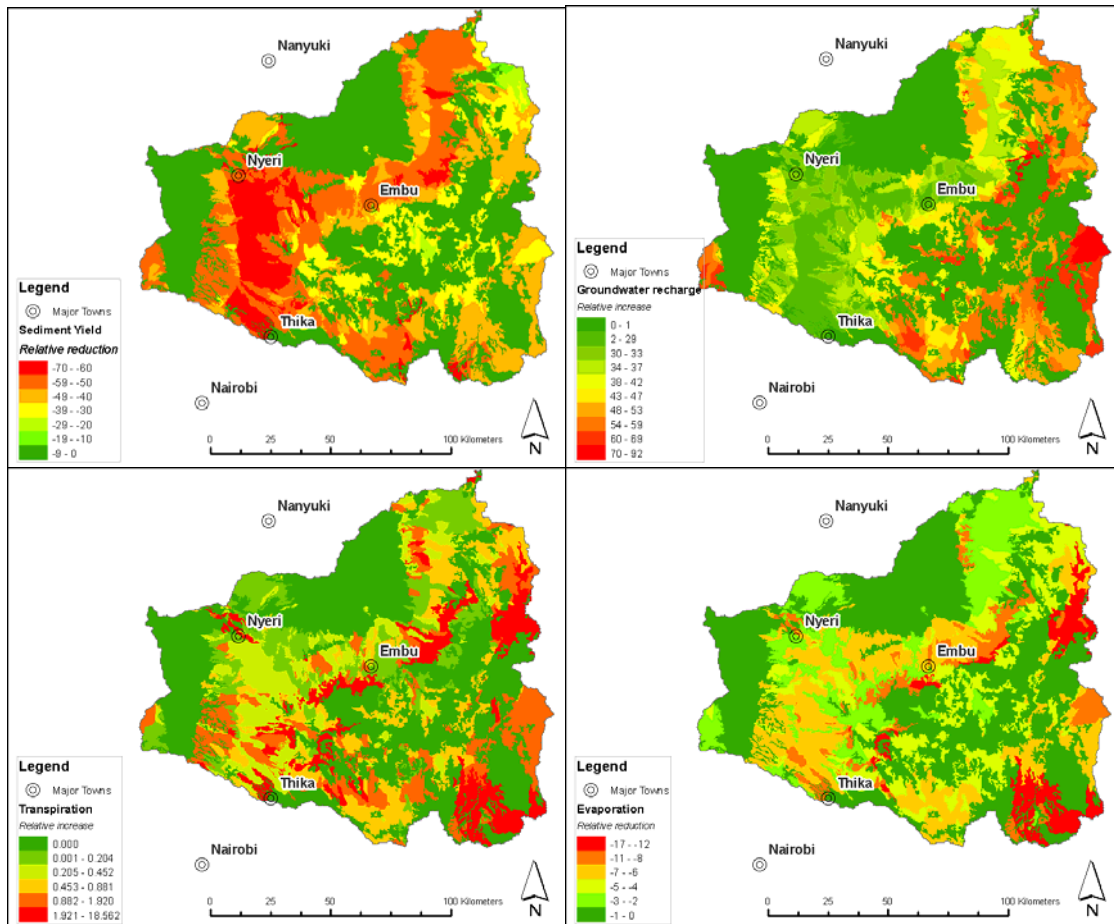


**Figure 69: Spatial distribution of relative changes of four selected parameters for target area identification: erosion reduction (a), groundwater recharge (b), crop transpiration (c) and soil evaporation (d).**

The previous figures show clearly that the identification of target areas is a multi-criteria problem, as the spatial distribution of the maximum changes for each parameter is very different. Therefore, for the target area identification from a biophysical point of view, it is necessary to define weights to each of the parameter of interest. Given the objectives of Green Water Credits, it was decided to give equal importance to erosion reduction (weight = 0.5) as to the optimization of green and blue water resources: groundwater recharge (0.25) and evapotranspiration (reduction evaporation 0.125 and increase transpiration 0.125). The relative changes as shown in Figure 69 were rescaled to a value between 0 and 1, in which 0 means no benefit and 1 is the maximum benefit for the selected parameter. These 4 parameters were then used with the mentioned weights within the following formula:

$$TA = \frac{0.5 \cdot SedYield + 0.25 \cdot GwRch + 0.125 \cdot T + 0.125 \cdot E}{(TA)_{max}}$$

The result of this scaled index TA used for target area identification is shown in Figure 70.

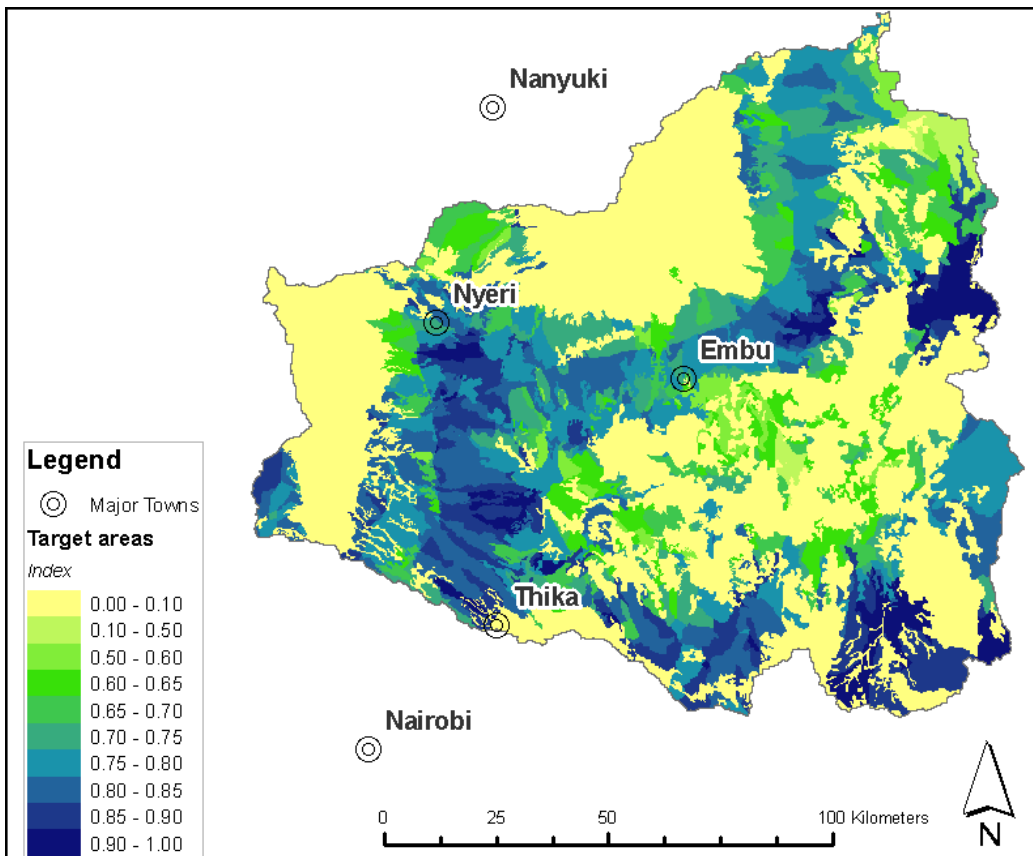


**Figure 70: Spatial distribution of potential target areas.**

#### 4.7 Conclusions

This biophysical assessment quantifies the benefits on the sediment and water flows of Green Water Credits management practices for the Upper Tana basin. It showed how much erosion and reservoir sediment input can be reduced and the green-blue water flows can be optimized through the implementation of the different management options. Also the key areas were identified and the corresponding most effective practices.

It is concluded that the implementation of vegetative contour strips or tied ridges at the most erosive parts of the basin could lead to a reduction of the sediment inflow into the Masinga reservoir of almost a million tons. The yearly sediment loss can be up to 4 times higher during a year with abundant precipitation than during a dry year. The highest erosion reductions are observed at the higher, steep slope areas, where the implementation of one of the practices is able to lead to a reduction of about 50%. Moreover, GWC options are more effective in these areas as they receive more rainfall than the lower parts of the basin.

This assessment shows that there is an unambiguous benefit in optimizing the use of the aquifer as a natural water storage in the basin. The reduction of runoff and the parallel enhancement of percolation and groundwater recharge reduce the need of unproductive spills from the reservoirs during intense rainfall periods as more water is retained upstream within the soil and aquifer. This stimulates a more continuous and reliable water supply during following dry periods. GWC options are able to improve the usage of the aquifer storage by about 20%. Moreover, it was confirmed that no significant reduction of reservoir inflow is caused during a dry year.



The mulching scenario showed that a considerable reduction of water evaporated from the soil surface can be obtained, both during a dry as a wet year. This additional water available is made available for crop transpiration (leading to a higher productivity) and blue water sources.

The identification of potential target areas for pilot operation was done using the impact assessment of the wet year 2006 as in general the GWC options are more effective during wet years (more erosion and more benefits for optimal use of aquifer storage capacity). The selection of target areas was done using the reachable changes of the following parameters: soil erosion, groundwater recharge, crop transpiration and soil evaporation.

The distributed approach used in this assessment allowed taking into account the spatial heterogeneity of the terrain. Therefore, the location of the target areas (Figure 70) depends on many factors as topography, soil type, etc. In general can be concluded that pilot operation of GWC is most interesting on the higher slopes of the Aberdares and Mount Kenya where coffee and maize is cultivated (average Target Area Index = 0.83 and 0.84 resp.). The use of a spatial index to summarize the benefits on each of the parameters of interest gives insight in the exact spatial distribution of the most appropriate areas. Results of these biophysical analysis indicating the most suitable GWC areas will be combined with the socio-economic and institutional studies resulting in the final selection of the pilot operation areas.



## 5 References

- Asadullah A., N. McIntyre and MAX Kigobe M. 2008. Evaluation of five satellite products for estimation of rainfall over Uganda. *Hydrological Sciences Journal* 53(6) December 2008
- Chen S.Y., X.Y. Zhang, D. Pe, H.Y. Sun and S.L. Chen 2007. Effects of straw mulching on soil temperature, evaporation and yield of winter wheat: field experiments on the North China Plain. *Annals of Applied Biology* Volume 150 Issue 3, Pages 261 – 268
- Droogers, P., A. Van Loon, W. Immerzeel. 2008. Quantifying the impact of model inaccuracy in climate change impact assessment studies using an agro-hydrological model. *Hydrology and Earth System Sciences* 12: 1-10FAO 2000. World-wide agroclimatic database, version 2.01, FAO, Rome
- Droogers, P., M. Torabi, M. Akbari, and E. Pazira. 2001. Field scale modeling to explore salinity in irrigated agriculture. *Irrigation and Drainage* 50: 77-90.
- Droogers, P., and G. Kite. 2001. Simulation modeling at different scales to evaluate the productivity of water. *Physics and Chemistry of the Earth* 26: 877-880.
- Gatebe, C. K., P. D. Tyson, H. J. Annegarn, S. Piketh, and G. Helas, 1999. A seasonal air transport climatology for Kenya, *J. Geophys. Res.*, 104, 14,237–14,244
- Jabro JD 1992. Estimation of saturated hydraulic conductivity of soils from particle distribution and bulk density data. *Trans. ASEA* 35(2), 557-560
- Jaetzold R and Schmidt H 1983. Farm management handbook of Kenya, Volume II - Natural conditions and farm management information. Ministry of Agriculture, Nairobi
- KSS 1996. The Soil and Terrain Database for Kenya at scale 1:1,000,000 (ver. 1.0), Kenya Soil Survey, National Agricultural Laboratory, Kenya Agricultural Research Institute
- KSS and ISRIC 2007. Kenya Soil and Terrain database - version 2. Kenya Soil Survey and ISRIC - World Soil Information
- Ministry of Water Development. 1992. The Study on the National Water Master Plan. Prepared with the assistance of Japan International Cooperation Agency (JICA).
- NASA 1998. The NASA GSFC and NIMA (National Imagery and Mapping Agency) Joint Geopotential Model EGM96 (<http://cddis.nasa.gov/926/egm96/egm96.html>)
- Neitsch SL, Arnold JG, Kiniry JR, Williams JR and King KW 2002. Soil and Water Assessment Tool (SWAT). Theoretical Documentation, version 2000, Texas Water Resources Institute, College Station, Texas
- Rallison RE and Miller N 1981. Past, Present and Future SCS Runoff Procedure. International Symposium on Rainfall-Runoff Modeling. Mississippi State University, Littleton pp 355-364
- Roose E. 1977. Application of the USLE in West Africa. In: *Soil Conservation and Management in the Humid Tropics*". Greenland and Lal (eds.). John Wiley. pp 177-188.
- Roose, E, 1996. Land husbandry - Components and strategy. *FAO Soils Bulletin* 70
- Shaxson F and Barber R 2003 Optimizing soil moisture for plant production: The significance of soil porosity, *FAO Soils Bulletin*, Rome: FAO
- Sobierja JA, Elsenbeer H and Vertessy RA 2001. Pedotransfer functions for estimating saturated hydraulic conductivity: implications for modeling storm flow generation. *Journal of Hydrology* 251, 202-220





- Sombroek WG, Braun HMM and van der Pouw BJA 1982. Exploratory soil map and agro-climatic zone map of Kenya, 1980, scale 1:1,000,000. Exploratory Soil Survey report No E1. Kenya Soil Survey, Ministry of Agriculture, Nairobi
- Tolk J. A., T. A. Howell and S. R. Evett, 1999. Effect of mulch, irrigation, and soil type on water use and yield of maize. Soil and Tillage Research Volume 50, Issue 2, 22 March 1999, Pages 137-147
- USDA-SCS 1972. National Engineering Handbook, Hydrology Section, Chap.4-10. US Dept. of Agriculture, Soil Conservation Service, Washington, DC, USA
- USDA-SCS 1986. Urban hydrology for small watersheds, Us Dept. of Agriculture, Soil Conservation Service, Washington, DC, USA
- USGS 2004. Seamless Data Distribution System, Earth Resources Observation and Science (EROS) Centre <http://seamless.usgs.gov/>
- van Engelen VWP and Wen TT 1995. Global and National Soil and Terrain Digital Database (SOTER). Procedures Manual. ISRIC - World Soil Information, Wageningen
- Vieux, B. E., Z. Cui, and A. Gaur (2004), Evaluation of a physics-based distributed hydrologic model for flood forecasting, J. Hydrol., 298, 155– 177.
- Wischmeier W.H. and Smith D 1978. Predicting rainfall erosion losses: a guide to conservation planning. USDA-ARS Agriculture Handbook N° 537, Washington DC. 58 p.

